

Article

Carbon Dioxide Capture and Storage (CCS) in Saline Aquifers versus Depleted Gas Fields

Richard H. Worden 

Department of Earth, Ocean and Ecological Sciences, University of Liverpool, Liverpool L69 3GP, UK; r.worden@liverpool.ac.uk

Abstract: Saline aquifers have been used for CO₂ storage as a dedicated greenhouse gas mitigation strategy since 1996. Depleted gas fields are now being planned for large-scale CCS projects. Although basalt host reservoirs are also going to be used, saline aquifers and depleted gas fields will make up most of the global geological repositories for CO₂. At present, depleted gas fields and saline aquifers seem to be treated as if they are a single entity, but they have distinct differences that are examined here. Depleted gas fields have far more pre-existing information about the reservoir, top-seal caprock, internal architecture of the site, and about fluid flow properties than saline aquifers due to the long history of hydrocarbon project development and fluid production. The fluid pressure evolution paths for saline aquifers and depleted gas fields are distinctly different because, unlike saline aquifers, depleted gas fields are likely to be below hydrostatic pressure before CO₂ injection commences. Depressurised depleted gas fields may require an initial injection of gas-phase CO₂ instead of dense-phase CO₂ typical of saline aquifers, but the greater pressure difference may allow higher initial injection rates in depleted gas fields than saline aquifers. Depressurised depleted gas fields may lead to CO₂-injection-related stress paths that are distinct from saline aquifers depending on the geomechanical properties of the reservoir. CO₂ trapping in saline aquifers will be dominated by buoyancy processes with residual CO₂ and dissolved CO₂ developing over time whereas depleted gas fields will be dominated by a sinking body of CO₂ that forms a cushion below the remaining methane. Saline aquifers tend to have a relatively limited ability to fill pores with CO₂ (i.e., low storage efficiency factors between 2 and 20%) as the injected CO₂ is controlled by buoyancy and viscosity differences with the saline brine. In contrast, depleted gas fields may have storage efficiency factors up to 80% as the reservoir will contain sub-hydrostatic pressure methane that is easy to displace. Saline aquifers have a greater risk of halite-scale and minor dissolution of reservoir minerals than depleted gas fields as the former contain vastly more of the aqueous medium needed for such processes compared to the latter. Depleted gas fields have some different leakage risks than saline aquifers mostly related to the different fluid pressure histories, depressurisation-related alteration of geomechanical properties, and the greater number of wells typical of depleted gas fields than saline aquifers. Depleted gas fields and saline aquifers also have some different monitoring opportunities. The high-density, electrically conductive brine replaced by CO₂ in saline aquifers permits seismic and resistivity imaging, but these forms of imaging are less feasible in depleted gas fields. Monitoring boreholes are less likely to be used in saline aquifers than depleted gas fields as the latter typically have numerous pre-existing exploration and production well penetrations. The significance of this analysis is that saline aquifers and depleted gas fields must be treated differently although the ultimate objective is the same: to permanently store CO₂ to mitigate greenhouse gas emissions and minimise global heating.



Citation: Worden, R.H. Carbon Dioxide Capture and Storage (CCS) in Saline Aquifers versus Depleted Gas Fields. *Geosciences* **2024**, *14*, 146. <https://doi.org/10.3390/geosciences14060146>

Academic Editors:
Jesus Martinez-Frias and Tadeusz Marek Peryt

Received: 29 March 2024
Revised: 11 May 2024
Accepted: 16 May 2024
Published: 28 May 2024



Copyright: © 2024 by the author. Licensee MDPI, Basel, Switzerland. This article is an open access article distributed under the terms and conditions of the Creative Commons Attribution (CC BY) license (<https://creativecommons.org/licenses/by/4.0/>).

Keywords: global heating; energy transition; saline aquifers; depleted gas fields; carbon dioxide; sequestration; carbon capture and storage; fluid pressure; monitoring; CO₂ leakage-risk

1. Introduction

Given the global requirement for energy, the long historical use of fossil fuels, the relatively slow rate of adoption of energy transition technologies, and the well-recognised links between carbon emission, atmospheric CO₂ concentration, and global heating [1], there is an abiding requirement to mitigate greenhouse gas emissions via CO₂ capture and geological disposal, known as carbon capture and storage (CCS) [2]. Global CO₂ emissions are continuing to rise despite various governments' pledges, with fossil fuel use predicted to fall slowly from about 2030 onwards [3]. This means that technologies to trap and dispose of CO₂ need to move quickly to help minimise global heating. This paper is focused on some of the geological disposal aspects of CCS, specifically comparing saline aquifers and depleted gas fields (Figure 1). Note that key terms employed throughout the discussion are defined in Appendix A.

Aquifers, in hydrogeological terms, are volumes of porous and permeable rock that contain water (Figure 1A). At the depths required to store CO₂ in its supercritical state (typically > 800 to 1000 m), the water in the aquifer is typically saline, rendering it unlikely to be suitable for drinking or any type of agricultural or industrial usage. Saline aquifers occur in all continents and are known to be present in most countries. They occur both onshore and offshore. Saline aquifers can be in both sandstones and carbonates.

Depleted hydrocarbon accumulations are volumes of porous and permeable rock that, until recently, contained liquid- or gas-phase hydrocarbons [4]. Most oil fields have pressure support mechanisms, such as water injection, to enhance recovery; towards the end of an oil field's life, much of the produced oil has been replaced by water. This leads to depleted oil fields, like aquifers, having close to hydrostatic pressures and a complex mix of remaining oil and water. CO₂ injection is being increasingly used to increase oil production via CO₂-enhanced oil recovery (EOR) activities at projects such as Weyburn [5], Olla [6], and Farnsworth [7]. CO₂-EOR is not the same as dedicated CCS as the purpose of the former is to increase oil production and not to mitigate greenhouse gas emissions. There are lessons to be learned for dedicated CCS projects from CO₂-EOR projects, but they have fundamentally different objectives.

Depleted gas fields are typically dominated by methane and do not routinely have water injection to maintain pressure [8] (Figure 1B). Gas fields can occur at a range of depths from a few hundred to thousands of metres below the surface. The term depleted means these gas fields have had their hydrocarbons largely or, in practical economic terms, completely extracted. Depleted gas fields can occur both onshore and offshore; and can be hosted by both sandstone and carbonate reservoirs. Depleted gas fields are restricted to sedimentary basins that contain effective source (organic-rich) rocks that have been heated to appropriate temperatures to generate gas and where migration has directed the gas towards porous and permeable reservoir rocks that have suitable trapping structures and effective top-seals [9]. Depleted gas fields are therefore geographically relatively restricted compared to saline aquifers.

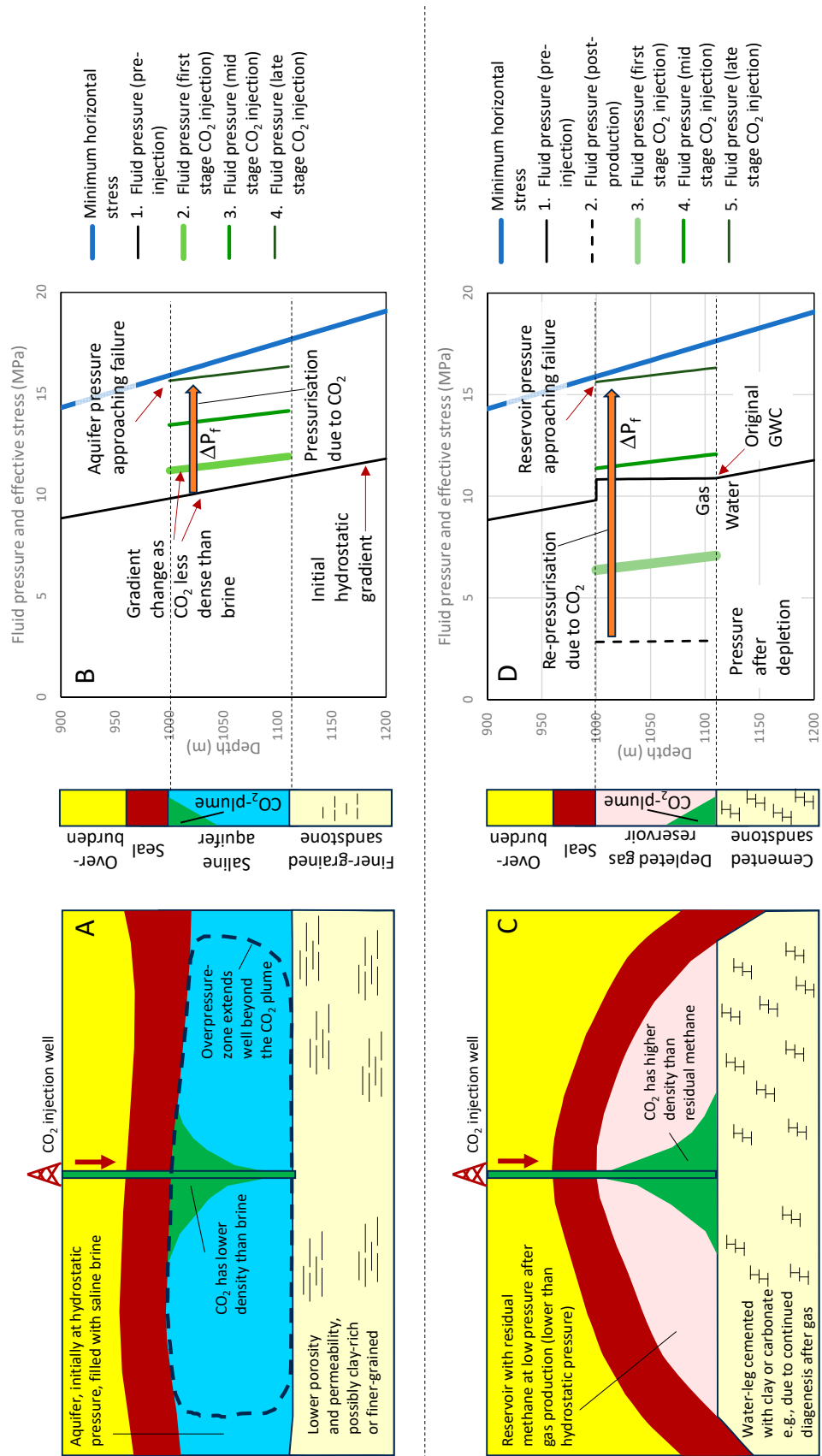


Figure 1. Schematic representation of a saline aquifer and a depleted gas field used for injection and storage of CO₂ with representations of pre- and post-CO₂ injection pressure variation together with the minimum horizontal stress (fracture pressure) also represented. Red arrows represent CO₂ injection.

(A) Schematic diagram of a saline aquifer with the rising CO₂ plume, driven by buoyancy and the much bigger pressure envelope [10]. (B) Pressure and effective stress variation versus depth for the saline aquifer; the pressure was initially hydrostatic (contour 1), CO₂ injection progressively increases the pressure in the aquifer (see contours 2, 3 and 4). The term ΔP_f (shown by the orange arrow moving to the right) represents the maximum additional fluid pressure that the structure can safely contain. (C) Schematic diagram of a depleted gas field with the sinking CO₂ plume, driven by the higher density of CO₂ compared to the residual methane in the gas field. (D) Pressure and effective stress variation versus depth for the depleted gas field. Before gas production (contour 1), the fluid pressure was initially elevated in the gas leg but hydrostatic in the water leg. After production, the pressure dropped to values much lower than hydrostatic (contour 2); in this model, there is no aquifer support so that the GWC was static. CO₂ injection then increases the pressure in the depleted gas field (see contours 3, 4 and 5), by a gradient dictated by the density of CO₂. In this figure, fluid pressure is approaching fracture pressure at the latest stages of filling. The term ΔP_f (shown by the orange arrows moving to the right) represents the maximum additional fluid pressure that the structure can safely contain.

There is an increasing number of saline aquifers being employed globally for CCS [11]. There have also been some CCS pilot studies of aquifers that have been developed to test the efficacy and consequences of injecting CO₂ into the subsurface. The plans, execution, and outcomes for some of these early saline aquifer and CCS pilot projects have been published. Some depleted gas fields have been tested for CO₂ disposal, also with some of the results helpfully published. Given the global need to accelerate the deployment of CCS to mitigate global heating, it is important that regulatory authorities and companies involved in these early stage CCS projects publish the outcomes of their work so that lessons can be learned, mistakes or oversights learned from, and improved decisions made for projects still in development. Regulatory authorities and companies that do not publish the results of their CCS projects are effectively thwarting the global attempt to slow, and then reverse, global heating. Based on available data published so far, this paper seeks to compare saline aquifers and depleted gas fields as geological sites for CO₂ disposal and address the following issues:

- Pressure evolution, CO₂ trapping mechanism, and storage capacity;
- Fluids present in the reservoir before CO₂ injection, relative permeability, and injectivity;
- Stress evolution pathways, risk of failure, and fluid pressure management;
- Risk of halite-scale and limitations to injection rate;
- Relative likelihood of rock property-altering chemical reactions in the reservoir;
- Risk factors, especially geomechanical and geochemical, linked to the possible leakage of CO₂;
- Optimum monitoring strategies.

2. Overview of the Main Existing Saline Aquifer Storage Projects

Before any CO₂ injection has happened, saline aquifers start at approximately hydrostatic pressure; fluid pressure increases during the lifetime of a CCS project as a function of the rate of injection of CO₂, reservoir permeability, the pressure- and temperature-controlled density of CO₂, and the compartmentalisation (plumbing) of the reservoir (Figure 2A). CO₂ injection rates into saline aquifers are controlled by a combination of reservoir effective permeability, pressure- and temperature-controlled CO₂ viscosity, the difference in pressure between the reservoir and the bottom of the injection well, and the ratio of the radius of the injection well and reservoir compartment [12,13].

The longest-lived saline aquifer CCS project is Sleipner, in the Norwegian North Sea Basin, which started injecting CO₂ in 1996 [11]. Production of CO₂-bearing hydrocarbons from the Sleipner Mid Jurassic sandstone reservoir, at about 3450 m, is linked to injection of separated CO₂ into the shallower sandstone saline aquifer of the 250 m-thick Miocene

Utsira Formation at a minimum depth of about 800 m [14]. Via one injection well, after some initial issues with injectivity linked to the completion of the injection well [13], this saline aquifer CCS project has successfully injected about 1 MT-CO₂/yr since 1996.

Snøhvit, in the Norwegian Barents Sea Basin, in 2008 started injecting co-produced CO₂ from the hydrocarbon-bearing sandstone of the Lower Jurassic Stø Formation at about 2300 m, into the slightly deeper (2700 m) and older sandstones of the Tübaen Formation [11,15]. No shallow aquifer exists at the Snøhvit site [16]. The aim was to inject all the CO₂ being emitted from the separator into the deeper saline aquifer, at the rate of about 0.7 MT-CO₂/yr. There were initial problems with the injection rate linked to pressure build-up, caused by reservoir connectivity and halite-scale formation leading to insufficient injectivity of the CO₂ (65 T-CO₂/h, equal to about 0.57 MT-CO₂/yr) [12]. The project adapted the strategy after a short period of time by changing the injection horizon to the off-structure Stø Formation (the reservoir interval). The part of the Stø Formation selected for CO₂ injection is not in direct contact with the reservoir and thus does not enhance hydrocarbon production [13,16].

The In Salah project, in Algeria, injected CO₂ co-produced from hydrocarbons from Lower Carboniferous sandstone reservoirs of the Krechba gas field, at about 1800 m, at a rate of up to 1.4 MT-CO₂/yr from 2004 to 2010. The In Salah project, like the second incarnation of the Snøhvit project, involved injecting the CO₂ into the reservoir interval, but well below the gas–water contact [18]. CO₂ injection did not enhance hydrocarbon production at the Krechba gas field. There were several problems, including ground-up-lift [19], microseismic events linked to high injection rates [20], and a risk of partial dissolution of the top-seal [21], that led to the In Salah CCS project being abandoned after about 6 years and the CO₂ disposed of in conventional ways that therefore did not then help mitigate greenhouse gas release and global heating.

The Gorgon CCS project was planned to inject gas separated from Triassic reservoirs of the Greater Gorgon Gas Fields in the Barrow Basin, Australia, into the 2000 m-deep Dupay Formation at up to 4 MT-CO₂/yr. Relatively little peer-reviewed literature seems to have been released about this project but it is clear that the mooted injection rates have not been achieved [22]. It seems that the Gorgon CCS project was designed to involve an aquifer pressure management system, controlled by water production wells situated away from the injection wells. The water production wells at Gorgon reportedly have experienced sand-production and clogging issues that limit the amount of water that can be produced and thus limit the amount of CO₂ that can be safely injected [23].

The Quest CCS project in Canada has injected about 1.1 MT-CO₂/yr into the Basal Cambrian Sand aquifer at about 2000 m in the Western Canada Sedimentary Basin since 2015 [11,24,25]. Like In Salah, there was a microseismic response to the injection of CO₂ but not sufficient to influence the operation of the project [26]. Like Snøhvit, there was halite-scale build-up, which has been treated by periodic injections of water [24].

Other saline aquifer CCS sites that have been widely published include CCS demonstration (pilot) projects such as Decatur in Illinois, USA [27,28], Nagaoka in Japan [29,30], Ketzin in Germany [31,32], and Heletz in Israel [33,34]. These projects have served as testbeds to prove the efficacy of CCS to politicians and the wider public, to develop monitoring strategies, and to refine the planning of the large-scale deployment of CCS.

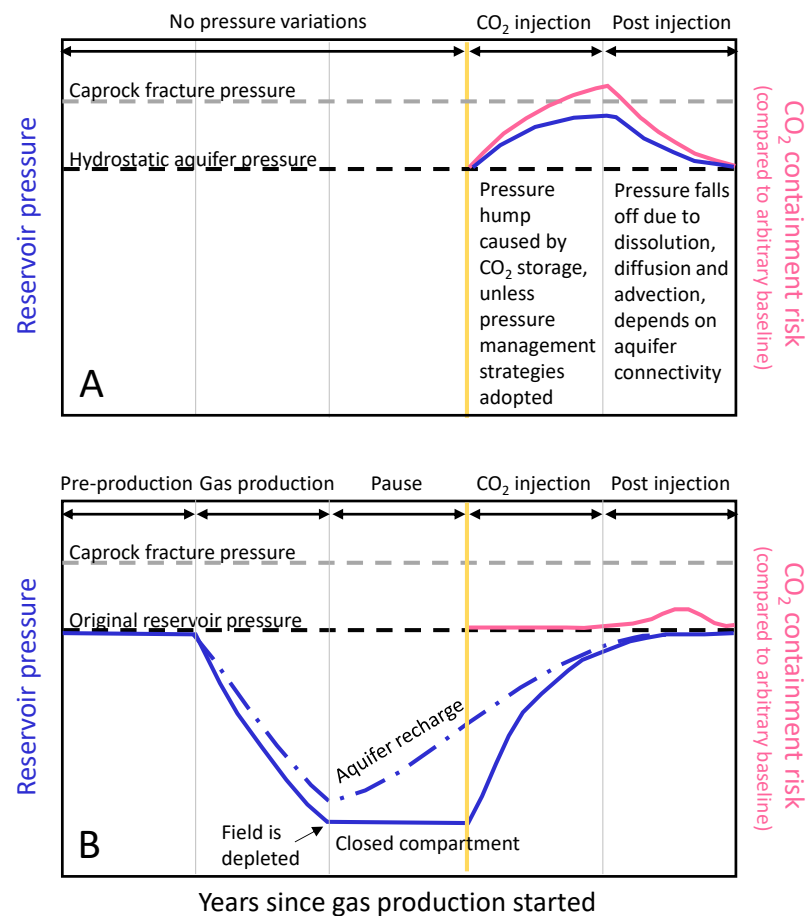


Figure 2. Comparison of possible pressure histories in (A) saline aquifers versus (B) depleted gas fields; modified after IEAGHG (2017) [17]. The different stages in the development of the CO₂ store are stated at the top of parts (A,B). The dashed lines represent the caprock fracture pressure (minimum horizontal stress, grey) and the original gas field or saline aquifer pressure (black). The blue lines represent fluid pressure in the CO₂ store a difference displayed for reservoirs with no aquifer support (Type 1, solid) and some aquifer support (Type 2, dot-dashed) (see Figure 3) and pressure variation in the aquifer, above original hydrostatic but below fracture pressure (solid). The pink lines represent the evolution of risk of CO₂ not being contained. Pressure management might be used in saline aquifers to limit the degree of fluid pressure increase.

3. Carbon Dioxide Storage in Depleted Gas Fields

During production and resource depletion, the pressure in a gas leg decreases as the hydrocarbon is extracted. The pressure evolution of the gas leg depends on the presence and strength of aquifer support, as well as engineering decisions linked to the method of extraction; fluid pressure in the reservoir will increase once CO₂ injection has commenced (Figure 2B). Depleted gas fields have been classified as Types-1 to -3 (Figure 3) [8]. A major source of energy to enhance production from some gas fields comes from a large water-bearing aquifer in direct contact with the hydrocarbons below the gas-water contact; this is known as water-drive, or aquifer support [35]. The aquifer needs to be more than ten times the volume of the hydrocarbon-bearing volume to be effective at assisting production [35,36]. If there is a high degree of aquifer support, the gas-water contact will rise upwards as hydrocarbons are extracted. If there is a negligible degree of aquifer support, then the gas-water contact will remain roughly static when hydrocarbons are produced. The permeability as well as the size of the aquifer influence the degree of aquifer support and whether water from the aquifer occupies reservoir pore space previously filled with hydrocarbons.

Type 1 depleted gas fields represent structures with negligible aquifer support. In this case, the pressure in the gas field decreases to significantly below hydrostatic pressures during gas production and, at the end of field life, the pressure will remain low because there are no fluids from the aquifer capable of rapidly replenishing fluid pressure. This situation can occur when the original hydrocarbon-water contact marked a boundary in the diagenetic evolution of the reservoir, with water-bearing rocks undergoing continued diagenesis and porosity- and permeability-decrease whereas the hydrocarbon leg had inhibited diagenesis because the low water saturation slowed the rate of diagenetic water-rock interaction [37–39]. An example of this phenomenon is the Morecambe Field in the UK's East Irish Sea Basin [40,41].

CO₂ injection rates into depleted gas fields are controlled by the same factors that control CO₂ injection into saline aquifers: reservoir permeability, reservoir and bottom hole pressure, CO₂ viscosity, and density, and the well and compartment radius values [12,13]. The low pressure in the reservoir at the end of gas production, especially for Type 1 depleted gas fields, may result in relatively high injection rates being achievable.

Type 3 depleted gas fields have active aquifers and experience some degree of water-drive during production; fluid pressure falls at a slower rate than Type 1, for the same rate of gas production because water from the aquifer helps keep pressure relatively high (Figure 3). At the end of field life, the fluid pressure rebounds to close to the pre-production pressure values. In Type 3 fields, the gas–water contact demonstrably moves upwards through the structure during the lifetime of the field. Type 3 gas fields probably have a lot of the attributes of saline aquifers as the pores progressively fill with water, especially after a lengthy period (decades) after gas production has ceased. Type 2 gas fields are roughly halfway between Types 1 and 3, having a semi-active aquifer.

It has been suggested that Type 1 and Type 3 depleted gas fields represent the best options for CO₂ storage [8]; Type 1 represents a pressure sink ready to accept injected CO₂. It has been proposed that Type 3 depleted gas fields may be useful because, just as water could easily flow into the aquifer, so water could be easily expelled by the injected CO₂ [8]. Type 2 depleted gas fields may represent a more difficult case as it may be harder, than in the case of Type 3, to expel the water by the injected CO₂ [8].

Depleted gas fields have not yet been widely used for CCS although there are numerous projects at the development stage. K12-B, in the Dutch sector of the North Sea, was developed as a project to test the long-term performance of a depleting gas field for CO₂ storage, by reinjecting CO₂ co-produced with the natural gas. K12-B has a Permian Rotliegend Group, Slochteren Formation gas reservoir at about 3744 m below sea level and 127 °C [45]. Gas production started in 1987 with CO₂ injection commencing in 2004. About 20 KT-CO₂/yr was injected for approaching 15 years at K12-B [46]. Significantly, no problems of CO₂ leakage from the structure, or excess corrosion of the cement or the liner, have been reported [46].

The Otway CCS pilot project in Australia successfully tested CO₂ injection into a depleted gas field. [47]. Similarly, the Rouse CCS pilot project in France involved CO₂ injection into the Lacq gas field, hosted in Cretaceous dolomitised carbonates at about 4000 m in the Aquitaine Basin. About 50 KT of CO₂ was injected for the Rouse project over 3 years from 2010 to 2013. This depleted gas field CCS pilot project led to relatively intense microseismic activity [48], probably because the host reservoir rocks have unusually low permeability (0.1 mD in unfractured core plugs) [49].

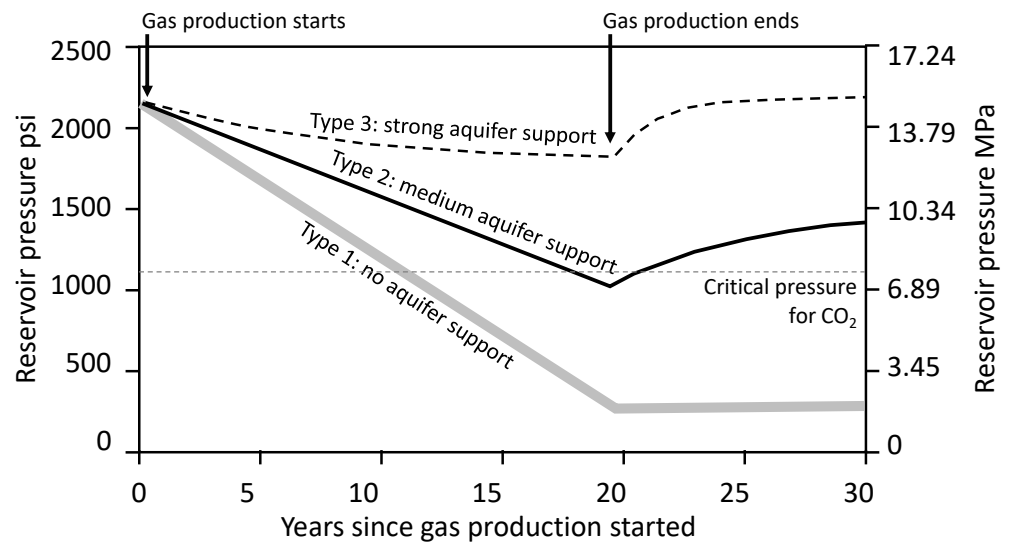


Figure 3. Different types of depleted gas fields as a function of the degree of aquifer support (diagram modified after Hughes [8]) are defined by the ability of fluid in the aquifer (brine) to move up into the pore spaces previously occupied by gas. A manifestation of aquifer support would be the upward movement of the gas–water contact (GWC) during gas production. Type 1 gas fields have very limited aquifer support and display an extreme decrease in reservoir pressure during production; the original gas–water contact may reflect a change from good quality (permeability) reservoir above the GWC to very poor reservoir quality (permeability) below the GWC, perhaps due to negligible diagenetic cementation after gas emplacement but continued diagenesis (e.g., clay or quartz growth [42]) in the water leg. A possible example of a Type 1 gas field is North Morecambe, in the UK East Irish Sea Basin, reported to have very limited water drive due to illite clay cementation in the aquifer [40,43]. Type 3 gas fields have very strong aquifer support indicated by muted pressure decrease during production; these will have GWCs that rise during production and presumably have a large, connected aquifer with good reservoir quality (permeability). Type 2 gas fields display behaviour intermediate between Type 1 and Type 3. An example of a gas field that seems to have re-pressurised (Type 3) is Esmond, in the UK Southern North Sea Basin [44]. The critical pressure for transforming gas into supercritical CO₂ is displayed (7.38 MPa).

4. Similarities between Depleted Gas Fields versus Saline Aquifers

As well as the overall common objective of reducing greenhouse emissions, and thus reducing the effect of global heating, there are numerous important similarities between saline aquifers and depleted gas fields for CCS. However, as discussed in the following section, there are also many differences (see Section 5).

4.1. Role of Reservoir Porosity

The quantity of CO₂ that can be stored in a CCS project is a function of the volume of porous rock to be exploited, the porosity of the host rock, the density of CO₂ at the pressure and temperature of the host rock, and the coefficient that depends on the fraction of the pore space that can be filled with CO₂ (known as the storage efficiency factor) [50]. Saline aquifers and depleted gas fields both will work better, in terms of quantity of CO₂ stored, if they have higher porosity (assuming no other variables change). All other factors being equal, a rock with 15% porosity will be able to store half the quantity of CO₂ as a rock with 30% porosity. Thus, both saline aquifers and depleted gas fields require the careful study of the porosity of the host rock, ideally including an appreciation of what has controlled porosity, e.g., depositional characteristics such as grain size or matrix content, diagenetic characteristics such as degrees of compaction or cementation [51], or structural characteristics such as extent of fracture development.

4.2. Role of Reservoir Permeability

The rate at which CO₂ can be injected is a function of a number of characteristics including effective reservoir permeability, reservoir and bottom hole pressure, CO₂ viscosity and density at the pressure and temperature of the host rock, and the well and compartment radius values [12,13]. If a rock has 10 mD effective permeability, it will have CO₂ injection rates of approximately 10% of a rock with 100 mD effective permeability if all other factors are the same. Permeability may decrease during CO₂ injection due to a range of processes such as fines migration or, in some cases, mineral precipitation [50] but note that higher permeability reservoirs will undergo a smaller degree of loss of injectivity than lower permeability reservoirs making the former easier to model and make predictions [52]. Both saline aquifers and depleted gas fields require careful study of the permeability of the reservoir rock to be able to predict injection rates per well. Saline aquifers and depleted gas fields also need to be understood in terms of the controls on permeability and how they might vary across the subsurface volume of rock planned for CCS. If CO₂ injection is part of an enhanced gas recovery (EGR) scheme [53], then care might need to be taken to understand permeability architecture to avoid the injected CO₂ finding its way to a production well via a high permeability thief zone.

4.3. Need for Reservoir Characterisation

There needs to be characterisation of the architecture of both saline aquifers and depleted gas fields before models can be developed and predictions made about the storage capacity and injectivity. This typically requires seismic imaging of the extent of the reservoir, top-seal, and overburden as well as information about structures such as faults and folds. There is also a need for high-quality well logs interpreted in terms of lithology, reservoir quality, fluid saturation, and geomechanical properties. Well logs are typically used to calibrate the rock characterised by seismic interpretation. Well tests (both historical gas production and water injection test data plus new CO₂ injection test data) can also provide important information about the CO₂ injectivity of the selected reservoir interval [54,55]. There is a strong need to have access to rock samples from the reservoir, and ideally the cap-rock top-seal, via core [56]. Seismic, wireline, and core data [56] are needed to provide an understanding of the internal architecture of the CO₂ storage site, helping to reveal internal baffles and barriers and so help to show how the CO₂ will move and then be stored in the subsurface.

4.4. Need for Data about Fluid Pressure and Effective Stress Responses

Information about fluid pressures is essential for both saline aquifers and depleted gas field storage sites. Fluid pressure variations, e.g., during well tests or from long-term production data, can be used to refine models of the reservoir architecture. Both saline aquifers and depleted gas fields need to have bottom hole fluid pressure increased at such a rate, and to such an extent, that the fracture pressure (minimum horizontal stress, σ_{hmin}) is not exceeded, especially in the top-seal (Figure 2), to avoid causing new fractures to develop. Perhaps even more important, in both saline aquifers and depleted gas fields, is to avoid exceeding the fracture pressure of existing faults that penetrate the reservoir and top-seal. In essence, saline aquifers and depleted gas fields need to minimise the risk of leakage and escape of CO₂ from top seals, fault seals, and wells.

4.5. Need to Understand the Role of Pre-Existing in-Use or Abandoned Wells

Wells in saline aquifers and depleted gas fields need to be designed to minimise corrosion, especially of the liner and the cement bonding the liner to the formation. Existing well penetrations through both types of CO₂ storage type (saline aquifers and depleted gas fields) need to be assessed for the durability of these wells in the presence of CO₂ as it is not automatic that such wells were designed to be in the presence of high CO₂ concentrations. Legacy wells pose one of the greatest threats to the secure subsurface storage of CO₂ in both saline aquifers and depleted gas fields due to poor practices applied at the time of

abandonment or corrosion of casing cements and plugs [57]. It is likely that depleted gas fields will have more well penetrations than deep saline aquifers so the problem will likely be more acute with the former than the latter.

4.6. Need for Monitoring, Measurement, and Verification (MMV)

Saline aquifers and depleted gas fields have some monitoring techniques and approaches in common (Table 1) [58,59]. Microseismic (passive) monitoring reveals whether new fractures are being created, or existing fractures might be caused by shear, due to the increasing fluid pressures in the CO₂ store. CO₂ injection rates and bottomhole pressures and temperatures need to be continuously monitored in both types of storage sites. Distributed acoustic sensors (DAS) and distributed thermal sensors (DTS) along the injection well provide opportunities to monitor the consequences of CO₂ injection in the reservoir, top-seal, and overburden at both saline aquifer and depleted gas field sites. Surface leakage needs to be monitored for saline aquifers and depleted gas field CO₂ storage sites.

5. Differences between Depleted Gas Fields versus Saline Aquifers

5.1. Data Availability and Physical Infrastructure

Two significant differences between saline aquifer and depleted gas field CCS sites are the quantity of data available before the project begins, and the availability of pre-existing physical infrastructure that could be repurposed to save money [60,61].

Depleted gas fields probably have extensive seismic data available from the exploration and appraisal stages of field life. Depleted gas fields have multiple exploration appraisal, and development or production wells with available wireline logs, core, and cuttings providing information about the reservoir and the top-seal. They will also have flow rate data from the testing phase and from the long history of gas production. Core data will typically be available in terms of porosity and permeability, wettability, pore size distribution, and mineralogy. Core samples will be available to allow tests of CO₂ flux through the reservoir. Saline aquifers must have been imaged and drilled through to allow the operator to expect that the body of rock will be suitable for storing CO₂. But, in contrast to depleted gas fields, the aquifer and top-seal rocks from aquifers are unlikely to have been cored ahead of the CCS project and they might not even have a full suite of wireline logs. The pre-existing seismic data from saline aquifer CCS projects will possibly be of lower quality than the equivalent from depleted gas fields.

Depleted gas fields have production platforms that could potentially be repurposed to save money and time. There will also be gas pipelines that could be re-used to send CO₂ to the CCS site rather than hydrocarbons away from the original gas field to collection terminals or distribution networks. Production wells at depleted gas fields, under favourable circumstances, could be re-used for CO₂ injection if the previous completions are appropriate and there has not been too much corrosion. Saline aquifers are unlikely to have comparable infrastructure that could be repurposed unless the aquifer happens to physically lie on top of older, deeper hydrocarbon-bearing intervals such as happened at Sleipner with the Utsira Sand sitting stratigraphically above the Jurassic reservoir.

Table 1. Monitoring techniques for saline aquifers and depleted gas fields.

Monitoring Technique	Saline Aquifer	Depleted Gas Field	Key or Example References
3D or 4D seismic imaging	Possible	Unlikely in most cases	Arts, et al. [62], Urosevic, et al. [63], Luth, et al. [64]
Cross well seismic (Vertical Seismic Profiling)	Only possible if other suitable wells in the area	Possible under some circumstances	Daley, et al. [65]
Electrical resistivity tomography	Possible under favourable circumstances	Unlikely in most cases	Bergmann, et al. [66]
Microseismic (passive) monitoring	Possible	Possible	Stork, et al. [67], Harvey, et al. [68]
CO ₂ composition monitoring	Possible	Possible	GCCSI [69]
CO ₂ injection rate monitoring	Possible	Possible	Ringrose, Greenberg, Whittaker, Nazarian and Oye [13]
Bottom hole pressure monitoring	Possible	Possible	Bergmann, Schmidt-Hattenberger, Labitzke, Wagner, Just, Flechsig and Rippe [66]
Bottom hole temperature monitoring	Possible	Possible	Miri and Hellevang [12]
Injection well-distributed thermal sensors (DTS)	Possible	Possible	Ali, et al. [70]
Injection well-distributed acoustic sensors (DAS)	Possible	Possible	Sidenko, et al. [71]
Monitoring borehole: pressure	Unlikely	Possible	Ringrose, Greenberg, Whittaker, Nazarian and Oye [13]
Monitoring borehole: gas composition	Unlikely	Possible	Vandeweyer, et al. [72]
Monitoring borehole: water composition	Unlikely	Possible	Jang, et al. [73]
Monitoring borehole: continuous log analysis	Unlikely	Possible	Sato, et al. [74]
Monitoring borehole: stable isotopes	Unlikely	Possible	Boreham, et al. [75]
Monitoring borehole: noble gas isotopes	Unlikely	Possible	Gyore, et al. [76], Utley, et al. [77]
Ground/seabed leakage detection: gas composition	Possible	Possible	Lescanne, et al. [78]
Ground/seabed leakage detection: isotopes	Possible	Possible	Gilfillan, et al. [79]
Ground/seabed elevation	Possible	Possible	Morris, et al. [80]

5.2. Pre-CO₂ Injection Fluid Pressures

Reservoir fluid pressures at the start of CO₂ injection tend to be significantly different in saline aquifers than depleted gas fields (Figures 1 and 2). Saline aquifers tend to be at approximately hydrostatic pressure (or above, if over-pressured) (Figures 1B and 2A). The gradient of the initial pre-CO₂ injection fluid pressure will be defined by the density of the water. CO₂ has a small but finite degree of solubility in brine with about 1.5 mole % CO₂ dissolving in low salinity brine at about 30 MPa and 80 °C [81]. The injected CO₂ will therefore predominantly lead to a separate CO₂-rich phase and increased fluid pressure. As the structure starts to fill with the largely insoluble CO₂, then the pressure gradient may start to change as high-density water is progressively replaced by lower-density CO₂. The fluid pressure will increase, especially near the injection well, and the system may approach failure conditions if the fluid pressure approaches fracture pressure conditions (Figure 2A). Pre-CO₂ injection, depleted gas fields probably have pressure much lower than hydrostatic, therefore there is the possibility of a much greater net increase in pressure than in saline aquifers before fracture pressure conditions would be reached (Figure 1, Figure 2B, and Figure 3).

5.3. CO₂ Phase and Density

The density of CO₂ varies with pressure and temperature (Figure 4). Saline aquifers are mostly chosen to be at such a depth that the CO₂ is in the relatively dense supercritical state in the reservoir. The critical point for CO₂ is 7.38 MPa and about 31 °C (Figure 5) so saline aquifers need to be at depths greater than about 800 m for a typical extensional sedimentary basin; for example, the crest of Sleipner is at about 800 m near the injection well [62] (Figure 5).

Because fluid pressure is relatively low in depleted gas fields (Figures 1–3), it is possible that CO₂ will, at least initially, be stable in the reservoir in the gas form rather than as a supercritical fluid. It is energetically expensive to compress CO₂ from gas into

the supercritical or liquid state so there may be advantages in injecting CO₂ as a gas into depleted gas fields until the subsurface fluid pressure has increased sufficiently to put the CO₂ in the supercritical state. It may be preferable to inject denser phase CO₂ once the fluid pressure in a depleted gas fields has exceeded the critical 7.38 MPa. There could be another side effect of injecting dense phase CO₂ into a sub-critical pressure reservoir as evaporation of CO₂ would lead to Joule–Thomson cooling [82] and the possibility of pore-plugging clathrate [83] developing in the near wellbore regions. Figure 5 illustrates a possible fluid pressure pathway for CO₂ injection into depleted gas fields involving first gas phase injection and then supercritical CO₂ injection as the pressure increases (Figure 5, pathway A to D). Thus, saline aquifers and depleted gas fields possibly will have different strategies for the initial phase of CO₂ injection.

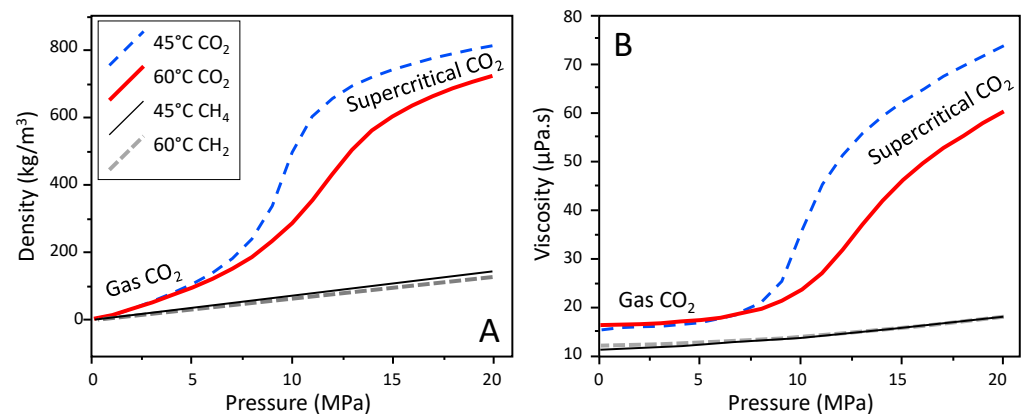


Figure 4. Comparison of physical properties of CO₂ and methane (CH₄) as a function of pressure and temperature, modified from Liu, Yuan, Zhao, Zhang and Song [53]. **(A)** Density variation with pressure at 45 and 60 °C for CO₂ and CH₄. The abrupt increase in CO₂ density, between 7 and 12 MPa, reflects the progressive change from gas-phase to supercritical-phase CO₂. In contrast, CH₄ does not display any phase changes. Gas phase CO₂ has a higher density than methane so the injection of gas phase CO₂ into pressure-depleted gas fields will not result in CO₂ rising buoyantly to the top of the structure. Water has a density of between 990 and 999 kg/m³ at 45 °C and between 983 and 991 kg/m³ at 60 °C between 0.1 and 20 MPa so CO₂ will always rise relative to water in a saline aquifer, whether it is gas or supercritical CO₂. **(B)** Viscosity variation with pressure at 45 and 60 °C for CO₂ and CH₄. The abrupt increase in CO₂ viscosity, between 7 and 12 MPa, reflects the progressive change from gas-phase to supercritical-phase CO₂. In contrast, CH₄ does not display any phase changes and so has a steady increase in viscosity with increasing pressure. For reference, water has a viscosity of between 596 and 599 μPa.s at 45 °C and between 466 and 477 μPa.s at 60 °C between 0.1 and 20 MPa.

The proportions of CO₂, residual methane, and other hydrocarbons, will be highly variable in depleted gas fields, locally affecting the density and viscosity of the mixed fluid, with the number of phases also controlled by the pressure and temperature. It will be difficult to predict the exact proportions of different fluids in a given simulation grid cell, leading to some degree of uncertainty in fluid injection models. Injecting CO₂ into a saline aquifer does not have the same level of complexity for modelling phase types, thus removing this level of complexity.

5.4. Trapping Mechanisms

An early suggestion about how CO₂ will be trapped in saline aquifers was presented in a report by the UN Intergovernmental Panel on Climate Change [2] (Figure 6A). This diagram suggested that most of the CO₂ will initially be trapped by buoyancy processes in structural or stratigraphic traps, analogous to oil and gas in conventional hydrocarbon traps. With time, as the CO₂ plume moves away from the injection well, if water slowly

re-enters the part of the aquifer transiently occupied by the injected CO₂, some CO₂ will be left behind in the pores as disconnected droplets. This trapping leads to residual CO₂; it was suggested that this may be an important trapping mechanism between 100 and 1000 years. CO₂ has limited solubility in water as a function of pressure, temperature, and water salinity. When CO₂ dissolves in water, the water becomes about 1% higher density than CO₂-free water. The locally increased water density results in convection cells that cause the CO₂-saturated water to sink compared to CO₂-unsaturated water [84,85]. Over time, especially after 1000 years, solubility trapping was proposed to become an increasingly important trapping mechanism for the injected CO₂. Finally, the IPCC report suggested that the injected CO₂ will react with either dissolved metals in formation water or unstable, divalent metal-bearing minerals in the host aquifer, resulting in the creation of new carbonate minerals. Mineral trapping was proposed, according to the IPCC report, to become important on a thousand to ten thousand year-timescale. The viability of mineral trapping in saline aquifers will be discussed later. The expected security of the trapping type in saline aquifers is lowest with structural or stratigraphic trapping, increasing through residual and solubility trapping and is highest with mineral trapping [50].

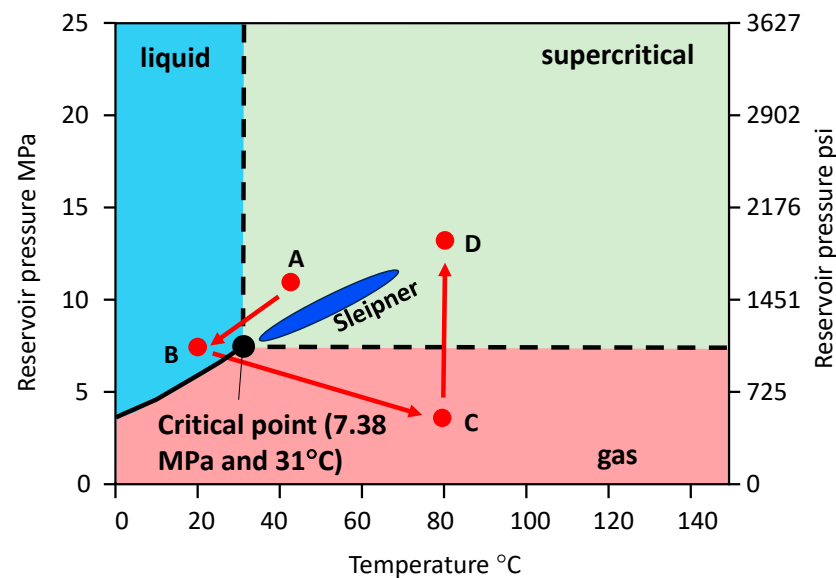


Figure 5. Phase diagram for CO₂ in a P-T region relevant to geological carbon storage. The critical point (black circle), at the upper end of the liquid–gas phase boundary, is at 30.98 °C and 7.38 MPa. The boundaries between the liquid (blue) and supercritical (green) and gas (pink) and supercritical CO₂ are shown as a dashed line as they are gradational. The blue oval represents downhole conditions for injection into the approximately normally pressured Sleipner saline aquifer [50]. Red points A to D represent a possible P-T trajectory (red arrows) for an industrial CO₂ source injected into a depleted gas field that is at fluid pressure lower than hydrostatic pressure [86,87]. For the depleted gas field, point A represents conditions after compression at the capture site. Point B represents the well head conditions of a CO₂ injector. Point C represents downhole conditions at the beginning of CO₂ injection into a depleted gas field when the CO₂ may be stable in the gas phase. Point D represents reservoir conditions towards the end of CO₂ injection when the reservoir has CO₂ in the supercritical state. The assumption in the diagram is that the depleted gas field will initially contain gas phase CO₂ that then evolves to supercritical CO₂ during the injection work.

The diagram proposed for saline aquifers by the IPCC (Figure 6A) is not relevant to depleted gas fields because there is limited water in the pore system and because the fluid that remains after gas production will be dominated by low-pressure and low-density methane. In direct comparison to saline aquifers, there will be no CO₂ buoyancy processes leading to structural or stratigraphic trapping (Figure 6B). Instead, there is likely to be the opposite of buoyancy trapping, as injected gas and supercritical CO₂ have higher densities

than methane so that injected CO_2 will sink to the base of the structure and act as a cushion to the remaining methane [88]. The gas field will have a finite quantity of water as defined by irreducible water saturation (S_{wirr}); this water will predominantly exist as thin films on grain surfaces and may be associated with high microporosity clay minerals, such as chlorite [89]. On a multi-thousand-year timescale, even the least active aquifer (Figure 3) is likely to contribute some water to the low-pressure structure so there may be an influx of water from below the original gas–water contact. These various types of water will dissolve a small quantity of CO_2 , probably leading to some solubility trapping, but convective overturn, analogous to saline aquifers [84,85], seems to be unlikely in depleted gas fields. If mineral trapping is feasible in saline aquifers (Figure 6A), it may be feasible in depleted gas fields, but to a lesser extent due to the relative paucity of water (Figure 6B).

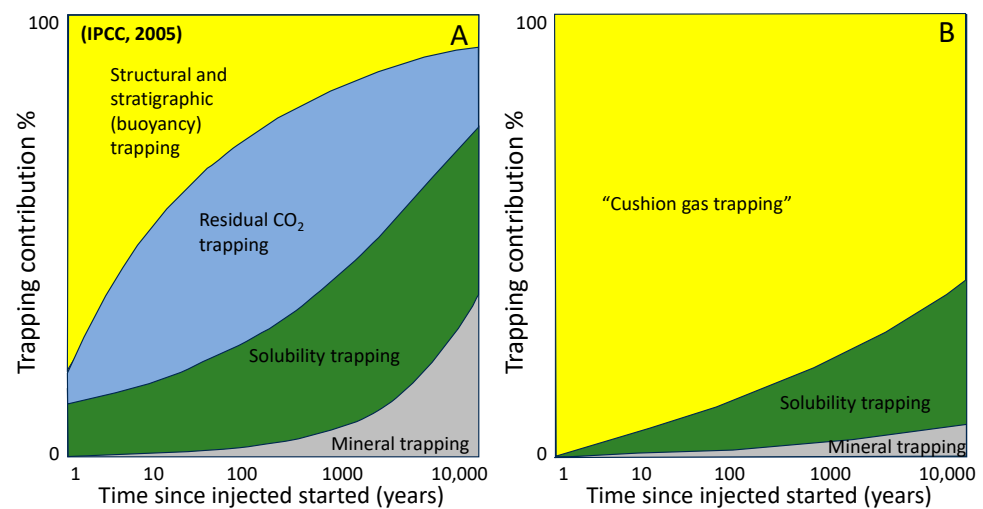


Figure 6. Sketch diagrams of the ways in which CO_2 will exist in the subsurface in saline aquifers and depleted gas fields as a function of time. (A) based on the IPCC [2] report, there were four forms of CO_2 proposed. The first dominant form will be a discrete form of CO_2 that is held in structural or stratigraphic traps by buoyancy forces. Residual CO_2 trapping will become increasingly important as the injected CO_2 moves through the aquifer; residual CO_2 develops to hysteresis of the rel-perm curve of CO_2 during increasing and then decreasing CO_2 saturation. Solubility trapping of CO_2 also becomes increasingly important as CO_2 dissolves in the dominant aqueous fluid phase; CO_2 -saturated water can be up to about 1% higher density than CO_2 -free water resulting in density-drive convection [90] although the effect diminishes at increasingly saline water [91]. Mineral trapping was suggested in the IPCC [2] report to become increasingly important with time, although the proportion of CO_2 that can be trapped in minerals is limited by the availability of divalent metal cations (Ca, Mg, Fe) not already linked to carbonate minerals. (B) Speculative diagram representing the possible forms of CO_2 when it is injected into a depleted gas field. Given that depleted gas fields will contain a small amount of residual water and low-pressure and low-density methane, then, unlike in saline aquifers, the CO_2 will not be buoyant and instead will sink to lower parts of the structure. The CO_2 will act effectively as a cushion and squeeze the remaining methane gas to the crest of the structure [88]. It is likely that there will be some minor influx of water, especially when the depleted gas field remains

at sub-hydrostatic pressure for a long time, and some CO_2 may dissolve in the residual water that remains after depressurisation. Given there is likely to be less solubility trapping of CO_2 in depleted gas fields than in saline aquifers, it is likely that there will also be commensurately less mineral trapping. It seems unlikely that there will be any residual trapping of CO_2 in depleted gas fields.

An attempt to better constrain the trapping mechanisms of CO_2 in closed aquifers, flat open aquifers, dipping open aquifers and depleted gas fields with small original oil contents, was undertaken via modelling by Snippe and Tucker [92] (Figure 7). Inevitably for modelling, they made various assumptions about porosity, permeability, relative per-

meability, hydrocarbon and water composition, pressure, and temperature. Snippe and Tucker [92] also undertook some geochemical modelling but the modelled rates of reactions were somewhat unconstrained and so will not be included here. It was shown [92] that the majority of the CO₂ remains mobile in the simulated hydrocarbon accumulation, with small amounts of CO₂ dissolved in the oil leg and residual water (Figure 7).

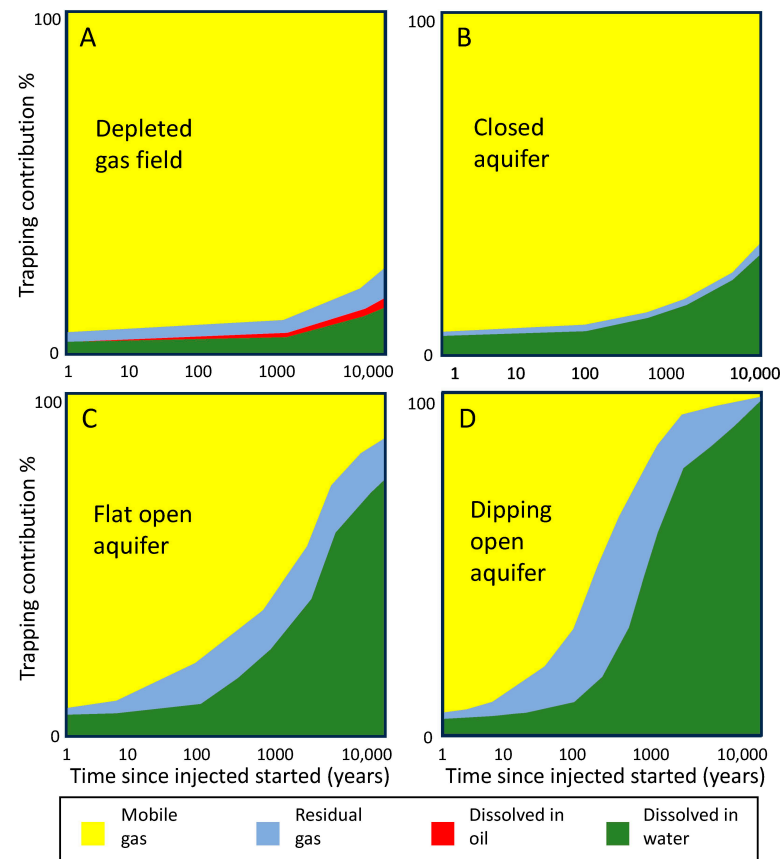


Figure 7. Simulated result of CO₂ phase distribution versus time (1 to 10,000 years) for: (A) depleted gas field with a small original oil content, (B) closed aquifer, (C) flat open aquifer, (D) dipping open aquifer; diagrams modified from Snippe and Tucker [92]. The simulations shown here have not considered geochemical-mineral forming reactions (although other simulations from the same study employed some kinetically controlled reactions). The depleted gas field had most of the CO₂ in a mobile state with minor amounts of residual (immobile) CO₂ and CO₂ dissolved in the remaining oil and a slightly greater amount of CO₂ dissolved in water. The closed aquifer also had most of the CO₂ in a mobile state, with only a small amount of dissolved CO₂ (due to inhibited convective overturn) and even less residual CO₂. The flat open aquifer allowed more density-driven convective overturn than the closed aquifer leading to the domination of water-dissolved CO₂ with moderate residual CO₂. The dipping open aquifer led to the greatest degree of convective overturn and the greatest proportion of dissolved CO₂ of all four models illustrated here. In all cases, the CO₂ is dominated by the discrete mobile form for the first 100 to 500 years.

The relative proportions of mobile, residual, and dissolved (in water) CO₂ in saline aquifers depend on the structural configuration of the aquifer, with the greatest quantity of dissolved CO₂ in dipping aquifers and the smallest quantity of dissolved CO₂ in closed (i.e., compartmentalised) aquifers (Figure 7B–D). A possible lesson from this model is that it may be best to avoid injecting CO₂ into pressure compartmentalised structures; i.e., highly faulted aquifers or those divided into horizontal slices by stratigraphical or diagenetic barriers such as calcite cemented horizons [93,94]. Instead, in terms of security of trapping, it may be preferable to inject CO₂ into large but dipping open aquifers. According to Snippe

and Tucker [92], depleted gas fields also do not lead to high degrees of security of trapping (Figure 7), but this may not take account of other factors such as the pre-CO₂ pressure regime and other benefit of infrastructure re-use.

5.5. Flow of CO₂ through Depleted Gas Fields and Saline Aquifers: Relative Permeability

In low-pressure, depleted gas fields that undergo gas-phase CO₂ injection, the incoming CO₂ will largely encounter low-viscosity methane (Figure 8A). Gas phase CO₂ is miscible with methane [95] so there will be no relative permeability (rel-perm) considerations. The effective permeability will be close to the rock's absolute permeability.

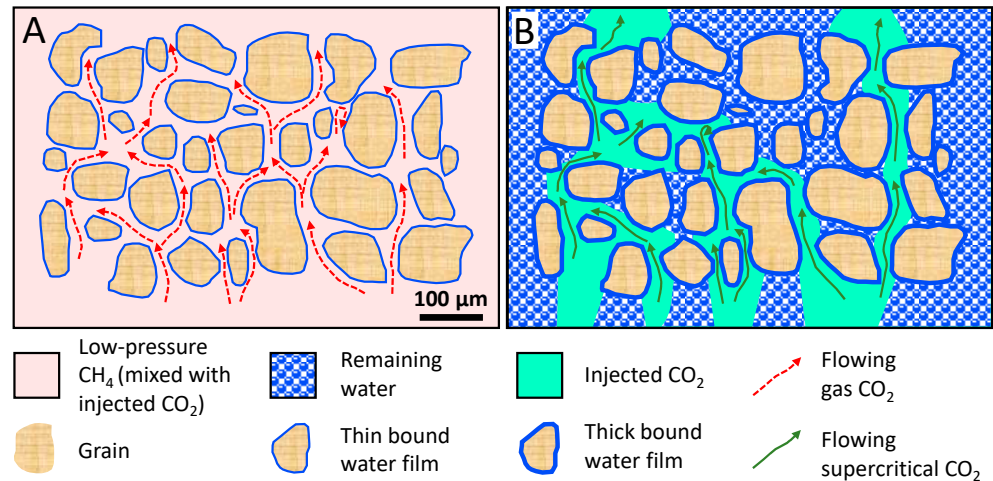


Figure 8. Schematic diagram of how CO₂ moves through a porous network in a depleted gas field and a saline aquifer, modified from Cao, Liao, Hou, Xu, Mehmood and Wu [88]. (A) Representation of gas phase CO₂ injected into a depleted gas field that contains low-pressure CH₄ and grains with a thin residual water film. Water saturation will likely be about 5 to 10%. Gas CO₂ is miscible with the remaining methane thus avoiding rel-perm effects. (B) Representation of supercritical CO₂ injected into a saline aquifer. The residual water films are probably thick (compared to long-lived gas accumulations, see part A) as there will have been little time to drive off water clinging to grain surfaces. Supercritical CO₂ is largely immiscible with saline water so there will be discrete patches of remaining water as well as fingers of CO₂ breaching the largest pore throats (capillaries). The difference in viscosity between supercritical CO₂ and water (Figure 7) will tend to lead to viscous fingering rather than a piston-like displacement [96].

In higher pressure depleted gas fields, or those in the mid-stages of CO₂ injection where the fluid pressure has exceeded the supercritical point (Figure 5), then there will be rel-perm considerations as supercritical CO₂ and methane have finite mutual miscibility (Figure 9A) [97]. In this case, the effective permeability to CO₂ will depend on the proportions of residual methane and injected CO₂. As the methane will likely be at low pressure, then the mole fractions of CO₂ are likely to be high compared to methane and the CO₂ rel-perm scaling factor is likely to be relatively high.

CO₂ has a rather limited ability to dissolve in water [98], so in saline aquifers, the injected CO₂, likely to be in the supercritical state in the subsurface, will be largely insoluble in the pore-filling brine [99]. It is widely assumed that common rocks will be preferentially water-wet as opposed to CO₂-wet [50]. The injected CO₂ will need to overcome the capillary entry pressure of the brine-filled pore (Figure 8B). At low CO₂ saturations, in the early stages of injection or in the far-field regions, the ratio of CO₂ to water will be low, leading to a low rel-perm scaling factor and low effective permeabilities to CO₂ (Figure 9B). At higher CO₂ saturations, possibly locally achieved by viscous fingering [96], then the CO₂ relative scaling factor will increase perhaps to 0.8 (Figure 9B) reinforcing the movement of CO₂ through preferred channels (Figure 8B). Once CO₂ injection ceases, the CO₂ plume will

migrate to higher structural levels in the saline aquifer and brine may flood back into the pores transiently occupied by CO₂. This sequence of events was suggested at the CCS pilot site at Nagaoka by long-term monitoring of a CO₂ injection site using repeat measurement of downhole resistivity via plastic-lined monitoring boreholes [100]. As CO₂ saturation starts to decrease, the CO₂ rel-perm curve moves down a different path to that during the CO₂ increasing phase, this is known as hysteresis. The decreasing CO₂-saturation rel-perm curve meets the base of the Y-axis at CO₂ fractions much less than zero (Figure 9B). This explains residual CO₂ saturation trapping (Figures 6 and 7). Depleted gas fields are rather unlikely to undergo this type of rel-perm hysteresis as the displaced pore fluid (methane) is unlikely to flood back into pores occupied by the injected CO₂. Thus, depleted gas fields seem to be unlikely to have a significant fraction, or possibly any, of the CO₂ trapped as a residual phase (Figure 6B).

5.6. Proportions of Fluids in Different Types of Depleted Gas Fields and Saline Aquifers

Saline aquifers probably contain only brine and trivial quantities of dissolved gas before CO₂ injection (Figure 10A). After CO₂ injection, the CO₂ will rise to the top of the structure but, due to viscosity differences and the probable viscous-fingering style of brine displacement by CO₂ [96], there will be a substantial volume of residual brine at the reservoir scale (Figure 10B). The proportion of CO₂ to brine in the aquifer effectively defines the storage efficiency of the saline aquifer [50,101,102].

In Type 3 depleted gas fields (Figure 3), before CO₂ injection, the present gas–water contact is likely to be at a higher position than before gas extraction and the remaining methane is likely to be at slightly higher pressure. There will be a small proportion of irreducible brine in the gas leg, remaining from when the structure was initially filled with hydrocarbons (Figure 10C). After a period of CO₂ injection into Type 3 depleted gas fields, the eventual gas–water contact may be at an even higher position than before the CO₂ injection started due to the strength of the aquifer (Figure 10D). The residual methane will be at higher pressure due to CO₂ injection. There will still be a small proportion of irreducible brine in the gas leg, and this will also be present in the CO₂-filled portion of the structure. CO₂ probably fills more of the pores in Type 3 depleted gas fields than in saline aquifers as there was only low-pressure residual methane to displace.

In contrast to Type 3, Type 1 depleted gas fields (Figure 3) will have the gas–water contact at effectively the same position as before gas extraction because the aquifer cannot supply water to the depleted structure and the remaining methane will be at low pressure (Figure 10E). There will be a small proportion of irreducible brine in the gas leg, left over from when the structure was initially filled with hydrocarbons. After a period of CO₂ injection, the Type 1 depleted gas field will have the residual methane at higher pressure due to CO₂ injection (Figure 10F). There will still be a small proportion of irreducible brine in the gas leg, and this will also be present in the CO₂-filled portion of the structure. CO₂ probably fills more of the pores than in a saline aquifer or Type 3 depleted gas field (active aquifer) as there will only be low-pressure residual methane to displace and a negligible supply of brine from below the original gas–water contact.

5.7. Locations of CO₂ and Displaced Fluids in Depleted Gas Fields and Saline Aquifers

The physical distribution of CO₂ and displaced fluids will be significantly different in saline aquifers and depleted gas fields (Figure 11).

In saline aquifers with supercritical CO₂ injected, the near wellbore zone will contain residual brine but only CO₂ can flow because the CO₂ saturation will be high and the rel-perm scaling factor for brine will be close to zero (Figures 9B and 11A) [50]. Further away from the injector, where CO₂ saturation is lower, both CO₂ and brine will flow outwards, pushed away from the injector well by the incoming CO₂. The CO₂ rises relative to the brine due to buoyancy effects (density differences, Figure 4A) leading to an inverted trumpet-shaped plume. At the furthest edge of the plume, the CO₂ saturation will be

very low, resulting in low CO₂-relative permeabilities (Figure 9B) and very low plume movement velocity.

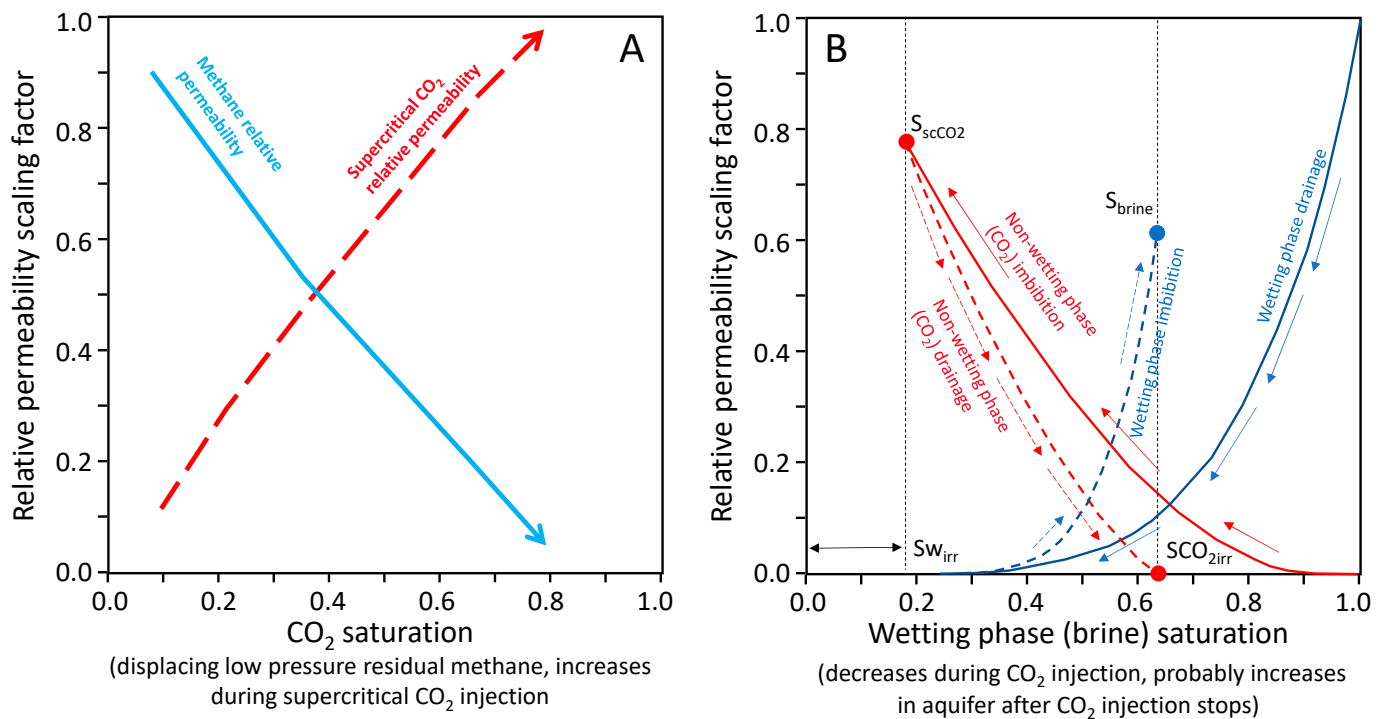


Figure 9. Relative permeability scaling factor; examples for different types of CCS projects. (A) Supercritical CO₂ injection into a depleted gas field, modified from Sidiq and Amin [103]. The red-dashed line is the variable relative permeability scaling factor for CO₂; the blue-solid line is the equivalent for methane. (B) CO₂ injection into a saline aquifer, modified from Burnside and Naylor [104]. The red lines are the variable relative permeability scaling factor for CO₂; the blue lines are the equivalent for water. The solid lines represent the system being flood with CO₂ (displacing water). The dashed lines represent the system undergoing increasing water saturation (displacing CO₂), for example when active CO₂ injection has stopped.

Depleted gas fields, with fluid pressure at a fraction of the original gas field pressure and probably below hydrostatic pressure, may initially have CO₂ injection as a gas phase to avoid (i) unnecessary (and energy-intensive) compression or (ii) evaporation and Joule–Thomson cooling [105] with concomitant risk of clathrate formation and formation damage [83]. The miscibility of gas phase CO₂ and methane will likely prevent a defined boundary between discrete phases of CO₂ and methane, but CO₂, having a higher density than methane (Figure 4), will tend to be more concentrated at the base of the structure (Figure 11B). The remaining methane will tend to be displaced upwards and away from the injector well [88]. Residual brine saturation will probably be similar to the value before any gas production, typically 5 to 15%, with the brine mainly occurring as a thin film on grain surfaces and associated with microporous clay minerals.

In re-pressurised depleted gas fields after injection of CO₂, or injection into a gas field that remains above the CO₂ critical point (Figure 5), then dense phase CO₂ will probably be injected; this will be immiscible with the remaining methane (Figures 9A and 11C). It is likely that there will be a zone near the injection well where the relatively higher viscosity supercritical CO₂ (Figure 4B) has swept most of the methane, a zone of mixed supercritical CO₂ and methane, that sinks relative to the crest of the structure due to the density difference between supercritical CO₂ and methane (Figure 4), and a zone of unswept methane that may have been displaced upwards and away from the injector well (Figure 11C). Residual brine saturation will, at least to start with, probably be like the value

before any gas production, typically 5 to 15%, with the brine mainly occurring as a thin film on grain surfaces and associated with microporous clay minerals. As injection proceeds, the residual brine in the near-wellbore region may evaporate into the injected CO₂ [106].

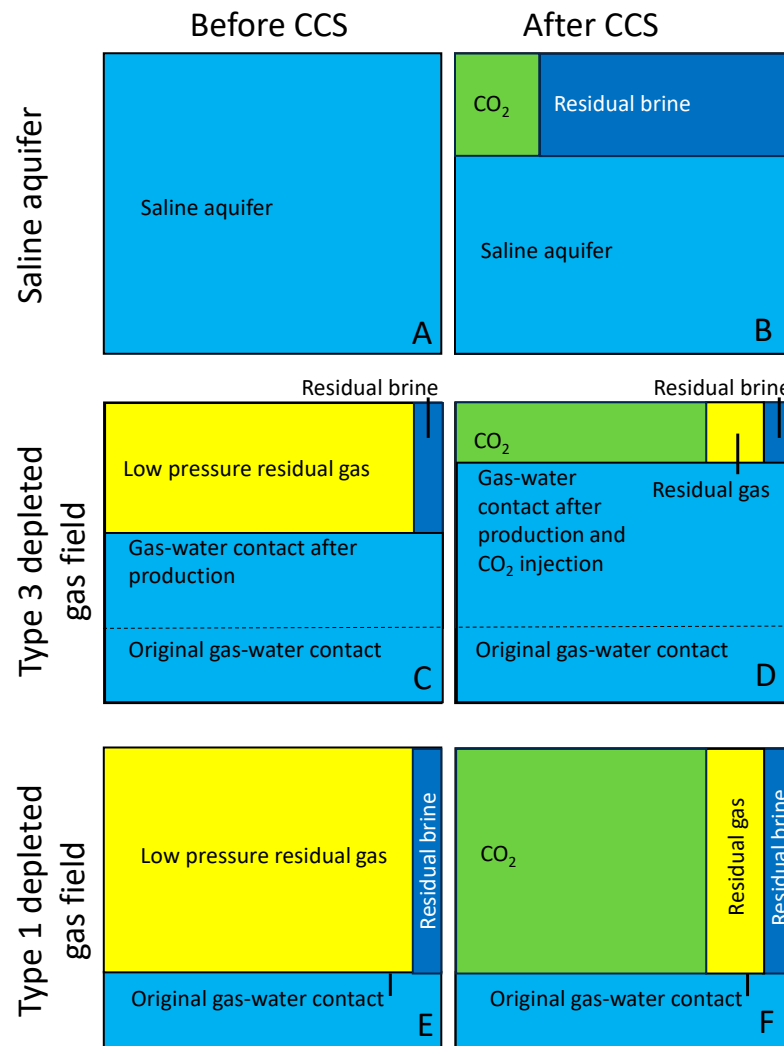


Figure 10. Schematic diagram illustrating the proportions of fluids in saline aquifers and depleted gas fields before, and after, CO₂ injection, modified from Tan, et al. [107]. (A) Saline aquifer before CO₂ injection. (B) Saline aquifer after CO₂ injection. (C) Type 3 depleted gas field with the present gas–water contact at a higher position than before gas extraction and a small proportion of irreducible brine in the gas leg. (D) Type 3 depleted gas field after a period of CO₂ injection with the present gas–water contact at a higher position than before CO₂ injection and a small proportion of irreducible brine in the gas-leg, and a CO₂-filled portion of the structure. (E) Type 1 depleted gas field with the present gas–water contact at the same position as before gas extraction and a small proportion of irreducible brine in the gas leg. (F) Type 1 depleted gas field after a period of CO₂ injection. The residual methane may be at higher pressure due to CO₂ injection, but the residual brine saturation probably remains.

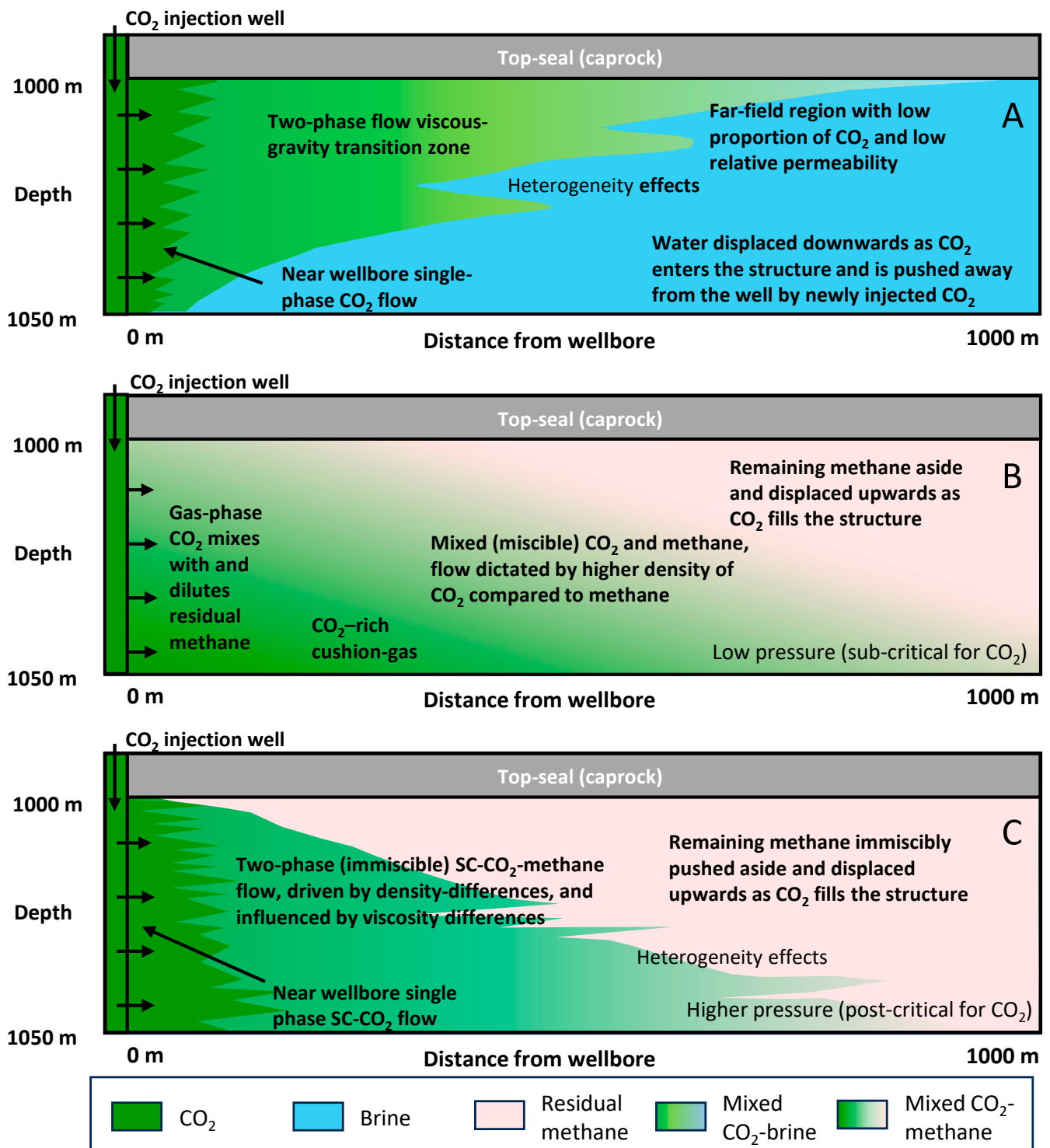


Figure 11. Schematic diagrams illustrating phase distribution in saline aquifers and depleted gas fields, at a nominal depth of 1000 m with a thick top-seal, used for CO₂ storage via a vertical injection well. (A) Saline aquifer with supercritical (SC) CO₂ injected; modified after Ringrose [50]. (B) Depleted gas field with fluid pressure at a fraction of the original gas field pressure and probably below hydrostatic pressure, modified from Cao, Liao, Hou, Xu, Mehmood and Wu [88]. (C) Depleted gas field after re-pressurisation by the injected CO₂ or injection into a gas field that remains above the CO₂ critical point.

5.8. Storage Efficiency of Saline Aquifers and Depleted Gas Fields

Storage efficiency is an important parameter that reflects the volume proportion of pore space within the saline aquifer or depleted gas field that can be filled with CO₂ [55]. It is a function of geological controls (e.g., pre-injection fluid in the porous rock) and the engineering (development) options selected, in terms of phase of CO₂, injection rate, and well-bore diameter. Storage efficiency ranges from as low as 0.02 to 0.05 (2 to 5%) in some open aquifers without structures, through to 0.70 to 0.80 (70 to 80%) in highly depleted gas fields [108].

In saline aquifers, there is a strong contrast in the viscosity of the injected supercritical CO₂ and the pre-existing saline brine, with which supercritical CO₂ has very limited ability to mix. As a function of pressure and temperature, the CO₂ will have a viscosity in the range 0.002 to 0.010 mPa.s (Figure 4B); the brine will have a viscosity in the range 0.3 to 0.6 mPa.s [109]. This contrast in viscosity will lead to viscous fingering of CO₂ into the brine-filled medium instead of stable (piston-like) displacement of the brine by the injected CO₂ [96]. Viscous fingering of the injected CO₂, as it displaces brine, leaves a lot of the brine-filled rock unswept and this will consequently result in a low storage efficiency, likely to be of the order of 0.10 if no other factors are at play [96]. However, there is likely to be a significant difference in density between the injected CO₂ and the brine. Depending on pressure and temperature, the injected supercritical CO₂ will have a density of about 400 to 800 kg/m³ (Figure 4A). In contrast, the brine will have a density of close to 1000 kg/m³ increasing with salinity (but with only a minor role for pressure and temperature due to the very limited compressibility of water [109]). The difference in density leads to the CO₂ being buoyant compared to brine in saline aquifers and results in plume-shaped accumulations (Figure 11A). Increasing the differences in the density of the injected and the displaced fluids leads to higher gravity–viscous ratios, which have been shown to be inversely proportional to storage efficiency [101,110]. Gravity–viscous ratios are also affected by injection rates, host rock permeability, and rel-perm factors, as well as fluid viscosities; under typical conditions, the density difference between supercritical CO₂ and brine will lead to storage efficiency factors of about 0.02 to 0.10 in saline aquifers [50,101].

Storage efficiency can be estimated from saline aquifer CCS projects by comparing the monitored amount of CO₂ injected to a seismically defined extent (radius) of a CO₂ plume (Figure 12) [50,102]. For a given set of conditions, larger plume radius values imply lower storage efficiency values as more of the saline aquifer has not been swept by the injected CO₂. Analysis of seismic and injection rate data from Sleipner showed that the storage efficiency was about 0.05 after 20 years of injection, closely matching theoretical considerations of the gravity–viscous ratio [50]. Storage efficiency values in closed saline aquifer compartments might be as low as 0.005, due to the incompressibility of water and the inability of injected fluid to move out from the injection site [111]. Modelling has suggested that storage efficiency values are likely to be higher in saline aquifers with large structural closures (e.g., anticlines) than in open flat aquifers; storage efficiency values might be as high as 0.20 in large anticlinal structures [54].

The question of storage efficiency values in depleted gas fields has not received as much attention as in saline aquifers, but values have been estimated, based on modelling, to be much higher than saline aquifers. In essence, the issues of viscosity difference are negligible (for methane and miscible gas phase CO₂ [95]) or much lower (for methane and immiscible supercritical CO₂; Figure 9A) for depleted gas fields than saline aquifers. In contrast to saline aquifers, the CO₂ is not fighting to move through the low-pressure methane-filled pores in depleted gas fields so there may be limited issues of viscous fingering. For depleted gas fields, a fundamental assumption can be made in storage capacity calculations that the volume previously occupied by the produced gas is available for CO₂ storage. This assumption is most valid for pressure-depleted reservoirs that are not in hydrodynamic contact with an aquifer, and/or that were not injected with any sort of fluid during secondary and tertiary recovery. If 70 to 80% of the original gas-in-place has been recovered, then that space may be available to be filled with injected CO₂. In this

case, the storage efficiency may be as high as 0.70 to 0.80 [112,113]. Field-specific estimates for depleted gas fields are 0.70 for the Permian Rotliegend sandstones of the Viking Field in the UK's Southern North Sea Basin [114] and 0.78 for the Triassic Sherwood (Bunter) sandstones of the Hamilton Field in the UK's East Irish Sea Basin [55].

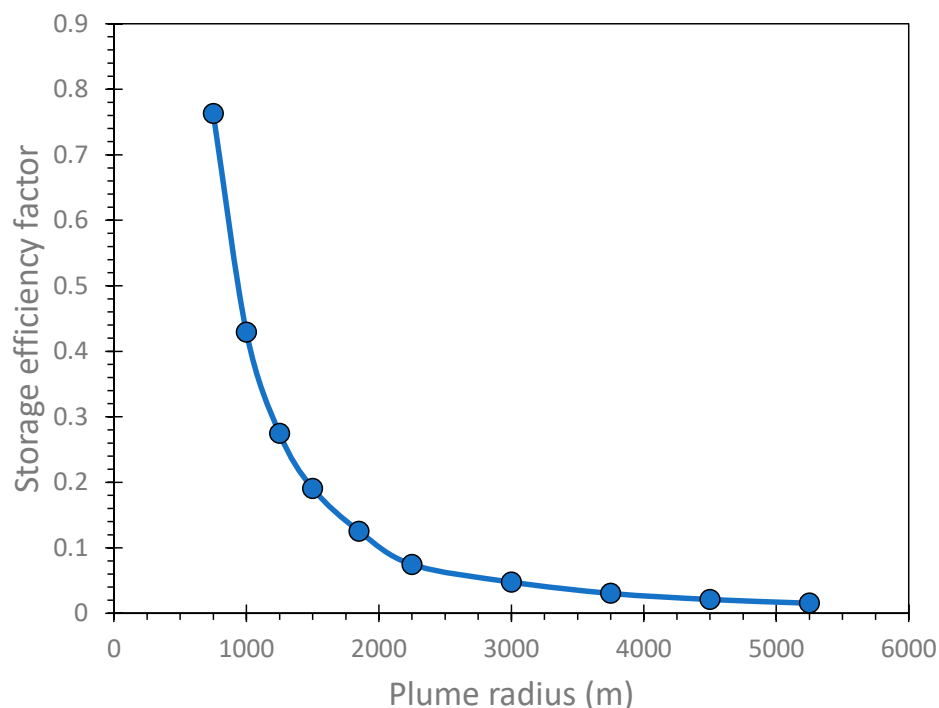


Figure 12. Modelled variation of storage efficiency of a saline aquifer as a function of the radius of the CO₂ plume, based on Ringrose [50]. In this case, the aquifer has been assumed to be a 50 m thick sand with 35% porosity, with CO₂ at a density of 650 kg/m³, injected at 3000 t/d for 14 years. The reservoir is here assumed to have isotropic horizontal permeability. A plume with a radius of about 2500 m would imply a storage efficiency of about 0.07 under these conditions.

In summary, the storage efficiency of saline aquifers is typically relatively low (0.02 to 0.20), whereas it is likely to be relatively high (up to 0.80) in depleted gas fields. This difference implies that the volume of rock to be exploited for depleted gas field storage of CO₂ may be up to an order of magnitude smaller than the volume of rock required for saline aquifer storage of CO₂, for the same mass quantity of CO₂ to be stored.

5.9. Proven versus Unproven Trap and Top-Seal Effectiveness

Depleted gas fields have both static data, such as seismic cross sections, wireline logs, core data, and even special core analysis data, and dynamic data about fluid production rates, sometimes from discrete horizons [60]. These sources of deep knowledge about the reservoir can be directly applied to the use of a depleted gas field as a CO₂ storage site [56]. There should be relatively low levels of uncertainty about how the field will behave in terms of CO₂ injection rate, reservoir architecture, and CO₂ storage capacity (but see subsequent section of geomechanical issues).

In comparison to reservoir-focused studies of conventional; hydrocarbon accumulations, top-seal caprocks to gas fields are relatively rarely studied: quite simply, if a gas field has been discovered, there must be an effective top-seal. Although depleted gas fields have a proven trap configuration with a top-seal caprock that has demonstrably been sufficient to trap some fluids as methane has been held in situ for many millions of years. Nonetheless, care must be taken in assessing the effectiveness of the caprock at a depleted gas field as there may have been geomechanical changes to its efficacy and the caprock may have some finite degree of reactivity to CO₂-rich fluids that were not manifest when it sealed

unreactive methane. It is likely that there will need to be a renewed research focus into caprocks to depleted gas fields to ensure that they will function effectively to hold CO₂ in place [115].

In contrast to depleted gas fields, saline aquifers may have limited pre-existing seismic, well-log, or core data as they are unlikely to have been exploited for fluid production [60]. This difference implies that there may be a need for greater time and expense for the site characterisation stage for saline aquifers than depleted gas fields.

Saline aquifers may not have a trapping configuration, but the large-scale details of the structure still need to be understood ahead of CO₂ injection. Saline aquifers will typically require a top-seal caprock to prevent upward flux of the buoyant CO₂, although some have suggested complex interlayering of reservoirs and thin seals may be sufficient to contain CO₂ [116]. Caprock systems to saline aquifers deserve substantial attention, which is likely to be a requirement imposed by regulatory authorities [117].

5.10. Dilation and Compaction Effects on Porosity and Permeability in Saline Aquifers and Depleted Gas Fields

Depending on the degree of diagenetic increase in the geomechanical strength of a reservoir, depressurisation during gas production may lead to some degree of compaction (Figure 13). Every reservoir will be different in detail, but generalities can be made about rock strength and susceptibility to compaction during depressurisation with prior knowledge of burial and thermal history and the initial mineralogy of the reservoir [38]. Older hotter and deeper clastic reservoir rocks, or those that have been deeply buried and heated and then inverted and consequently cooled, tend to be strong and are relatively unlikely to undergo significant compaction during gas production. Younger, cooler clastic rocks, buried to shallow depths are likely to undergo compaction during gas production.

If a depleted gas field that underwent compaction due to pressure depletion is then re-pressurised due to CO₂ injection, then there are a range of possible outcomes [86]. In terms of porosity, it is possible that the reservoir will simply elastically re-inflate (Figure 13A). Alternatively, the compaction may have been permanent and there may be no increase in porosity during re-pressurisation. It is also possible that there will be partial re-inflation of the reservoir (Figure 13A). At present, there are not enough published case studies of re-pressurisation with which to develop rules. It seems likely that reservoirs that are susceptible to ductile compaction, i.e., those that are rich in clay minerals, may be most susceptible to non-reversible compaction because clay aggregates may have undergone permanent plastic deformation during depressurisation.

There are also a variety of outcomes in terms of porosity-permeability trajectories during depressurisation and re-pressurisation (Figure 13B,C). Gas production may lead to a significant decrease in permeability as, presumably, the biggest pore throats collapse first. It is possible to speculate that one type of response is that CO₂ injection may partly re-open some of the collapsed pore throats and increase permeability to some degree [86]; another type of response is that the compaction may have been permanent and so permeability will not increase when fluid pressure increased due to CO₂ injection. The precise relation between porosity and permeability during re-pressurisation depends on which pores re-inflate and whether they increase the overall connectivity as CO₂ pressure increases. More published research work is required on the topic of the geomechanical response of reservoir rocks to re-pressurisation during injection of CO₂.

The porosity-permeability response to decreasing and then increasing fluid pressure in depleted gas fields will be different to the response of saline aquifers to CO₂ pressure increase. It is not impossible that there will be a degree of dilation of the saline aquifer reservoir, as evidenced by ground elevation monitoring at the In Salah saline aquifer CO₂ storage site [19,59]. However, there has not yet been a detailed synthesis of porosity-permeability evolutionary paths due to CO₂ injection into saline aquifers.

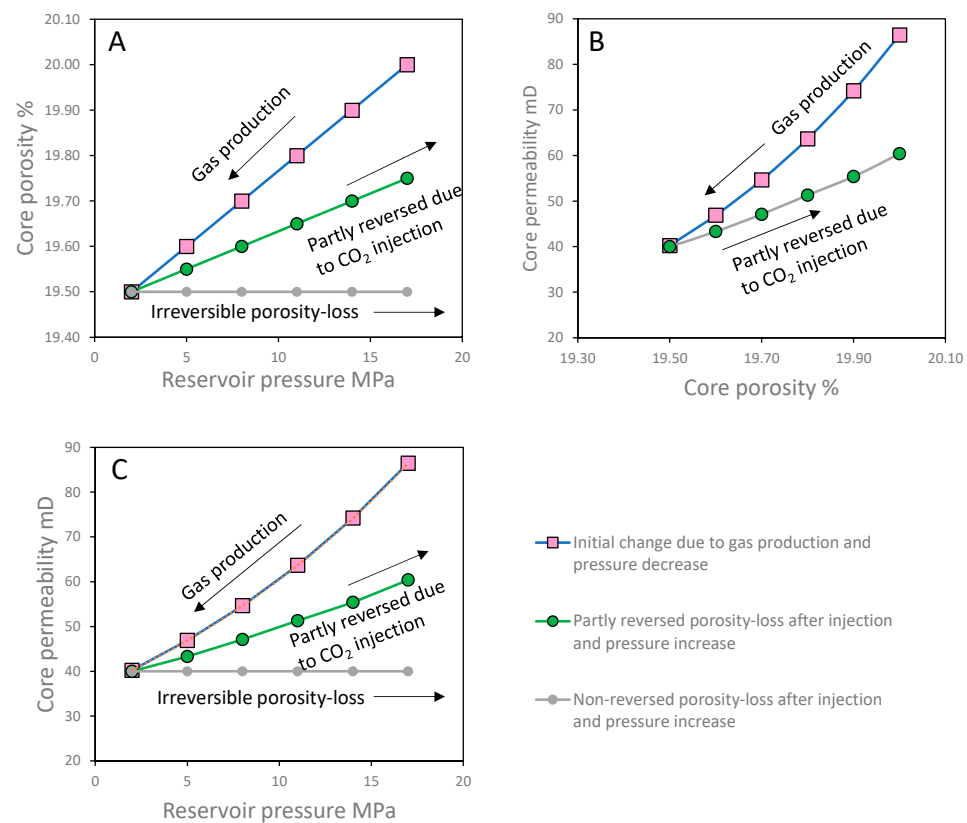


Figure 13. Suggested range of evolutionary paths of porosity and permeability with changing pressure due to initial gas production and then CO₂ injection, modified from Akai, Saito, Hiyama and Okabe [86]. (A) Porosity change with reservoir pressure; compaction due to depressurisation here initially occurred at the rate of $1.25 \times 10^{-3} \text{ MPa}^{-1}$ leading to a 0.5% decrease in porosity for a 15 MPa pressure decrease. Two paths are illustrated, one with minor reversal of the porosity loss at a rate of $6.25 \times 10^{-4} \text{ MPa}^{-1}$ leading to a 0.25% increase in porosity for a 15 MPa pressure increase; the other experienced no porosity increase as the production-related compaction was permanent (irreversible). (B) Permeability change with reservoir pressure linked to the porosity changes illustrated in (A). Gas production, in this model, led to a significant decrease in permeability, presumably as the biggest pore throats collapsed first. One type of response is that CO₂ injection partly reinflated the rock and presumably reopened some of the collapsed pore throats and permeability increased to some degree; another type of response is that the compaction was permanent, and permeability did not increase as pressure increased due to CO₂ injection. (C) Comparison of the porosity-permeability evolutionary paths due to gas production and CO₂ injection, illustrated in (A,B).

5.11. Geomechanical Evolution and Stress Paths in Saline Aquifers and Depleted Gas Fields

As well as the dilation of reservoirs, increasing fluid pressure in depleted gas fields has been linked to microseismic activity due to fluid pressure-related shear failure. Rock failure can be related to shear and effective normal stress values and evolving fluid pressure via a Mohr's circle construction (Figures 14 and 15). The Mohr's circle joins, as an arc, the maximum (σ_1) and minimum (σ_3) effective stresses for a rock on a diagram of effective normal stress versus shear stress. In normal extensional or quiescent basins, σ_1 is equivalent to vertical effective stress (σ_v), and σ_3 is equivalent to minimum horizontal stress (σ_{hmin}). Stability occurs when the range of stresses remains lower than the failure envelope which is defined by the friction coefficient (which describes the slope) and the cohesion (defined as the intercept of the failure envelope with the shear stress axis at zero effective normal stress). The cohesion (intercept) for a fault is routinely assumed to be zero so that the failure envelope is lower for faulted rocks than for intact rocks. Failure by shear (on the right-hand side of the diagrams in Figures 14 and 15) or tensional failure (on the left-hand

side of these figures) can occur when some part of the Mohr’s circle plots on, or above, the failure envelope. Effective normal stress increases if fluid pressure decreases so that the Mohr’s circle moves to the left, e.g., during the production of natural gas. Conversely, effective normal stress decreases if fluid pressure increases so that the Mohr’s circle moves left (in Figures 14 and 15) towards the failure envelope, for example during the injection of CO₂. Based on poroelastic theory, vertical effective stress changes by the full extent of fluid pressure change, whereas minimum horizontal stress changes by a lesser amount influenced by the Poisson’s ratio of the rock [118]. The rate of change of minimum horizontal stress ($\Delta\sigma_{hmin}$) with changing fluid pressure (ΔP_f) is controlled by the Biot coefficient (α) and the Poisson’s ratio (ν) [118]:

$$\frac{\Delta\sigma_{hmin}}{\Delta P_f} = \alpha \cdot \left(\frac{1 - 2\nu}{1 - \nu} \right) \tag{1}$$

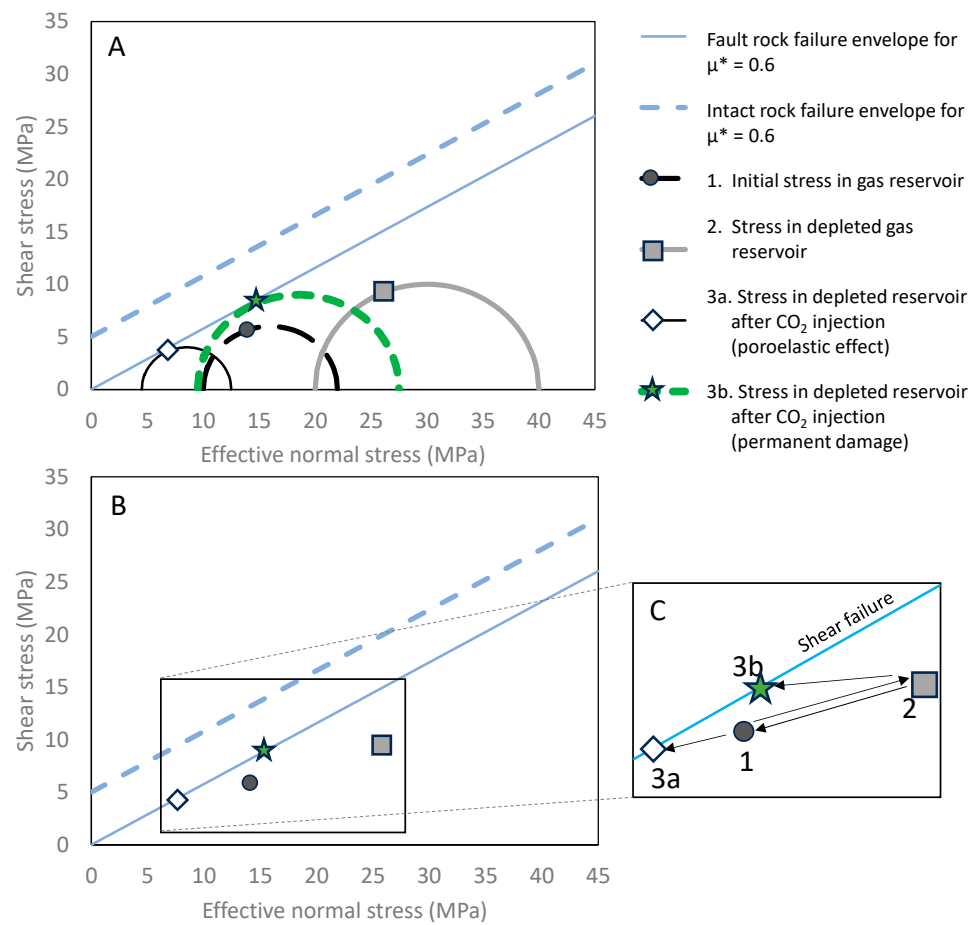


Figure 14. Effective normal stress versus shear stress diagram for a depleted gas field, modified from Orlic [10]. (A) Diagram with full Mohr’s circle constructions for the initial reservoir, after depletion, and two scenarios following re-pressurisation by CO₂ injection. (B) Like part (A) but only with potential contact points between the Mohr’s circles and the failure envelope shown. (C) Like part (B) but enlarged showing the range of possible stress paths. The failure envelopes for intact rock and fault rock are shown, both with a friction coefficient (μ^*) of 0.6. In this example, the initial effective stress states of system (σ_{hmin} and σ_v) both increase as the fluid pressure decreases but in comparing Mohr’s circle 1 to 2, it is apparent that σ_{hmin} does not increase by as much as σ_v due to poroelastic effects [10,118].

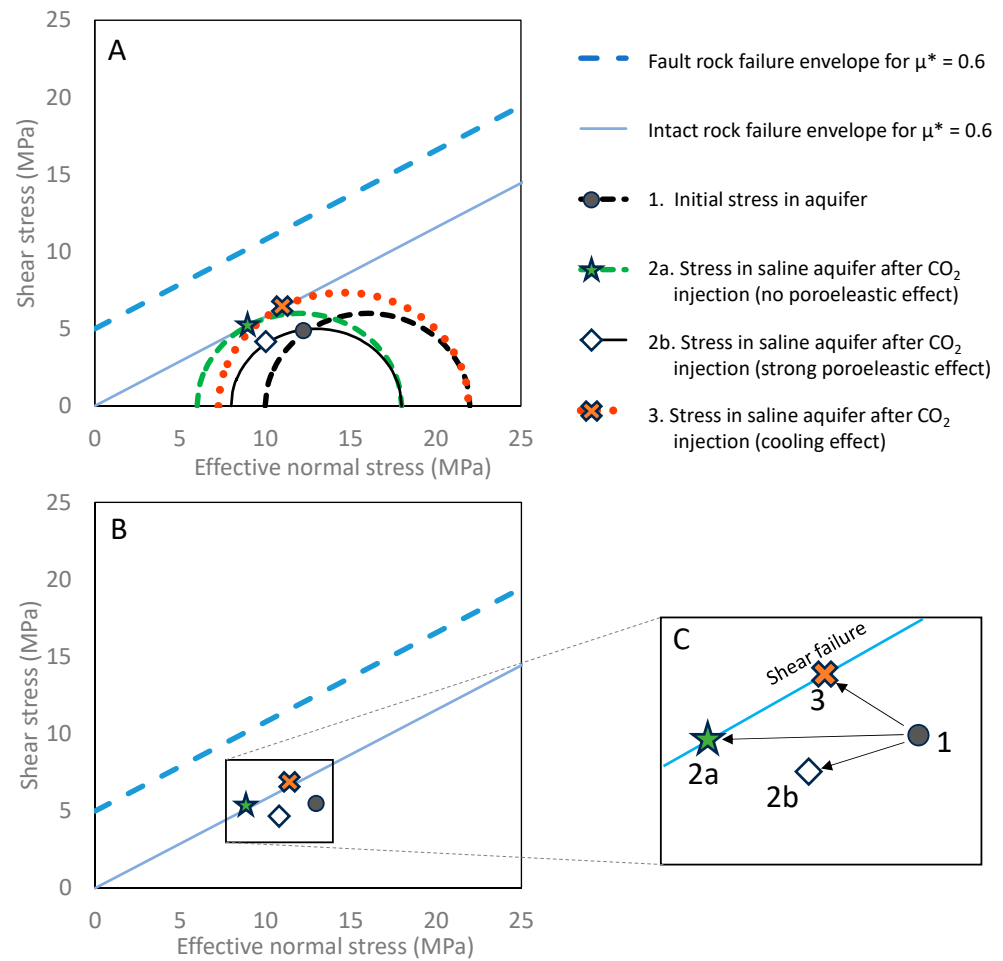


Figure 15. Effective normal stress versus shear stress diagram for a saline aquifer, modified from Orlic [10]. (A) Diagram with full Mohr’s circle constructions for the initial saline aquifer, after two scenarios following pressurisation by CO₂ injection and a scenario mimicking the effects of cooling and thermal stress due to the injection of relatively low-temperature CO₂ into an aquifer. (B) Like (A) but only with potential contact points between the Mohr’s circles and the failure envelope shown. (C) Like (B) but enlarged showing the range of possible stress paths. The failure envelopes for intact rock and fault rock are shown, both with a friction coefficient (μ^*) of 0.6.

The Biot coefficient is typically assumed to be 1 [119]. The Poisson’s ratio is represented by lateral strain divided by longitudinal strain and is a fundamental geomechanical property that can be defined by high-quality wireline logs [120] or laboratory-based studies. High Poisson’s ratio rocks (e.g., 0.3) tend to be characteristic of poorly cemented materials such as shallow buried sandstones [119]. Low Poisson’s ratio rocks (e.g., 0.15) tend to be typical of well-cemented materials such as quartz- or calcite-cemented sandstones [121]. The Poisson’s ratio defines the changing diameter of the Mohr’s circle as pore fluid pressure changes and the stress path [10,122,123].

In actively depleting gas fields, the Mohr’s circle moves to the right of the diagram and gets bigger as fluid pressure decreases and σ_3 (σ_{hmin}) changes by less than σ_1 (σ_v) (Equation (1)). Under some conditions, depressurisation can result in shear failure if the Mohr’s circle meets the failure envelope. Figure 14 shows a rock where the Mohr’s circle moves to the right and gets slightly further from the failure envelope suggesting that shear failure would not have occurred during depletion in this case (Figure 14, curve 1 to curve 2). During re-pressurisation resulting from injection of CO₂, it is possible that the stress path simply reverses what happened during depressurisation, in which case, shear failure can occur at elevated pore fluid pressures, due to CO₂ injection, that is higher

than the original reservoir pressure (Figure 14, curve 3a) [10]. Alternatively, if there had been permanent compaction during depressurisation, then the stress path is likely to be weaker (flatter). If there had been a permanent change in the rocks during depressurisation, then the intersection with the failure envelope, and thus shear, potentially happens at a lower degree of fluid pressure increase than if there had been elastic deformation during depressurisation (Figure 14, curve 3b). This suggests that understanding the result of depressurisation on reservoirs is of renewed interest now that they are to be used for CO₂ storage and undergo re-pressurisation. More research needs to be undertaken on the effects of depressurisation on rock properties.

Saline aquifers do not have a long history of pre-injection fluid pressure change, but they still respond to CO₂ injection in a manner controlled by geomechanical properties (Figure 15). If there is little or no poroelastic effect in a saline aquifer, then increasing CO₂ fluid pressure can cause intersection of the Mohr's circle with the failure envelope and thus shear failure of fault rocks (Figure 15, curve 2a). If there is a significant poroelastic effect, then σ_{hmin} will not decrease by as much as σ_v and thus intersection of the moving Mohr's circle with the failure envelope will be unlikely unless extreme CO₂ pore pressures are imposed (Figure 15, curve 2b). Thermal effects, resulting from the injection of low-temperature CO₂ into a higher-temperature aquifer (Figure 15, curve 3), may lead to decreasing σ_{hmin} for invariant σ_v and thus intersection of Mohr's circle with the failure envelope and thus shear failure of fault rocks.

The differences between depleted gas fields and saline aquifers, in terms of the geomechanical stress paths during CO₂ injection, arise from the lack of pre-CO₂ pressure decrease in saline aquifers. This may have effects on the response of the rock to CO₂ injection. It is not yet well-defined whether depressurisation weakens reservoirs and leads to shear failure as fluid pressure increases due to CO₂ injection. Rocks that undergo inelastic (permanent) compaction during depressurisation may likely be susceptible to shear failure at lower fluid pressures during re-pressurisation than those that do not undergo inelastic (permanent) change. There are few case studies to guide us at this stage, but re-pressurisation of depleted gas fields needs to be carefully monitored (e.g., with microseismic techniques, Table 2). However, CO₂ injection into saline aquifers also needs to be carefully monitored; there are numerous case studies where microseismic activity has been reported in saline aquifers, presumably due to shear failure (In Salah, Quest, and numerous CO₂-EOR projects; Table 2), although it is worth noting that some case studies seem not to have had seismic activity reported suggesting minimal shear failure (e.g., Sleipner, Snøhvit, Ketzin; Table 2).

Table 2. Synthesis of microseismic activity and implied shear failure in various reservoirs used for CO₂ injection (CCS represents dedicated greenhouse gas mitigation projects, EOR represents enhanced oil recovery projects, and CCS pilot represents confidence-building demonstration projects).

CCS Reservoir and/or Field	Type	Seismic Activity Reported	Comments	Reference
Sleipner, Norway	CCS	No	No seismic events seem to have been reported	Non-reported
Snøhvit, Norway	CCS	No	No seismic events seem to have been reported	Non-reported
In Salah (Krechba), Algeria	CCS	Yes	Reservoir fracturing occurred as well as ground uplift due to reservoir dilation. Magnitude from -1 to 1	White and Foxall [124]
Quest, Canada	CCS	Yes	Reservoir fracturing occurred as well as ground uplift due to reservoir dilation.	Harvey, O'Brien, Minisini, Oates and Braim [68]

Table 2. Cont.

CCS Reservoir and/or Field	Type	Seismic Activity Reported	Comments	Reference
Weyburn, Canada	EOR	Yes	Seismic activity occurred but no problems. Magnitude from -3 to -1	White and Foxall [124]
Aneth, USA	EOR	Yes	Seismic activity occurred but no problems. Magnitude from -1.2 to 0.8	White and Foxall [124]
Cogdell, USA	EOR	Yes	Seismic activity occurred but no problems. One magnitude 4.4 , 18 magnitude > 3 events over 6 years	White and Foxall [124]
Decatur, USA	CCS pilot	Yes	Seismic activity occurred but no problems were encountered with the top seal. Magnitude from -2 to 1	White and Foxall [124]
Rousse (Lacq), France	CCS pilot	Yes	Magnitude 2 earthquakes reported	Payre, Maisons, Marble and Thibeau [48]
Heletz, Israel	CCS pilot	No	No seismic events seem to have been reported	Non-reported
Ketzin, Germany	CCS pilot	Probably no	No definitive seismic events seem to have been reported (some suspected)	Paap, et al. [125]

5.12. Risk of Halite-Scale Impacting Injectivity in Saline Aquifers and Depleted Gas Fields

Some saline aquifers utilised for CO₂ storage, such as at the Snøhvit and Quest CCS sites, have been reported to have problems with halite-scale forming in the near-wellbore zone [126,127]. This build-up of crystalline material in the reservoir has been shown to have a detrimental effect upon flow properties which may affect the rate at which CO₂ can be injected, and consequently on the effectiveness of a given CCS project [126]. Halite precipitation in saline aquifers has also been demonstrated experimentally when CO₂ has been fluxed through brine-filled core plugs [128,129].

CO₂ has a limited miscibility with H₂O but it can dissolve about 1% H₂O by weight at 80 °C and 10 MPa [98]. When anhydrous CO₂ is injected into porous rocks bearing saline water (Figure 16A), there will be a finite degree of evaporation of water into the CO₂ (Figure 16C), up to the point at which the CO₂ is saturated with water [130]. This causes the remaining saline brine to become more concentrated with its dissolved load. Almost all formation waters are dominated by sodium, as the dominant cation, and chloride, as the dominant anion [131,132]. Therefore, when anhydrous CO₂ is continually fluxed through the porous aquifer, and as salinity increases due to water evaporation, the formation water may start to approach halite saturation. Once saturation has been exceeded, crystalline halite will start to develop. Porous rocks are assumed to be water-, as opposed to CO₂-, wet [50], so that there will be a film of brine on all mineral surfaces. It could be assumed that halite would develop as some sort of thin conformal coat on mineral surfaces, perhaps similar to other diagenetic mineral coats, such as chlorite or microcrystalline quartz, found in some reservoirs [89,133]. When water evaporates into the CO₂ near the injection well, the brine from the aquifer flows towards the well via the thin aqueous film that adheres to grain surfaces. This is known as capillary back-flow [12,106] as the Na- and Cl-ion-bearing aqueous flow occurs in the opposite direction to the flux of CO₂. This process feeds the components required to create halite in the vicinity of the injection well. The consequence of this chain of events is that halite develops as dense clusters in pore throats, in relatively close proximity to the injection well (Figure 16B), thus locally reducing permeability and inhibiting the injection of CO₂ [106].

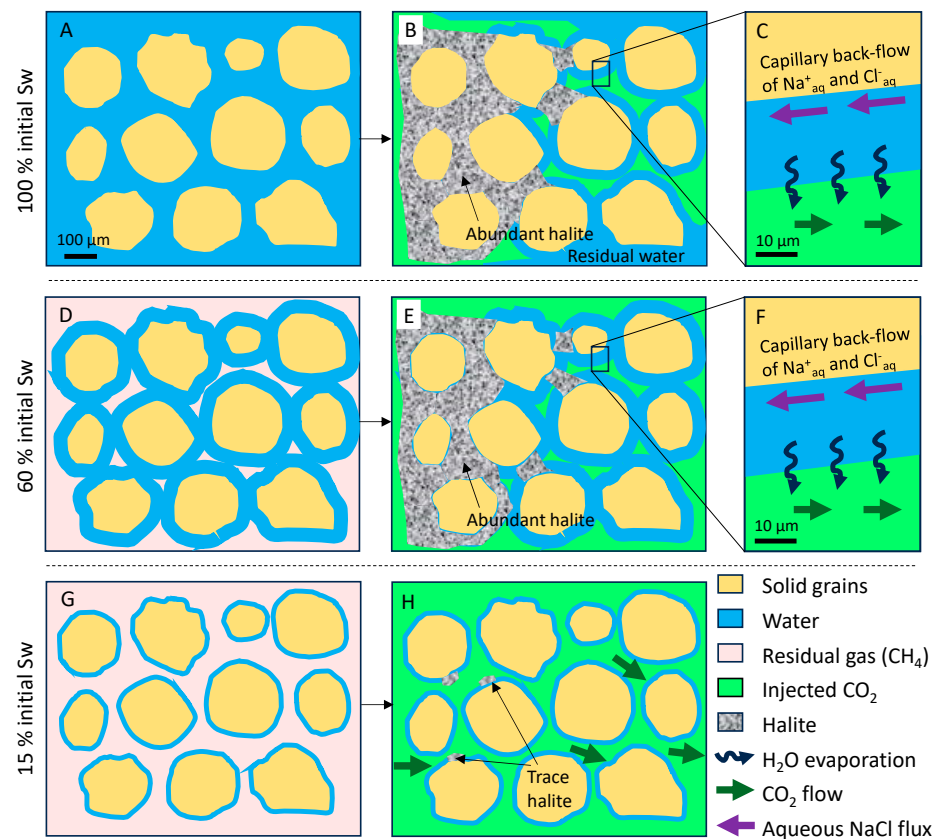


Figure 16. Schematic diagrams representing the likelihood of halite precipitation from saline brines associated with saline aquifers, high-residual-water-saturation depleted gas fields, and low residual water saturation depleted gas fields, partly based on Giorgis, Carpita and Battistelli [134]. (A) Initial saline aquifer with water salinity $>150,000$ mg/L. (B,C) The same saline aquifer as (A) but after CO_2 injection (from the left). There will be locally high residual water saturation and thick films of bound water on water-wet grain surfaces even after CO_2 injection. H_2O from the brine evaporates into the anhydrous CO_2 leaving the residual water at ever increasing salinities. Halite starts to precipitate once the local brine has exceeded halite saturation. There is a capillary back-flow of brine, including the dissolved Na^+ and Cl^- , from right to left, as halite precipitates and transiently, locally, leaves the water close to or at halite saturation. This leads to mass halite precipitation towards the injection well and thus a significant skin effect and reduced injectivity. (D) Initial depleted gas field with high residual water saturation (about 60%), where the water salinity $>150,000$ mg/L. (E,F) The same depleted gas field as (D) but after CO_2 injection (from the left). Although the depleted gas phase will be swept by the injected CO_2 , it is not impossible that there will be high residual water saturation, as there was in the depleted gas field. In this regard, a depleted gas field with a high residual water saturation may behave in a similar manner to saline aquifers. H_2O from the brine evaporates into the anhydrous CO_2 leaving the residual water at ever-increasing salinities, with halite precipitation, supported by capillary back-flow of brine, and the dissolved Na^+ and Cl^- , leading to mass halite precipitation, a significant skin effect and reduced injectivity. (G) Initial depleted gas field with low residual water saturation (about 15%), where the water salinity $>150,000$ mg/L. (H) The same depleted gas field as (G) but after CO_2 injection (from the left). The depleted gas phase will be swept by the injected CO_2 and the low residual water saturation will remain. Minimal halite will form due to inhibited capillary back flow and the relative lack of the aqueous medium needed to grow halite.

Halite scale is likely to be an issue in saline aquifers with high salinity brines. The halite-scale-affected Quest site had salinities of 294,000 mg/L, or approximately 27% salinity [25]. The halite-scale-affected Tübaen Formation at the Snøhvit CCS site had about 14% salinity [126]. Aquifer salinity values lower than this may also lead to halite-scale but there

is not yet a cut-off below which salinity and halite scale may not lead to injectivity problems that require systematic and regular remediation treatments. The problem of halite-scale and injection rate reduction has been dealt with in practice by periodic injections of methyl ethyl glycol (MEG) [126] or periodic injections of water [127]. MEG forms complexes with sodium and chloride ions, thus increasing their aqueous solubility and inhibiting halite-scale formation. MEG also modifies the crystal surfaces of halite by binding to the crystal faces and disrupting the normal orderly addition of ions needed for crystal growth. Injections of water will cause the dissolution of any halite that has formed, pushing the ions away from the injection well. The problem of halite scale can therefore be overcome but there will be a need to consider the minor cost implication, well design and slightly reduced time for CO₂ injection when these treatments are being undertaken.

Gas fields, before any production has happened, tend to have relatively low (water) brine saturations, typically in the range of 5 to 15% at the maximum. When the gas is produced there is, in some cases, a small amount of aqueous condensate produced but most of the residual brine will remain in place, clinging to grain surfaces and associated with clusters of fine-grained and microporous clay minerals. Thus, by the time the field has been depleted of hydrocarbons, there will still be about 5 to 15% of the pore volume filled with brine that still occurs as thin films on grain surfaces. The role of the residual brine fraction in depleted gas fields was examined by Giorgis, et al. [134], who showed by modelling that at a very high value of 60% S_w (brine saturation), then there is still a strong capacity to allow halite to develop as dense clusters of minerals in the vicinity of a CO₂ injector well, just as it does for saline aquifers (Figure 16D–F). The 60% of residual brine permitted capillary back-flow, as happens in saline aquifers. Conversely, Giorgis, Carpita and Battistelli [134], showed that a more typical 15% S_w did not lead to capillary back-flow as there was insufficient water to permit a substantial flux of sodium and chloride ions towards the injector well (Figure 16G,H). Instead, it is likely that the thin film of brine progressively evaporated into the injected CO₂ and so reached halite saturation, but instead of permitting a flux of ions, the halite simply precipitated as a thin film in situ, leaving pore throats little reduced and CO₂ injectivity unaltered.

In summary, saline aquifers with relatively concentrated brine may be susceptible to treatable formation damage due to halite precipitation. In contrast, a depleted gas field with a typically low residual brine saturation (15%) is unlikely to lead to excessive halite precipitation as there will be less dissolved NaCl per unit volume of rock (as there is less brine) and as the thin film of brine on grain surfaces will inhibit capillary back-flow.

5.13. Feasibility of Geochemical Processes in Saline Aquifers and Depleted Gas Fields

There has been substantial focus on mineral processes in CO₂ storage sites, not least because the conversion of fluid-phase CO₂ into solid-phase carbonate minerals offers the safest way of locking CO₂ in the subsurface with negligible opportunity for escape [2]. An initial hope was that CO₂-water-rock interaction would lead to a substantial fraction of the injected CO₂ being locked up as new carbonate minerals within a few thousand years.

Much early effort was focused on examining natural analogues of subsurface reservoirs that contain large quantities of CO₂, such as CO₂-rich gas and oil fields, and nearly pure natural CO₂ accumulations such as Bravo Dome, New Mexico [135–137]. These natural analogue studies demonstrated that some CO₂ can be locked up as minerals, but much can remain in the fluid phase. There is now an additional focus on the effect of CO₂ on mineral dissolution processes as this can fortuitously lead to enhanced porosity and permeability but with consequences for weakening of rocks and altered risks of shear failure [138].

Saline aquifers will naturally retain relatively high brine saturations since the overall storage efficiency of saline aquifers will fall somewhere between 0.02 and 0.20 (2 and 20%), as described in Section 5.7. If only 2 to 20% of the pores are filled with CO₂, then between 80 and 98% of the pores must be filled with remaining brine. This means that there will be much brine to catalyse CO₂-mineral interactions within the CO₂ accumulation. In detail,

even where CO₂ is present, there will be a residual brine film on grain surfaces since minerals are water-wet rather than CO₂-wet [50].

One of the issues with mineral trapping of CO₂ as minerals is that there must be a plentiful supply of divalent cations such as iron, magnesium, or calcium that are not already locked up as pre-existing carbonate minerals, such as calcite, dolomite, or siderite. There may be a limited amount of these cations in the brine, but most of these divalent cations will have to be supplied by iron, magnesium, or calcium silicate-bearing minerals, and to a lesser extent from Fe-oxides. Most calcium in sedimentary rocks exists within calcite and dolomite which are inevitably incapable of creating new carbonate minerals, as the calcium is already within a carbonate mineral. Calcium sulphate minerals (anhydrite and gypsum) are stable in the presence of high concentrations of CO₂ and cannot provide calcium to precipitate new calcite. Calcium feldspar (anorthite) has been used in modelling studies to simulate the effect of CO₂ injection in sedimentary rocks [139,140] but this misses the key point that calcium feldspar is not stable at, or near, the Earth's surface; during weathering of Ca-feldspar-bearing rocks such as basalt or andesite (or metamorphic equivalents), anorthite breaks down so quickly that it is relatively rare in modern or ancient clastic depositional environments and the sedimentary rocks that are result from burial and diagenesis [141]. Anorthite, or any form of Ca-feldspar, should not be counted on to allow mineral sequestration of injected CO₂ as it is absent from most sandstones, siltstones and mudstones. Magnesium and iron also mainly exist as carbonates (dolomite and siderite) but they may also be present within clay minerals such as chlorite and glauconite [142]. Smectite may also be capable of supplying iron, magnesium, or calcium [143] to help create new carbonate minerals and lock up some of the injected CO₂, but smectite is not common in most reservoir rocks.

Rates of reaction are another important consideration in an assessment of CO₂-rock interactions. It has been demonstrated that calcite dissolution can occur in experiments [128,144,145] or engineering timescale at CO₂-EOR sites [4,146,147]. Calcite dissolution increases the porosity of the rock formation where CO₂ is being injected; as calcite dissolves, pore spaces are created or enlarged, providing pathways for CO₂ to flow more easily through the rock [4,145]. Dissolution of calcite can also alter the permeability of the rock. Higher dissolution rates can lead to increased permeability, which could enhance the injectivity of injected CO₂ [56,144,148]. The rate of dissolution of calcite can be assessed by geochemical modelling using appropriate kinetic constants and the textural parameter that dictates exposed reactive surface area [149,150]. For the growth of new carbonate minerals that trap the injected CO₂, there must be a supply of cations, mainly from silicate minerals. Thus, carbonate precipitation will probably be rate-limited by the speed at which silicate dissolution occurs (rate of delivery of cations) rather than the rate at which carbonate precipitation occurs. Herein lies the problem with any models that rely on CO₂ mineral trapping in conventional sedimentary reservoirs. Silicate dissolution rate constants are approximately five to seven orders of magnitude smaller than carbonate rate constants [150], thus if a carbonate dissolution reaction needs a few years to happen (e.g., during CO₂-enhanced oil recovery), a linked silicate dissolution reaction may take millions of years to be effective. This is perhaps not a surprise as natural diagenetic reactions have millions of years to proceed.

One puzzling exception is the mineral dawsonite [151], which is a sodium-aluminium carbonate reported from a few deeply buried sandstones [152]. From modelling studies, dawsonite has routinely been shown to be a common reaction product of CO₂ injection to rocks with Na-rich saline brines or those rich in Na-feldspar (albite). However, the thermodynamic constants for dawsonite used in geochemical modelling routines may not be correct and the kinetic constants used to model dawsonite are almost certainly incorrect as they are typically assumed to be similar to the rate constants of alkaline earth carbonate minerals such as calcite [151]. These two issues lead to some doubts about the plausibility of dawsonite as a routine way to trap CO₂ in a new mineral form at CCS sites.

In a saline aquifer, where the water is saturated with CO₂ due to CO₂ injection, geochemical reaction rates will be controlled by kinetic rate constants, grain size, degree of exposure of reactive minerals (extent of reactive surface area), and temperature [149,150]; for

example, calcite cement dissolution, detrital chlorite dissolution and the linked precipitation of Fe- and Mg-carbonate (Figure 17A,B). The presence of abundant aqueous pore fluid will possibly allow diffusive or even advective transport of newly dissolved species. It is likely that the newly reduced pH that occurs when CO₂ partial pressure suddenly increases will lead to an initial phase of dissolution of calcite (Figure 17B). On a longer timescale, there may be dissolution of chlorite (supplying Fe and Mg). The elevated aqueous CO₂ plus the elevated concentrations of Mg and Fe might lead to late-stage siderite precipitation, hosted on the calcite substrate, as reported by Forster, et al. [153] from the Ketzin CCS pilot site. Thus, the initial dissolution of calcite may be followed by the precipitation of subsequent carbonate minerals. It seems unlikely that a saline aquifer such as that represented in Figure 17A,B could lead to significant mineral trapping of CO₂ and it is more likely to lead to a small degree of carbonate dissolution.

In contrast, the typically low water saturation of depleted gas fields (as low as 5 to 15% of pore space filled with water; Figure 17C and Section 5.12) will lead to slow or negligible rates of reaction. While geochemical reactions such as calcite and chlorite dissolution are theoretically feasible based on thermodynamic driving forces, the lack of the essential aqueous medium required for CO₂-mineral reactions and the tortuous path that needs to be traversed between potential reactants means that CO₂-mineral reactions are generally unlikely to occur to any advanced degree in depleted gas fields (Figure 17D). Interestingly, the reactive surface area of minerals is likely to be similar in saline aquifers and depleted gas fields; the difference between them is the volume of reactive aqueous medium that minimises diffusive transport rates in depleted gas fields compared to saline aquifers. Thus, while for the rock illustrated in Figure 17C,D, calcite, chlorite, and plagioclase dissolution and even siderite precipitation are all thermodynamically possible and the reactive surface area is the same, the kinetics of dissolution and especially transport in low residual water saturation depleted gas fields, used for CO₂ storage are likely to be prohibitively slow.

Overall, mineral reactions even in saline aquifers, are likely to be relatively slow and there is unlikely to be any significant (e.g., 10 to 20% of injected CO₂) mineral trapping of CO₂ in real (i.e., plagioclase-free) reservoirs. Saline aquifers are more likely to undergo a small amount of calcite dissolution rather than new calcite precipitation. Depleted gas fields, especially Type 1 (Figure 3), with their paucity of brine, will have even less opportunity to undergo mineral trapping of CO₂ and there will be even less likelihood of large-scale dissolution of pre-existing carbonates.

5.14. Water Flow and Pressure Management via Water Production

Pressure management must be used in saline aquifers to limit the degree of fluid pressure increase, specifically to try to avoid exceeding fracture pressures (Figure 2) [17]. The need to carefully monitor and control fluid pressure in saline aquifer CCS projects was recognised following Snøhvit and In Salah CCS projects [13,154]. It has been reported that the Gorgon saline aquifer CCS project uses water production to try to minimise fluid pressure increase due to CO₂ injection and so presumably keep fluid pressure below the fracture gradient [22,23]. Due to the relative lack of water in depleted gas fields (especially Type 3 depleted gas fields, Figure 3), it seems unlikely that pressure management using water production will be employed for depleted gas field CCS projects.

The role of natural water flux in open saline aquifers was modelled showing that an active aquifer causes horizontal attenuation but reduces the vertical migration, of the CO₂ plume [155]. Most depleted gas fields will not have active aquifers influencing CO₂ movement patterns due to the trap configuration. This lack of influence of water flux in the aquifer will be strongest of all in Type 1 depleted gas fields (no aquifer support).

5.15. Relative Risk of Leakage of CO₂ in Saline Aquifers and Depleted Gas Fields

Avoiding leakage of CO₂ from CCS sites is of paramount importance; there is no merit in spending energy in injecting CO₂ underground if it simply escapes to the surface. However, if even a small amount of leakage occurs, such as 0.1% per annum, then the

vast majority (90%) of the CO₂ will have escaped within 2000 years [156]. Minimising risk means being aware of the factors that may potentially lead to the escape of CO₂ [57]. Saline aquifers and depleted gas fields have some risk factors in common, but they also have their own unique risks to consider.

Saline aquifers have risks of CO₂ leakage (Figure 18A) predominantly linked to fault reactivation (Figure 15) [157], induced fractures in the top-seal [118], reservoir dilation due to elevated pressure potentially leading to de-bonding of the liner and cement of the well to the rock formation [158], thermal (shrinkage) effects in the reservoir close to the injection well [157], and corrosion of the cement and liner in the injection well and other wells through the aquifer [159].

Depleted gas fields (Figure 18B) are likely to have far more boreholes drilled into them than saline aquifers. One of the biggest risks of CO₂ leakage will be the large number of potentially leaky well penetrations into the subsurface [57,60,61]. Depleted gas fields also have a unique set of risks linked to the geomechanical consequences of depletion including shear stresses at the reservoir seal interface, reactivation of faults due to reservoir compaction, and de-bonding the well (liner and cement) from the reservoir due to compaction [160]. There may also be hydraulic fractures in the top seal once CO₂ pressure exceeds the post-depletion strength of the seal [118], thermal effects in the reservoir close to the CO₂ injection well, and corrosion of cement and liner in the injection and other wells through the depleted gas field.

5.16. Monitoring Strategies in Saline Aquifers and Depleted Gas Fields

Monitoring subsurface CO₂ storage sites is required for a variety of purposes [50,161–163]. Monitoring is needed to establish such as the following:

- how much CO₂ is being injected for a given bottom hole pressure;
- the temperature in the subsurface;
- where the CO₂ has travelled to in the subsurface;
- if any geomechanical failure has occurred in the reservoir, the top-seal caprock or in the engineered environment;
- whether any uplift of the entire sediment column has occurred;
- what geochemical or biogeochemical processes have happened;
- if and how CO₂ has interacted with the materials used in well completions (tubing, cement, or liner);
- if the CO₂ has escaped to overlying porous beds or even to the surface.

The organisations involved in the injection of CO₂ need to know how to minimise the risk of escape of CO₂. The regulatory authority that oversees a given project, different in each country, will need to be reassured that the stated amount of CO₂ has been injected and that there are no increased levels of risk of escape of the CO₂, or any other problems [61]. Any organisation involved in trading carbon credits needs to be reliably informed of the amount of CO₂ disposed of. Monitoring, measurement, and verification are linked activities that will be a legal requirement of all CCS projects, whether they are in saline aquifers or depleted gas fields (Figure 19A,B).

Saline aquifer CCS sites have been monitored using a wide variety of techniques, some of which are listed in Table 1 (and see Figure 19). 3D and 4D seismic imaging have proved to be spectacularly successful at the Sleipner [50,62,167] and Snøhvit [16,126] CCS sites in Norway. The seismic imaging approach has revealed the details of plume movement and emphasised the importance of internal stratigraphy and lateral changes in permeability within defined sedimentary formations. Ringrose [50] suggested that 4D seismic provided the greatest benefit of all monitoring techniques despite the great cost. It has been suggested that seismic imaging may be much more difficult for depleted gas fields than saline aquifers due to the lack of a marked density difference or phase distinction at the early stages of a project when the CO₂ may be injected as a miscible gas into low-pressure reservoirs [63].

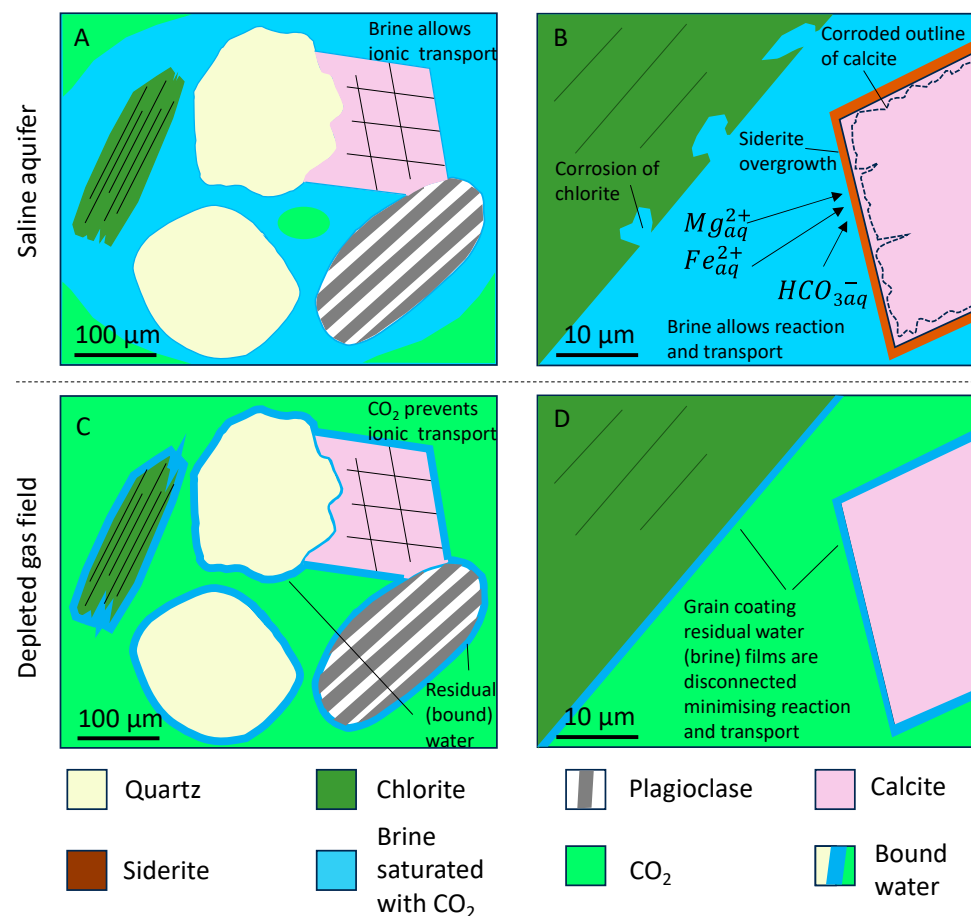


Figure 17. Schematic diagrams representing the effects of fluid type on geochemical processes on quartz-rich, feldspar- and chlorite clay-bearing, calcite-cemented sandstones that are saline aquifers and depleted gas fields. (A) Saline aquifer, where the water is saturated with CO_2 due to CO_2 injection. Geochemical reaction rate will be controlled by kinetic rate constants, grain size, exposure of reactive minerals, and temperature; for example, calcite cement dissolution, detrital chlorite, and feldspar dissolution, and potentially Fe- and Mg-carbonate and dawsonite precipitation. The aqueous pore fluid will allow diffusive or even advective transport of newly dissolved species. (B) Enlarged view of the saline aquifer from (A) where there was an initial dissolution of calcite as pH decreased due to the injection of CO_2 , followed by potentially much later dissolution of chlorite and consequent liberation of aqueous Mg and Fe. The elevated aqueous CO_2 plus the elevated concentrations of Mg and Fe led, in this case, to late-stage siderite precipitation, hosted on the calcite, as reported by Forster, Wilke, Block, Eisner, Forster, Norden and Schmidt-Hattenberger [153] from the Ketzin CCS pilot site. (C) The depleted gas field, with a low residual water saturation, where the low-pressure methane has been largely replaced by the injected CO_2 . While geochemical reactions are possible, the lack of water in the depleted gas field, and especially the tortuous path that needs to be traversed between potential reactants, means that reactions are generally unlikely to occur to any advanced degree. Thus while, for this rock, calcite dissolution, chlorite and plagioclase dissolution, and siderite and dawsonite precipitation are all thermodynamically possible, the kinetics of dissolution and transport in low residual water saturation depleted gas fields used for carbon storage may be prohibitively slow. (D) Details of the physical and geochemical disconnect between the thin films of water on neighbouring grains typical in depleted gas used for CO_2 storage. The medium for reaction (water) represents a small fraction (0.05 to 0.15) of the pore space and transport to, or from, reaction sites is largely impossible (in contrast to water-rich saline aquifers, as depicted in Figure 17B).

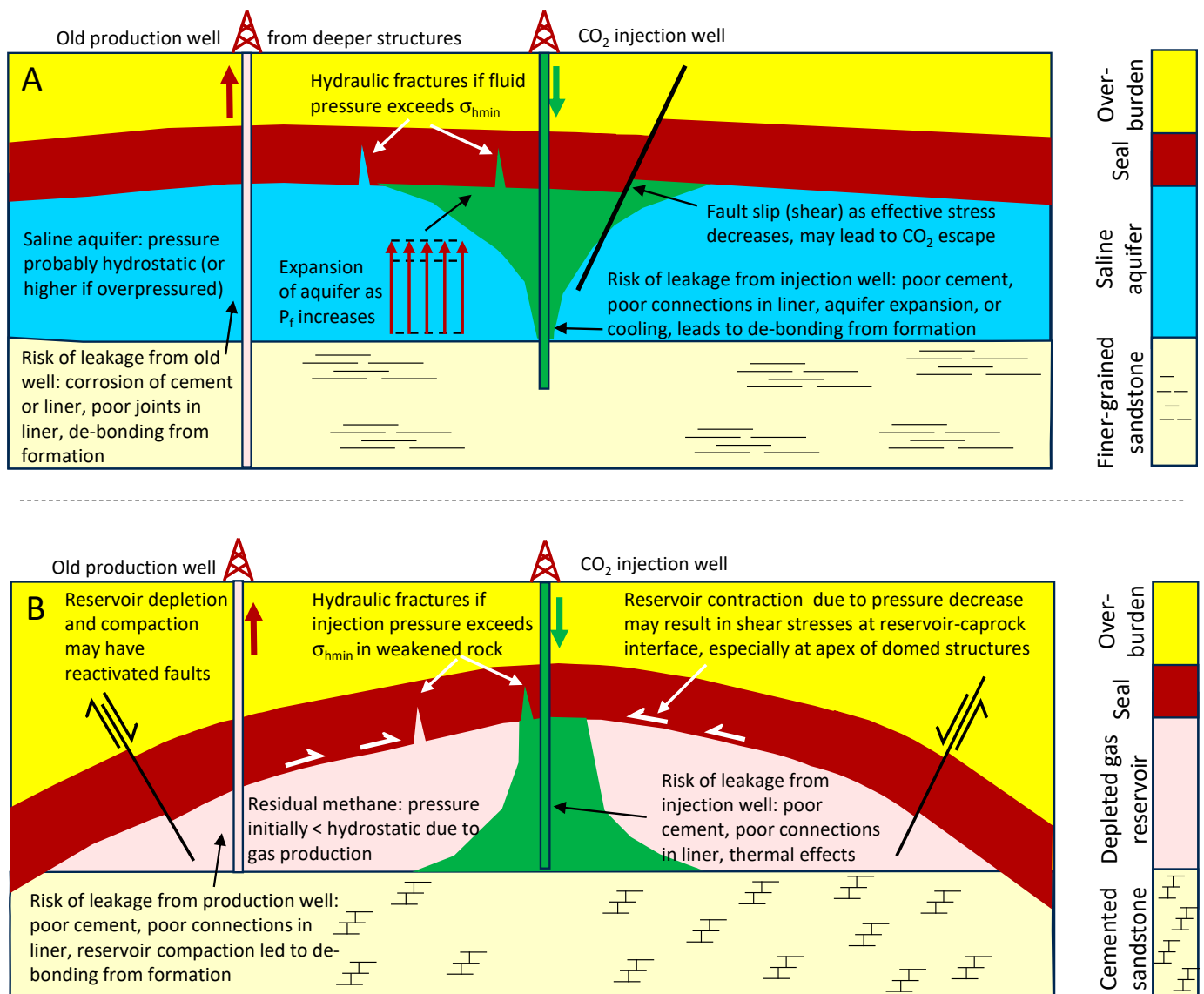


Figure 18. Factors influencing the risk of leakage in saline aquifers and depleted gas fields: green (down) arrow represents CO₂ injection, red arrows (up) represent the risk of fluid escape from old wells. **(A)** Saline aquifers, with risks linked to fault reactivation, induced fractures in the top-seal, reservoir dilation due to elevated pressure de-bonding the well, liner, and cement, thermal effects in the reservoir close to the injection well, corrosion of cement and liner in the injection well and other wells through the aquifer; modified from Gaurina-Medimurec and Mavar [164], Ringrose [50], Rutqvist, et al. [165], Rutqvist [157], Rutqvist, et al. [166]. **(B)** Depleted gas field, with risks linked to the geomechanical consequences of depletion including shear stresses at the reservoir seal interface, reactivation of faults due to reservoir compaction, de-bonding the well (liner and cement) from the reservoir due to compaction, modified from Hawkes, Bachu and McLellan [160]. There may also be hydraulic fractures in the top seal once CO₂ pressure exceeds the post-depletion strength of the seal, thermal effects in the reservoir close to the CO₂ injection well, and corrosion of cement and liner in the injection and other wells through the depleted gas field.

Cross-well or vertical seismic profiling requires at least a second well in addition to the injection well (Table 1). These options may therefore not be feasible in some of the smaller CCS projects in saline aquifers as there may only be one well (e.g., Sleipner). However, large saline aquifer CCS projects with multiple wells may be amenable to this approach (Figure 19A). It is possible that depleted gas fields, presumably with a host

of old exploration, appraisal, and production wells, will facilitate cross-well or vertical seismic profiling of the plume [65], especially once the depleted gas field has re-pressurised sufficiently to place the CO₂ in the supercritical phase giving it a density contrast to the remaining methane (Figure 19B).

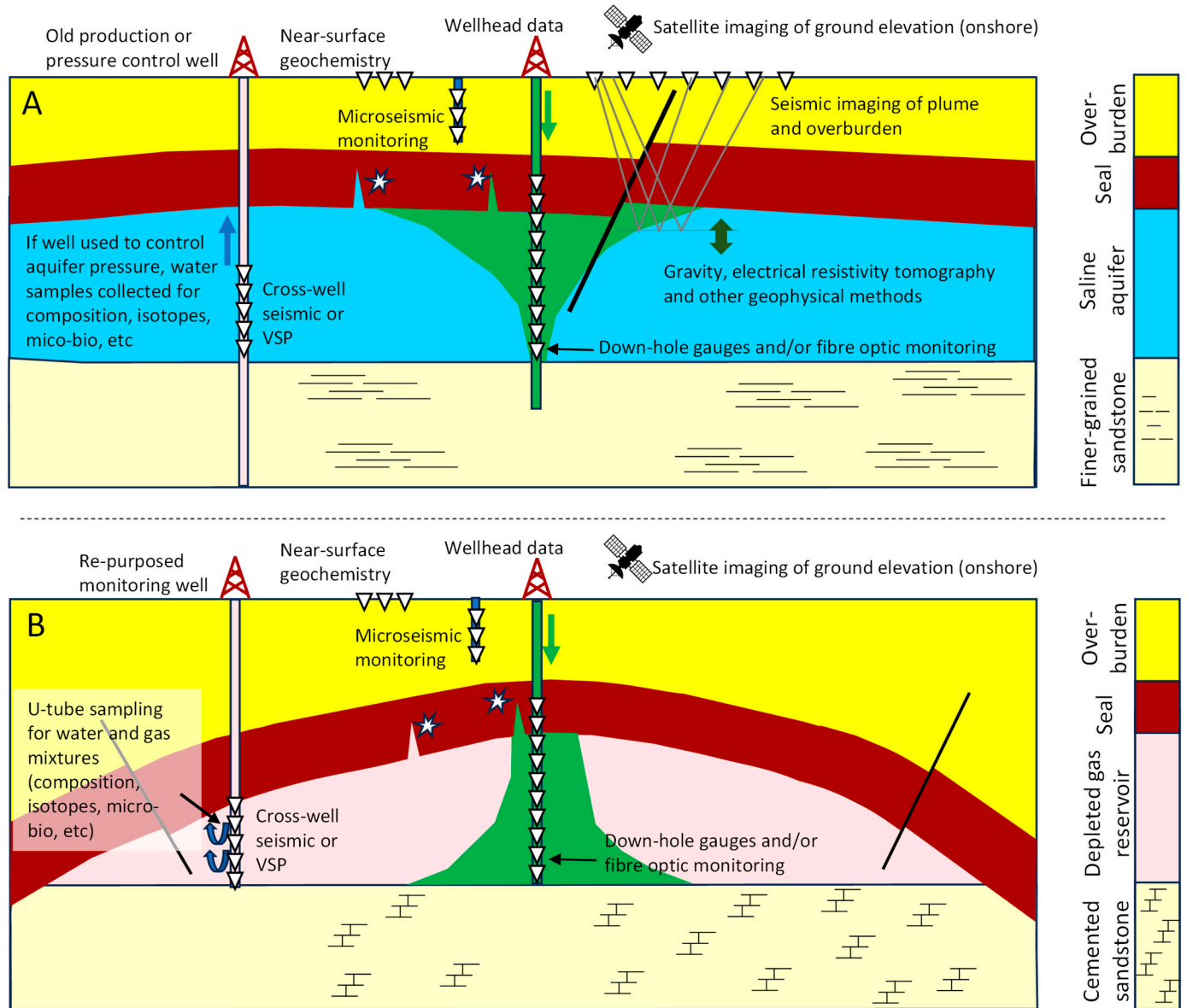


Figure 19. Common monitoring strategies that may be applied to saline aquifers and depleted gas fields: green arrow represents CO₂ injection, stars represent induced microseismic events. (A) Saline aquifer monitoring strategies, modified from Bergmann, Schmidt-Hattenberger, Labitzke, Wagner, Just, Flechsig and Rippe [66], Correa, et al. [168], Ringrose [50], Vasco, Rucci, Ferretti, Novali, Bissell, Ringrose, Mathieson and Wright [19], (B) Depleted gas field monitoring strategies, modified from Dean and Tucker [161], Freifeld, et al. [169], Utley, Martin-Roberts, Utting, Johnson, Györe, Zurakowska, Stuart, Boyce, Darrah, Gulliver, Haszeldine, Lawton and Gilfillan [77], Vandeweijer, van der Meer, Hofstee, Mulders, D’Hoore and Graven [72], Vasco, Rucci, Ferretti, Novali, Bissell, Ringrose, Mathieson and Wright [19].

Electrical resistivity tomography was successfully used in the Ketzin saline aquifer CCS pilot project [66] (Figure 19A). This works because there is a resistivity contrast between the pre-existing conductive saline brine and the injected non-conductive CO₂.

Electrical resistivity tomography seems to be unlikely to work in depleted gas fields as both the remaining methane and the injected CO₂ are non-conductive (Table 1).

Microseismic monitoring is a passive technique using permanent geophones, shielded from background vibration, for detecting rock failure events in the subsurface. It can reveal earthquakes of very low intensity (magnitude less than -2) and is likely to be used to assess the short-term effects of high fluid pressure on the integrity of both saline aquifers and depleted gas fields [20,48] (Figure 19A,B).

Monitoring of the rate of CO₂ injection and pressure and temperature at the point of injection of CO₂ into the reservoir will be required for all CCS projects. The rate of injection is needed to inform regulators and various stakeholders about the effectiveness of the project. Pressure data are needed to understand if there are formation damage issues [13] or if the CO₂ is unexpectedly not able to move away from the injection site to faulted-, stratigraphic-, or diagenetic-compartments [16].

Monitoring of the composition of the injected CO₂ is needed for both saline aquifer and depleted gas field CCS sites to ensure that the fluids fall within the safe parameters of the engineered part of the system (cement, tubing, liner) and are not excessively corrosive to the reservoir or top-seal caprock. CO₂ from industrial sources is unlikely to be pure CO₂; instead, it may contain acid gases, such as SO₂ or nitrogen-oxides, or reducing gases, such as H₂, H₂S, or even NH₃ [170]. The presence and amount of all contaminants being injected into the subsurface need to be checked regularly during injection [69].

Suites of distributed downhole sensors built into injection wells for both saline aquifer and depleted gas field CCS sites are likely to become routine as they maximise monitoring capabilities for a relatively low extra cost (Table 1; Figure 19A,B). Distributed acoustic sensors [71,171] and distributed thermal sensors [70] have already been employed. It seems likely that this technology will develop, and that new types of distributed downhole sensors will be developed.

Monitoring wells were used to great effect in CCS pilot projects, such as Cranfield, Heletz, Ketzin, and Nagaoka, that were designed to build knowledge and develop confidence in the plan for large-scale and long-term injection of CO₂ [34,172–174]. However, monitoring boreholes have not been routinely used in large-scale CCS projects in saline aquifers (e.g., Sleipner, Snøhvit, In Salah) due to the cost and the increased risk of leakage associated with additional well penetrations into the CO₂ storage domain (Table 1; Figure 19A). In contrast, depleted gas fields will have multiple pre-existing well penetrations that may offer opportunities for monitoring fluids and their pressures in the subsurface (Table 1, Figure 19B). Monitoring boreholes provide the opportunity to measure water and gas chemistry and stable isotope ratios to provide unique probes into chemical reactions in the CO₂ storage site. For example, one study revealed a substantial degree of methanogenesis (conversion of CO₂ into methane) by the microbial metabolization of the injected CO₂ during a CO₂-EOR project [6]. Noble gas concentrations and their isotopes provide another way to track processes at CO₂ injection sites and have been used to unequivocally refute suggestions that near-surface CO₂ was due to leakage from a CO₂-EOR project [79]. Novel U-tube sampling technology has been developed to allow fluids to be brought to surface from monitoring wells, thus allowing repeated analysis of gas and water geochemistry and stable isotope ratios [169].

Surface geochemical techniques have been used at both saline aquifer and depleted gas field CCS sites to demonstrate the lack of degree of leakage [78]. This approach will probably remain a requirement by regulators and will serve to placate any widespread societal anxiety about the escape of the injected CO₂. Atmospheric monitoring above continental projects will be important above CCS sites to demonstrate a lack of escape from the CO₂. Offshore projects require a different, seabed monitoring-based approach as any escaping CO₂ would potentially dissolve and disperse into the overlying water column [175,176].

Satellite-based ground surface elevation change monitoring, using such as InSAR [19], will probably be required at both saline aquifer and depleted gas field onshore CCS sites

whereas tiltmeters can be used, albeit less accurately, at offshore locations. Injected CO₂ led to about 30 mm of uplift at the In Salah saline aquifer CCS project in Algeria [177], which, in conjunction with elevated signals from microseismic monitoring, seemingly led to the authorities stopping the project. Onshore ground uplift can be determined with high precision by satellite monitoring. This option is not relevant to offshore projects, which instead will have to develop or use seabed-based technologies that are unlikely to be as accurate as onshore satellite methods.

6. Synthesis

Saline aquifer and depleted gas field CCS projects have several aspects in common, especially the need for characterisation and the objectives of monitoring, measurement, and verification. Both types need to have detailed models of the subsurface in terms of porosity and permeability distribution in the CO₂ storage domain. The internal architecture of the storage domain needs to be thoroughly understood for both saline aquifers and depleted gas fields to be able to predict how the CO₂ will move in the subsurface. Both need to have careful pressure management to minimise the consequences of the injected fluid on the security of the subsurface storage site. Top-seal caprocks at both saline aquifers and depleted gas fields need to be sufficient to hold the injected CO₂. The trapping mechanism for the injected CO₂ needs to be understood in both saline aquifers and depleted gas fields. Any old or abandoned wells that penetrate the host storage reservoir need to be assessed to ensure that they are not going to be routes for CO₂ escape to the surface. Saline aquifers and depleted gas fields need to be monitored before, during, and after CO₂ injection to track the movement and lack of release of the injected CO₂. Monitoring of fluid injection rate, fluid injection composition, bottom hole pressure and temperature, use of distributed sensors down the injection well, and microseismic monitoring all are possible and may be required at both saline aquifers and depleted gas fields.

The main differences between saline aquifers and depleted gas fields are summarised in Table 3. Saline aquifer and depleted gas field CCS projects will probably start with different knowledge bases about the subsurface with the latter having a wealth of information available about porosity, permeability, fault properties, internal stratigraphic and diagenetic baffles and barriers, and fluid flow history. Depleted gas fields have definitively had a working reservoir and top-seal caprock that have stored hydrocarbons for millions of years. In contrast, saline aquifers will probably have limited data about porosity, permeability, fault properties, internal stratigraphic and diagenetic baffles, barriers, or fluid flow history. Saline aquifers will require careful geological and petrophysical study to ensure that the top-seal caprock is sufficient to store the injected CO₂.

Saline aquifer and depleted gas field CCS projects have numerous differences that arise from the pre-CO₂ history of the sites, especially the artificially reduced pressure and relatively small volume of water in depleted gas fields. The fluid pressure ahead of CO₂ injection will be much lower in depleted gas fields than saline aquifers possibly putting the reservoir in the CO₂ gas phase (below critical pressure); some depleted gas fields may require initial injection of gas phase CO₂ until the reservoir pressure exceeds the critical point. Because the CO₂ is not displacing water in depleted gas fields, the CO₂ will not rise to create a buoyant plume as it does in saline aquifers; instead, it will probably sink to develop as a cushion at the base of the storage reservoir. Also as a consequence of the CO₂ not displacing water, unlike in saline aquifers, there may be muted effects of rel-perm in depleted gas fields, especially when CO₂ is injected in the gas phase. The difference in viscosity between CO₂ and water, and its likely consequence, viscous fingering, may not be a factor in depleted gas fields, as it is in saline aquifers. The differences in density and viscosity between CO₂ and water that lead to low storage efficiency factors in saline aquifers will not be dominant factors in depleted gas fields, which, also due to the sub-hydrostatic pressures ahead of CO₂ injection, will have relatively high storage efficiency factors.

The pre-CO₂ fluid pressure history of depleted gas fields has implications for the stress state of the reservoir; this, of course, is not an issue in saline aquifers. The depressurisation

may lead to compaction of the reservoir, shear stresses at the reservoir seal interface, reactivation of faults, and de-bonding of the well (liner and cement) from the reservoir due to compaction. The stress path of a depleted gas field undergoing re-pressurisation is not easy to predict as each reservoir will be different in terms of geomechanical properties of the reservoir and top-seal and there are very few case studies of re-pressurisation to refer to. The stress paths of saline aquifers also need consideration, but they will not have the complications of the pre-CO₂ fluid pressure changes that are attendant with depleted gas fields.

Table 3. Summary of differences between saline aquifers and depleted gas fields.

Key Difference	Saline Aquifers	Depleted Gas Fields
Quantity of pre-CCS project-supporting data	Relatively little pre-existing data	Typically much supporting data
Pre-existing infrastructure (rigs, pipelines, wells)	Potentially little is available unless the aquifer sits stratigraphically above hydrocarbon-producing horizons	Rigs, pipelines, and wells linked to hydrocarbon production are all likely to be available to be considered for repurposing for CO ₂ injection
Pre-CCS project fluid pressure history	Simple: possibly hydrostatic	Complex: typically far below initial gas field fluid pressure, possibly well below hydrostatic pressure
CO ₂ phase	Typically supercritical CO ₂ will be injected	Initial injection may be as CO ₂ gas if the reservoir pressure is below critical after gas production. Later injection may change to supercritical CO ₂ once reservoir pressure exceeds supercritical
Fluids in the reservoir	CO ₂ and brine (water)	CO ₂ , remaining methane, and residual water (thin film on grains). The role of water will increase if the depleted gas field has an active (strong) aquifer
CO ₂ trapping mechanism	Buoyancy, residual, and solubility trapping dominate	CO ₂ forms a cushion below remaining methane, either miscible or immiscible depending largely on the pressure
Location of CO ₂ in the reservoir	CO ₂ will tend to rise (as a buoyant plume relative to brine)	CO ₂ will tend to sink (as a cushion relative to residual methane)
Confidence in CO ₂ top-seal (caprock)	Top seal properties need to be demonstrated	Top seal proven by geological trapping of hydrocarbon gas
Confidence in trap	Buoyancy (structural) trapping of CO ₂ needs to be proven (unless the CCS concept obviates the need for a trap)	Trap proven by geological storage of hydrocarbon gas
Storage efficiency (proportion of pores filled with CO ₂)	Typically low (2 to 20%)	Potentially high (up to 80%)
Injection rates	Potentially low as bottom hole pump pressure is limited by the risk of shear failure	Potentially high as pore-CO ₂ reservoir pressure is typically low compared to hydrostatic pressure
Stress path history	Simple (non-existent pre-CO ₂ injection)	Potentially complex with a risk of low-fluid pressure-related damage to the reservoir
Risk of halite-scale affecting injection rate	High if brines have high salinity	Low as there will be little brine in the reservoir
Risk of near wellbore mineral dissolution	Relatively high depending on reservoir mineralogy	Relatively low as there is little water in the system to catalyse dissolution
Leakage risk linked to reservoir compaction and well-cement-liner bonding	Zero to negligible risk as there was no pre-CO ₂ compaction	Possible risk if the reservoir was not strongly cemented (rigid) and fluid pressure dropped by a large amount due to production
Leakage risk from old abandoned wells	Relatively low as the structure is unlikely to have been exploited for petroleum fluids	Relatively high as the structure has been exploited for petroleum fluids
Leakage risk due to fluid pressure-related failure	Relatively high as the aquifer did not have low pressure to start with	Potentially low as the depleted gas field probably had low pressure after gas production
Leakage risk due to pre-CO ₂ stress path	Negligible as there was no pressure decrease ahead of the CO ₂ injection	Potentially high if there was permanent compaction due to fluid pressure decrease
Pressure management via water production from dedicated wells	Possible in cases where fluid pressure risks exceeding fracture pressure	Unlikely in the early stages when fluid pressures are well below the original reservoir conditions
Monitoring: seismic	Proven to be effective	Likely to be difficult due to the lack of fluid density contrast
Monitoring: fluid composition	Unlikely as there may be few opportunities for dedicated fluid sampling boreholes	Possible if pre-existing wells can be repurposed to bring fluid samples to the surface

The pre-CO₂ fluid composition histories of depleted gas fields are also quite different from those of saline aquifers. Saline aquifers were, of course, filled with brine and, as their low storage efficiencies show that they will retain high brine saturations, saline aquifers will tend to produce halite-scale if the brine is relatively concentrated (e.g., >15% wt %

salinity). This is distinct from depleted gas fields, which have low water saturations, and will be less liable to formation damage by halite-scale than saline aquifers. Although mineral trapping of CO₂ seems to be unlikely on an engineering timescale, some degree of carbonate dissolution is feasible in saline aquifers as the acidity increases due to high CO₂ partial pressures. In water-deficient, depleted gas fields, mineral dissolution remains possible, but the lack of the essential aqueous medium suggests that the effects will be muted compared to saline aquifers.

The risks of leakage from saline aquifers and depleted gas fields are strongly related to geomechanical (stress state) controls and the presence of old wells that were not correctly sealed at abandonment, or functioning wells that were not designed to be stable in the presence of elevated CO₂ pressures. Depleted gas fields are likely to contain more pre-existing wells than saline aquifers, but they will all require assessing for storage security whatever the CCS storage type. The pre-CO₂ fluid pressure history of depleted gas fields will afford different issues to saline aquifers; the lower pre-CO₂ pressure of the former may make shear failure less likely compared to the latter, but the reservoir and top-seal of the former may have undergone some degree of inelastic deformation that changes their strength characteristics.

Monitoring of saline aquifers can involve 4D seismic and electrical resistivity tomography whereas these are unlikely to be effective in many depleted gas fields due to the lack of density contrast, especially between low-pressure CO₂ and methane and the lack of resistivity contrast between CO₂ and methane. The use of monitoring wells for measurement of pressure and temperature away from the injection well and fluid composition and isotopes from the plume may be possible in depleted gas fields with a large number of pre-existing wells. The use of monitoring boreholes from saline aquifers seems to be less likely, in most cases.

7. Conclusions

- Depleted gas fields have a greater quantity of pre-existing information about the reservoir, top-seal caprock, internal architecture of the site, and information about fluid flow properties than saline aquifers due to the long history of project development and fluid production;
- Unlike most saline aquifers, depleted gas fields typically have pre-existing infrastructure (rigs, wells, pipelines) that may be suitable for repurposing CO₂ injection;
- The fluid pressure evolution paths for saline aquifers and depleted gas fields will be distinctly different because depleted gas fields will probably be well below hydrostatic pressure at the time CO₂ injection commences but saline aquifers are likely to be at close to hydrostatic conditions;
- CO₂ trapping mechanisms in saline aquifers will be dominated by buoyancy processes with residual CO₂ and dissolved CO₂ developing with time. Depleted gas fields will be dominated by CO₂ forming a cushion below the remaining methane;
- Saline aquifers, with their buoyant CO₂ plume, relative permeability controls, and the difference in viscosity of the CO₂ and the pre-existing brine, will have low to very low proportions of the pores (2 to 20%) filled with CO₂ whereas depleted gas fields may have up to 80% of the pores filled with CO₂;
- The low pressure of depleted gas fields may give them much higher CO₂ injection rates than saline aquifers as it may be possible to safely achieve a large pressure difference between the injection well and the reservoir in depleted gas fields;
- Depleted gas fields have more complex stress path histories than saline aquifers and it is likely that any compactional processes that accompany depressurisation of depleted gas fields will not be reversed during re-pressurisation;
- Saline aquifers have a greater risk of halite scale and inhibition of injectivity than depleted aquifers as the former have vastly more brine than the latter;

- Saline aquifers have a greater risk of minor mineral dissolution processes in the reservoir than depleted aquifers due to the relatively smaller quantity of the aqueous medium needed for geochemical processes;
- Saline aquifers have several different leakage risk factors compared to depleted gas fields that are mostly related to (i) the different fluid pressure histories once CO₂ injection has started, (ii) possible pre-CO₂ injection alteration of geomechanical properties, and (iii) the probability of the greater number of wells in depleted gas fields than in saline aquifers;
- Saline aquifers different have monitoring opportunities than depleted gas fields. These arise from the different pore fluids that the CO₂ displaces (high-density, electrically conductive brine rather than low-density, non-conductive methane) and the fact that monitoring boreholes are unlikely to be possible in previously unexploited saline aquifers whereas they may be available in some depleted gas fields due to their large number of pre-existing well penetrations.

Funding: This research received no external funding.

Data Availability Statement: No original data are available.

Conflicts of Interest: The author declares that there are no conflicts of interest.

Appendix A. Definitions of Key Terms

Term	Alternative Term or Acronym	Definition
Abandoned well		A former oil, gas, or water well that is no longer in use for its original purpose, and ideally has been permanently sealed and taken out of operation.
Aquifer	Water-leg	The water filled part of the reservoir. This volume sits beneath the gas-filled part of a reservoir.
Aquifer support		Buoyancy-derived energy from the aquifer connected to the gas leg. Strong aquifer support leads to enhanced gas production rates because the water maintains pressure in the gas leg as the gas–water contact moves upwards during production. Weak aquifer support leads to steep decreases in pressure in the gas leg and little upward movement of the original gas–water contact.
Biot coefficient		The ratio of the fluid volume gained (or lost) in a material element to the volume change of that element when the pore pressure is changed.
Bottom hole pressure	BHP	The pressure exerted by fluids (such as CO ₂) at the bottom of a wellbore or at the depth of the reservoir within a CO ₂ storage site.
Brine	Saline brine	Saline water present in aquifers as the dominant fluid or gas fields as a minor component. Can be anything from <1 to 35 wt % NaCl (and other salts).
Buoyancy trapping	Structural and stratigraphic trapping	The physical trapping and immobilisation of CO ₂ within underground reservoirs due to gravity (density) controlled buoyant forces acting on the injected CO ₂ .
Capillary back-flow		The flow of brine (water and dissolved salts) in the opposite direction to the flow of CO ₂ , driven by the evaporation of water into the CO ₂ at a drying front. Flow happens via the thin film of water that adheres to grain surfaces, present as minerals are preferentially water-wet.
Carbon capture		The removal of CO ₂ from waste streams such as power stations or industrial processes.
Carbon storage	Carbon dioxide disposal	The injection of CO ₂ underground for permanent geological trapping.
Cement (well cement)		The specialised cementitious material used to construct and seal wells drilled for the purpose of CO ₂ injection and storage in underground reservoirs. Well cement plays a crucial role in ensuring the integrity and containment of CO ₂ within the designated storage formations.
Clathrate	Gas hydrate	A crystalline structure formed by water molecules trapping gas molecules (such as methane) within a lattice-like framework that develops under specific conditions of low temperature and high pressure.
CO ₂ cushion		Sinking CO ₂ in depleted gas fields is controlled by the higher density of the CO ₂ compared to the low-pressure, residual methane, which, in contrast, is pushed up to the top of the structure.
CO ₂ plume		The buoyant column of CO ₂ in saline aquifers, roughly forming a trumpet shape against the base of the top seal.
CO ₂ -wet		A function of wettability, where minerals are largely assumed to be preferentially coated with a film of CO ₂ rather than water (CO ₂ -wetting is a situation that is broadly assumed to not arise in engineered systems).

Term	Alternative Term or Acronym	Definition
Compartmentalisation		Sealed faults or low permeability stratigraphic or diagenetic layers divide the subsurface storage formation into distinct compartments or zones with limited fluid/ flow communication between them.
Depleted gas field		A gas field that has produced as much hydrocarbon as is economically and technically feasible; usually has pressure lower than the pre-production fluid pressure.
Depressurised gas field		Former natural gas reservoirs that have been emptied of their gas content through extraction.
Diagenesis		Combination of chemical, physical, and biological processes that convert initially friable sediment into sedimentary rock.
Dissolution rate constant		The kinetic variable that dictates the rate at which a mineral dissolves at a given temperature.
Distributed acoustic sensors	DAS	Fibre-optic sensors (seismic receivers) built into the CO ₂ injection well to assess the full acoustic field (i.e., amplitude, wavelength) during and after CO ₂ injection.
Distributed thermal sensors	DTS	Fibre-optic sensors (temperature monitors) built into the CO ₂ injection well to assess the thermal effects of CO ₂ injection.
Effective normal stress		The stress perpendicular to a plane less the component linked to the fluid pressure.
Enhanced gas recovery	EGR	Gas production assisted by more than just pumping; for example, the injection of a gas with a higher density than methane, such as CO ₂ , to act as a cushion to encourage the remaining methane to rise to the top of the structure.
Enhanced oil recovery	EOR	Oil production assisted by more than just pumping; for example, by injection of CO ₂ which reduces oil viscosity and increases oil volume (thus encouraging the reconnection of previously separated droplets of oil).
Fault		A geological discontinuity that has experienced substantial displacement.
Fault reactivation		The process where existing geological faults become active again due to changes in stress conditions, potentially leading to pathways for CO ₂ escape.
Fault seal		Low-permeability geological faults that stop the movement of CO ₂ and other fluids, leading to localised trapping of CO ₂ or limitations on the lateral flow of CO ₂ .
Fracture		Any split in a body of rock; can be natural or induced and may have displacement across it.
Fracture pressure		The fluid pressure at which the strength (minimum horizontal stress) is exceeded, resulting in the failure of the rock.
Gas leg		The shallowest portion of a gas field occupied by hydrocarbon gas, as opposed to water, controlled by buoyancy.
Gas–water contact		The buoyancy-controlled interface between gas in the gas leg and water in the water leg. There will be a finite transition zone separating the water leg and the gas leg where the proportions of water and gas evolve upwards over several metres.
Halite scale		The growth of crystalline sodium chloride (halite), typically in the near wellbore zone, leading to impaired injectivity due to the blocking of pore throats.
Hydrostatic pressure		The pressure at a given depth equivalent to that imposed by a continuous column of water; a function of the density of water and depth.
Injection well	Injector	The well through which CO ₂ is injected into the reservoir.
Injection rate		The rate, in terms of mass or volume per unit time, at which CO ₂ is injected into the reservoir.
Irreducible water saturation	Irreducible brine saturation, S_{wirr}	The fraction of pore space occupied by water when the CO ₂ or hydrocarbon content is at maximum. This quantity of water can be locally reduced by the flow of anhydrous CO ₂ that allows the water to evaporate.
Joule–Thomson cooling		In CCS fields this refers to the decrease in temperature experienced by pressurised CO ₂ as it expands during injection or other processes, driven by the thermodynamic properties of the gas undergoing rapid expansion.
Kinetics		The study of the rate at which reactions happen, in this case related to CO ₂ injection.
Liner	Casing	Steel pipe placed in an oil or gas well as drilling progresses. The function of the liner (casing) is to prevent the wall of the hole from caving during drilling, provide control of the well if it meets an overpressured zone, and limit CO ₂ injection (or oil or gas production) to the perforated zone.
Lithostatic pressure	Vertical effective stress, VES	The pressure at a given depth equivalent to that imposed by the column of rock; a function of the cumulative density of rocks in a stratigraphic succession and depth.
Micropore	Microporous	Rocks dominated by pore throats that are in the micrometer and smaller range.

Term	Alternative Term or Acronym	Definition
Microseismic events	Microearthquakes or microseismicity	Small-scale seismic disturbances or vibrations that occur in the subsurface during carbon capture and storage (CCS) operations. These events are typically induced by changes in stress, fluid movement, or rock deformation associated with CO ₂ injection and storage activities.
Microseismic monitoring		Deployment of arrays of sensitive seismic sensors (geophones) either at the surface or downhole near the injection well to continuously monitor and record microseismic events. These events are typically very small in magnitude and are caused by stress changes and fluid movement in the subsurface.
Mineral dissolution		The act of minerals in the reservoir or top-seal (or cement) dissolving in the acidic conditions developed due to the injection of CO ₂ into a water-bearing saline aquifer or depleted gas field.
Mineral trapping		The act of minerals precipitating due to the injection of CO ₂ leading to the formation of water supersaturated with new carbonate minerals.
Minimum horizontal stress	S3 or σ_3 or σ_{hmin}	One of the three principal stresses that subsurface rocks are subjected to. Hydraulic fractures propagate perpendicular to the minimum horizontal stress.
Mohr circle	Mohr diagram	A diagram that shows how the normal and shear stresses within a material element (e.g., sedimentary rock) vary with orientation. Can be used to define stable and unstable conditions for rocks and how they vary with fluid pressure.
Monitoring well	Monitoring borehole	A borehole used to assess the fluid pressure and fluid composition of the reservoir at a site remote from the injection well. Could be a re-purposed gas production well.
Near wellbore zone		The volume of the reservoir near the injection well. The extent depends on the nature of the reservoir rock (especially permeability and strength), injection pressure, and water salinity (for halite scale effects).
Partial pressure		The pressure exerted by a component (such as carbon dioxide, CO ₂) within a mixture of gases, expressed as the fraction of the total pressure attributed to that specific component.
Permeability		The quantitative ability of rock to transmit fluid under a pressure gradient; has directionality; this depends on whether there is one fluid phase or a combination of immiscible fluids present (e.g., CO ₂ and water).
Poisson's ratio		The ratio of transverse contraction strain to longitudinal extension strain in the direction of the stretching force.
Pore throat		The narrowest space between a collection of sedimentary grains. Usually measured in micrometers, or nanometers for the finest-grained materials.
Poroelasticity	Poroelastic theory	The interaction between fluid flow, pressure, and bulk solid deformation within a porous medium (i.e., a reservoir).
Porosity		The quantitative measure of the proportion of pore (void) space in a rock.
Production well	Production borehole	The well through which hydrocarbons were originally extracted from the subsurface in a depleted gas field.
Reactive surface area	RSA	A kinetic variable controlled by how much of a mineral is exposed to reactive CO ₂ and water; negligible RSA leads to negligible extents of reaction.
Regulatory authority		The regional or national body that dictates if, how, and when CO ₂ storage projects happen. Different in every country.
Relative permeability	Rel-perm scaling factor	A variable between 1 and 0 that is multiplied by the absolute permeability of a reservoir that contains two or more fluids, leading to the effective permeability.
Re-pressurised gas field		Former reservoirs that have been largely emptied of their gas content through production, and then had fluid (e.g., CO ₂ , or hydrocarbons for storage) reinjected.
Reservoir		Body of porous rock that serves to store the injected CO ₂ ; typically sandstone or carbonate, but potentially also fractured basalt or shale.
Reservoir architecture		The overall organisation of a reservoir into flow units and compartments, typically separated by barriers and baffles (both depositional and diagenetic) and sealing faults
Reservoir compartment		A part of a reservoir in pressure isolation from other parts of the overall trap.
Reservoir pressure		The pressure of a reservoir, or specific compartment. For saline aquifers before CO ₂ injection probably hydrostatic. For depleted gas fields, the final (low) fluid pressure after hydrocarbons have been produced.
Reservoir temperature		The ambient temperature of a reservoir, mainly controlled by the regional geothermal gradient, but possibly affected by sub-surface interventions such as injection of cold fluids (CO ₂ , or even water for pressure support).
Residual brine saturation	Residual water saturation	The water that remains in a portion of the reservoir after non-wetting CO ₂ has been injected into the structure in engineered systems or after methane has occupied a structure in natural gas fields.
Residual methane	Remaining methane	Methane that is left in a reservoir when it is not economical or feasible to produce any more gas.

Term	Alternative Term or Acronym	Definition
Residual trapping		The storage of injected CO ₂ in the subsurface as discrete, separated droplets that cannot easily connect and thus flow up a pressure gradient.
Saline aquifer		A deeply buried (typically > 800 m) porous rock filled with brine.
Salinity		Measure of the dissolved load (mainly NaCl) of water in an aquifer or depleted gas field.
Seismic imaging		Seismic imaging plays a critical role in CCS projects by providing essential subsurface information for reservoir characterisation, caprock assessment, fault detection, and ongoing monitoring of a CO ₂ plume in a saline aquifer.
Shear stress		Forces acting parallel to a surface.
Solubility trapping		The storage of injected CO ₂ in the subsurface in a dissolved form (typically in brine)
Storage capacity		The quantity (in megatonnes) of CO ₂ that can be stored in a given structure; given the decisions about the numbers of wells, injection pressures, location of wells, and additional fluid pressure management plans.
Storage efficiency factor		The ratio of the amount of CO ₂ securely stored in the reservoir to the total amount of CO ₂ injected into the reservoir over a specific period. It is expressed as a percentage or fraction and provides a measure of how efficiently the storage site retains the injected CO ₂ without significant leakage or migration.
Stress path		The temporal evolution of stress in a reservoir that evolves due to changes in fluid pressure, both during hydrocarbon production and CO ₂ injection.
Supercritical CO ₂		CO ₂ beyond the P-T critical point that is neither liquid nor gas; it has a viscosity close to that of gas-phase CO ₂ but can approach the density of liquid CO ₂ .
Trap	Trapping mechanism	The physical closure mechanism that holds CO ₂ in place in the subsurface. May include folds, faults, or stratigraphic discontinuities. May involve capillary trapping.
Top-seal	Caprock	Impermeable rock layers that function as a cap over reservoirs, preventing fluids such as CO ₂ from escaping upwards.
Underburden		Non-reservoir rock that sits below the reservoir
Well logs		A range of electrical-, nuclear-, acoustic-, imaging-, and radioactivity-based detectors that generate a large amount of data from a borehole, capable of revealing porosity, lithology, fluid saturation, mineralogy, fracture orientation and extent and lithofacies from the walls of the borehole
Water leg		The deepest portion of a gas field occupied by water, as opposed to gas.
Water-wet		A function of wettability, where minerals are largely assumed to be preferentially coated with a film of water rather than CO ₂ (a situation that is assumed to arise in engineered CCS systems).
Water saturation		The proportion of the pore space filled with water, expressed as a percentage or a fraction.

References

1. IPCC. *Climate Change 2013: The Physical Basis*; IPCC: Cambridge UK, 2013.
2. IPCC. *Special Report on Carbon Dioxide Capture and Storage*; Cambridge University Press: Cambridge, UK, 2005; pp. 1–431.
3. McKinsey. *Energy Insights: Global Energy Perspectives*; McKinsey: New York, NY, USA, 2022.
4. Worden, R.H.; Smith, L.K. Geological sequestration of CO₂ in the subsurface: Lessons from CO₂ injection enhanced oil recovery projects in oilfields. In *Geological Storage of Carbon Dioxide. Special Publication*; Baines, S.J., Worden, R.H., Eds.; Geological Society: London, UK, 2004; Volume 233, pp. 211–224.
5. Riding, J.B. The IEA Weyburn CO₂ Monitoring and Storage Project—Integrated Results from Europe. In Proceedings of the NATO Advanced Research Workshop on Advances in CO₂ Geological Sequestration in Eastern and Western European Countries, Tomsk, Russia, 15–18 November 2004; pp. 223–230.
6. Tyne, R.L.; Barry, P.H.; Lawson, M.; Byrne, D.J.; Warr, O.; Xie, H.; Hillegonds, D.J.; Formolo, M.; Summers, Z.M.; Skinner, B.; et al. Rapid microbial methanogenesis during CO₂ storage in hydrocarbon reservoirs. *Nature* **2021**, *600*, 670–674. [[CrossRef](#)]
7. Kumar, A.; Chao, K.; Hammack, R.; Harbert, W.; Ampomah, W.; Balch, R.; Garcia, L. Surface-Seismic Monitoring of an Active CO₂-EOR Operation in the Texas Panhandle Using Broadband Seismometers. In Proceedings of the SEG International Exposition and Annual Meeting, Anaheim, CA, USA, 17 October 2018; 2018 ; p. SEG-2018-2997451.
8. Hughes, D.S. Carbon storage in depleted gas fields: Key challenges. In Proceedings of the 9th International Conference on Greenhouse Gas Control Technologies, Washington, DC, USA, 16–20 November 2008; Volume 1, pp. 3007–3014.
9. Tissot, B.T.; Welte, D.H. *Petroleum Formation and Occurrences*, 2nd ed.; Springer: Berlin, German, 1984; p. 699.
10. Orlic, B. Geomechanical effects of CO₂ storage in depleted gas reservoirs in The Netherlands: Inferences from feasibility studies and comparison with aquifer storage. *J. Rock Mech. Geotech. Eng.* **2016**, *8*, 846–859. [[CrossRef](#)]
11. GCCSI. *Global Status of CCS 2023*; Global CCS Institute: Melbourne, Australia, 2023.
12. Miri, R.; Hellevang, H. *Critical Factors for Considering CO₂ Injectivity in Saline Aquifers*; FME Success: Bergen, Norway, 2019; pp. 1–24.

13. Ringrose, P.; Greenberg, S.; Whittaker, S.; Nazarian, B.; Oye, V. Building confidence in CO₂ storage using reference datasets from demonstration projects. *Energy Procedia* **2017**, *114*, 3547–3557. [CrossRef]
14. Torp, T.A.; Gale, J. Demonstrating storage of CO₂ in geological reservoirs: The Sleipner and SACS projects. In *Greenhouse Gas Control Technologies*; Gale, J., Kaya, K., Eds.; Elsevier: Amsterdam, The Netherlands, 2003; Volume I–II, pp. 311–316.
15. Estublier, A.; Lackner, A.S. Long-term simulation of the Snohvit CO₂ storage. In Proceedings of the 9th International Conference on Greenhouse Gas Control Technologies, Washington, DC, USA, 16–20 November 2008; pp. 3221–3228.
16. Hansen, O.; Gilding, D.; Nazarian, B.; Osdal, B.; Ringrose, P.; Kristoffersen, J.B.; Eiken, O.; Hansen, H. Snohvit: The history of injecting and storing 1 Mt CO₂ in the fluvial Tubaen Fm. *Energy Procedia* **2013**, *37*, 3565–3573. [CrossRef]
17. IEAGHG. *Case Studies of CO₂ Storage in Depleted Oil and Gas Fields, 2017/01*; IEAGHG: Cheltenham, UK, 2017.
18. Iding, M.; Ringrose, P. Evaluating the impact of fractures on the long-term performance of the in salah CO₂ storage site. *Energy Procedia* **2009**, *1*, 2021–2028. [CrossRef]
19. Vasco, D.W.; Rucci, A.; Ferretti, A.; Novali, F.; Bissell, R.C.; Ringrose, P.S.; Mathieson, A.S.; Wright, I.W. Satellite-based measurements of surface deformation reveal fluid flow associated with the geological storage of carbon dioxide. *Geophys. Res. Lett.* **2009**, *1*, 2021–2028. [CrossRef]
20. Goertz-Allmann, B.P.; Kuhn, D.; Oye, V.; Bohlooli, B.; Aker, E. Combining microseismic and geomechanical observations to interpret storage integrity at the In Salah CCS site. *Geophys. J. Int.* **2014**, *198*, 447–461. [CrossRef]
21. Armitage, P.J.; Faulkner, D.R.; Worden, R.H. Caprock corrosion. *Nat. Geosci.* **2013**, *6*, 79–80. [CrossRef]
22. Robertson, B.; Mousavian, M. Gorgon Carbon Capture and Storage: The Sting in the Tail. Available online: <https://acrobat.adobe.com/link/review?uri=urn:aaid:scds:US:866ec6ca-0541-409a-a1b4-8b4fe2ea6d1d#pageNum=1> (accessed on 2 March 2024).
23. Lewis, J. Chevron’s Flagship Gorgon CCS Project still Failing to Live up to Expectations. Available online: www.upstreamonline.com/energy-transition/chevrons-flagship-gorgon-ccs-project-still-failing-to-live-up-to-expectations/2-1-1166185 (accessed on 2 March 2024).
24. Smith, N.; Boone, P.; Oguntimehin, A.; van Essen, G.; Guo, R.; Reynolds, M.A.; Friesen, L.; Cano, M.C.; O’Brien, S. Quest CCS facility: Halite damage and injectivity remediation in CO₂ injection wells. *Int. J. Greenh. Gas Control* **2022**, *119*, 103718. [CrossRef]
25. Tawiah, P.; Duer, J.; Bryant, S.L.; Larter, S.; O’Brien, S.; Dong, M.Z. CO₂ injectivity behaviour under non-isothermal conditions—Field observations and assessments from the Quest CCS operation. *Int. J. Greenh. Gas Control* **2020**, *92*, 102843. [CrossRef]
26. Goertz-Allman, B.P.; Langet, N.; Kuhn, D.; Baird, A.; Oates, S.; Rowe, C.; Harvey, S.; Oye, V.; Nakstad, H. Effective microseismic monitoring of the Quest CCS site, Alberta, Canada. In Proceedings of the 16th International Conference on Greenhouse Gas Control Technologies, GHGT-16, Lyon, France, 23–27 October 2022.
27. Finley, R.J. An overview of the Illinois Basin—Decatur Project. *Greenh. Gases-Sci. Technol.* **2014**, *4*, 571–579. [CrossRef]
28. Blakley, C.; Carman, C.; Korose, C.; Luman, D.; Zimmerman, J.; Frish, M.; Dobler, J.; Blume, N.; Zaccheo, S. Application of emerging monitoring techniques at the Illinois Basin—Decatur Project. *Int. J. Greenh. Gas Control* **2020**, *103*, 103188. [CrossRef]
29. Zwingmann, N.; Mito, S.; Sorai, M.; Ohsumi, T. Preinjection characterisation and evaluation of CO₂ sequestration potential in the Haizume Formation, Niigata Basin, Japan—Geochemical modelling of water-minerals-CO₂ interaction. *Oil Gas Sci. Technol. Rev. D Ifp Energ. Nouv.* **2005**, *60*, 249–258. [CrossRef]
30. Mito, S.; Xue, Z.Q.; Ohsumi, T. Case study of geochemical reactions at the Nagaoka CO₂ injection site, Japan. *Int. J. Greenh. Gas Control* **2008**, *2*, 309–318. [CrossRef]
31. Wildenborg, T.; Bentham, M.; Chadwick, A.; David, P.; Deflandre, J.P.; Dillen, M.; Groenenberg, H.; Kirk, K.; Le Gallo, Y. Large-scale CO₂ injection demos for the development of monitoring and verification technology and guidelines (CO₂ReMoVe). *Energy Procedia* **2009**, *1*, 2367–2374. [CrossRef]
32. Fischer, S.; Liebscher, A.; Wandrey, M.; Grp, C.S. CO₂-brine-rock interaction—First results of long-term exposure experiments at in situ P-T conditions of the Ketzin CO₂ reservoir. *Chem. Der Erde-Geochem.* **2010**, *70*, 155–164. [CrossRef]
33. Niemi, A.; Bensabat, J.; Fagerlund, F.; Sauter, M.; Ghergut, J.; Licha, T.; Fierz, T.; Wiegand, G.; Rasmusson, M.; Rasmusson, K.; et al. Small-scale CO₂ injection into a deep geological formation at Heletz, Israel. In Proceedings of the 6th Trondheim Conference on CO₂ Capture, Transport and Storage, Trondheim, Norway, 16–18 June 2012; Volume 23, pp. 504–511.
34. Niemi, A.; Bensabat, J.; Shtivelman, V.; Edlmann, K.; Gouze, P.; Luquot, L.; Hingerl, F.; Benson, S.M.; Pezard, P.A.; Rasmusson, K.; et al. Heletz experimental site overview, characterization and data analysis for CO₂ injection and geological storage. *Int. J. Greenh. Gas Control* **2016**, *48*, 3–23. [CrossRef]
35. Shepherd, M. Chapter 5 Factors influencing recovery from oil and gas fields. In *Oil field production geology. AAPG Memoir 91*; Shepherd, M., Ed.; American Association of Petroleum Geologists: Tulsa, OK, USA, 2009; pp. 37–46.
36. Jahn, F.; Cook, M.; Graham, C. *Hydrocarbon Exploration and Production*, 2nd ed.; Elsevier: Amsterdam, The Netherlands, 2008; Volume 55, p. 444.
37. Worden, R.H.; Bukar, M.; Shell, P. The effect of oil emplacement on quartz cementation in a deeply buried sandstone reservoir. *Am. Assoc. Pet. Geol. Bull.* **2018**, *102*, 49–75. [CrossRef]
38. Worden, R.H.; Armitage, P.J.; Butcher, A.; Churchill, J.; Csoma, A.; Hollis, C.; Lander, R.H.; Omma, J. Petroleum reservoir quality prediction: Overview and contrasting approaches from sandstone and carbonate communities. In *Reservoir Quality of Clastic and Carbonate Rocks: Analysis, Modelling and Prediction. Special Publication*; Armitage, P.J., Butcher, A., Churchill, J., Csoma, A., Hollis, C., Lander, R.H., Omma, J., Worden, R.H., Eds.; Geological Society: London, UK, 2018; Volume 435, pp. 1–31.

39. Worden, R.H.; Oxtoby, N.H.; Smalley, P.C. Can oil emplacement prevent quartz cementation in sandstones? *Pet. Geosci.* **1998**, *4*, 129–137. [[CrossRef](#)]
40. Cowan, G. The development of the North Morecambe Gas Field, East Irish Sea Basin, UK. *Pet. Geosci.* **1996**, *2*, 43–52. [[CrossRef](#)]
41. Woodward, K.; Curtis, C.D. Predictive model for the distribution of production constraining illites—Morecambe Gas Field, Irish Sea, Offshore UK. In *Petroleum Geology of North West Europe*; Brooks, J., Glennie, K.W., Eds.; Graham and Trotman: London, UK, 1987; Volume 1, pp. 205–215.
42. French, M.W.; Worden, R.H.; Mariani, E.; Larese, R.E.; Mueller, R.R.; Kliewer, C.E. Microcrystalline quartz generation and the preservation of porosity in sandstones: Evidence from the upper Cretaceous of the Sub-Hercynian Basin, Germany. *J. Sediment. Res.* **2012**, *82*, 422–434. [[CrossRef](#)]
43. Kirk, K.L. Potential for storage of carbon dioxide in the rocks beneath the East Irish Sea. In *Sustainable and Renewable Energy Programme Internal Report CR/05/127N*; British Geological Survey: Keyworth, UK, 2005; pp. 1–24.
44. Bentham, M.; Williams, G.; Vosper, H.; Chadwick, A.; Williams, J.; Kirk, K. Using Pressure Recovery at a Depleted Gas Field to Understand Saline Aquifer Connectivity. In Proceedings of the 13th International Conference on Greenhouse Gas Control Technologies (GHGT), Lausanne, Switzerland, 14–18 November 2017; pp. 2906–2920.
45. Van der Meer, L.G.H. The K12-B CO₂ injection project in The Netherlands (Chapter 13). In *Geological Storage of Carbon Dioxide (CO₂)*; Gluyas, J., Mathias, S., Eds.; Woodhead Publishing Limited: Cambridge, UK, 2013; pp. 301–331.
46. Vandeweyer, V.; Hofstee, C.; Pelt, W.V.; Graven, H. CO₂ injection at K12-B, the final story. GHGT-15. In Proceedings of the 15th International Conference on Greenhouse Gas Control Technologies, Abu Dhabi, United Arab Emirates, 5–8 October 2020.
47. Sharma, S.; Cook, P.; Jenkins, C.; Steeper, T.; Lees, M.; Ranasinghe, N. The CO₂CRC Otway Project: Leveraging experience and exploiting new opportunities at Australia’s first CCS project site. In Proceedings of the 10th International Conference on Greenhouse Gas Control Technologies, Amsterdam, The Netherlands, 19–23 September 2010; pp. 5447–5454.
48. Payre, X.; Maisons, C.; Marble, A.; Thibeau, S. Analysis of the passive seismic monitoring performance at the Rouse CO₂ storage demonstration pilot. *Energy Procedia* **2014**, *63*, 4339–4357. [[CrossRef](#)]
49. Mouillac, J. From the North Pyrenees Surface Outcrops to the Deep Aquitaine Basin Gas Fields: Geological Field Trip Guide Book. 16 June 2017. Available online: www.geolval.fr/images/Geoval/actualites/2017/06_juin/Escurets-guide-book--GeolVal-June-2017.pdf (accessed on 2 March 2024).
50. Ringrose, P. *How to Store CO₂ Underground: Insights from Early-Mover CCS Projects*; Springer: Cham, Switzerland, 2020.
51. Worden, R.H.; Utley, J.E.P. Automated mineralogy (SEM-EDS) approach to sandstone reservoir quality and diagenesis. *Front. Earth Sci.* **2022**, *10*, 794266. [[CrossRef](#)]
52. Machado, M.V.B.; Delshad, M.; Sepehrnoori, K. Injectivity assessment for CCS field-scale projects with considerations of salt deposition, mineral dissolution, fines migration, hydrate formation, and non-Darcy flow. *Fuel* **2023**, *353*, 129148. [[CrossRef](#)]
53. Liu, S.Z.; Yuan, L.; Zhao, C.Z.; Zhang, Y.; Song, Y.C. A review of research on the dispersion process and CO₂ enhanced natural gas recovery in depleted gas reservoir. *J. Pet. Sci. Eng.* **2022**, *208*, 109682. [[CrossRef](#)]
54. James, A.; Baines, S.; McCollough, S. *Strategic UK CCS Storage Appraisal—WP5A—Bunter Storage Development Plan*; Energy Technologies Institute: Loughborough, UK, 2016.
55. James, A.; Baines, S.; McCollough, S. *Strategic UK CCS Storage Appraisal—WP5C—Hamilton Storage Development Plan*; Energy Technologies Institute: Loughborough, UK, 2016.
56. Worden, R.H. Value of core for reservoir and top-seal analysis for carbon capture and storage projects. In *The Role of Core in 21st Century Reservoir Characterisation*; Neal, A., Ashton, M., Williams, L., Dee, S., Dodd, T.T., Marshall, J., Eds.; Geological Society of London: London, UK, 2023; Volume 527, pp. 365–385.
57. Edlmann, K.; Bensabat, J.; Niemi, A.; Haszeldine, R.S.; McDermott, C.I. Lessons learned from using expert elicitation to identify, assess and rank the potential leakage scenarios at the Heletz pilot CO₂ injection site. *Int. J. Greenh. Gas Control* **2016**, *49*, 473–487. [[CrossRef](#)]
58. Worth, K.; White, D.; Chalaturnyk, R.; Sorensen, J.; Hawkes, C.; Rostron, B.; Johnson, J.; Young, A. Aquistore Project Measurement, Monitoring, and Verification: From Concept to CO₂ Injection. *Energy Procedia* **2014**, *63*, 3202–3208. [[CrossRef](#)]
59. Ringrose, P.S.; Mathieson, A.S.; Wright, I.W.; Selama, F.; Hansen, O.; Bissell, R.; Saoula, N.; Midgley, J. The In Salah CO₂ storage project: Lessons learned and knowledge transfer. *Energy Procedia* **2013**, *37*, 6226–6236. [[CrossRef](#)]
60. European-Commission. *Guidance Document 2: Characterisation of the Storage Complex, CO₂ Stream Composition, Monitoring and Corrective Measures*; European-Commission: Luxembourg, 2011; pp. 1–155.
61. European-Commission Guidance Document 1. *CO₂ Storage Life Cycle Risk Management Framework*; European-Commission: Luxembourg, 2011.
62. Arts, R.; Eiken, O.; Chadwick, A.; Zweigel, P.; van der Meer, B.; Kirby, G. Seismic monitoring at the Sleipner underground CO₂ storage site (North Sea). In *Geological Storage of Carbon Dioxide. Special Publication*; Baines, S.J., Worden, R.H., Eds.; Geological Society: London, UK, 2004; Volume 233, pp. 181–191.
63. Urosevic, M.; Pevzner, R.; Shulakova, V.; Kepic, A.; Caspari, E.; Sharma, S. Seismic monitoring of CO₂ Injection into a Depleted Gas Reservoir—Otway Basin Pilot Project, Australia. In Proceedings of the 10th International Conference on Greenhouse Gas Control Technologies, Amsterdam, The Netherlands, 19–23 September 2010; pp. 3550–3557.

64. Luth, S.; Ivanova, A.; Juhlin, C.; Juhojuntti, N.; Kashubin, A.; Bergmann, P.; Gotz, J. 4D seismic monitoring of small CO₂ injection—Results from the Ketzin pilot site (Germany). In Proceedings of the 12th ISRM International Congress on Rock Mechanics, Beijing, China, 17–21 October 2011; pp. 1747–1751.
65. Daley, T.M.; Hendrickson, J.; Queen, J.H. Monitoring CO₂ Storage at Cranfield, Mississippi with Time-Lapse Offset VSP—Using Integration and Modeling to Reduce Uncertainty. *Energy Procedia* **2014**, *63*, 4240–4248. [[CrossRef](#)]
66. Bergmann, P.; Schmidt-Hattenberger, C.; Labitzke, T.; Wagner, F.M.; Just, A.; Flechsig, C.; Rippe, D. Fluid injection monitoring using electrical resistivity tomography five years of CO₂ injection at Ketzin, Germany. *Geophys. Prospect.* **2017**, *65*, 859–875. [[CrossRef](#)]
67. Stork, A.L.; Verdon, J.P.; Kendall, J.M. The microseismic response at the In Salah Carbon Capture and Storage (CCS) site. *Int. J. Greenh. Gas Control* **2015**, *32*, 159–171. [[CrossRef](#)]
68. Harvey, S.; O'Brien, S.; Minisini, S.; Oates, S.; Braim, M. Quest CCS Facility: Microseismic System Monitoring and Observations. In Proceedings of the 15th International Conference on Greenhouse Gas Control Technologies, GHGT-15, Abu Dhabi, United Arab Emirates, 15–18 March 2021.
69. GCCSI. *Effects of Impurities on Geological Storage of CO₂*; Global Carbon Capture and Storage Institute: Melbourne, Australia, 2011; pp. 1–87.
70. Ali, L.; Bentley, R.E.; Gutierrez, A.A.; Gonzalez, Y. Using distributed temperature sensing (DTS) technology in acid gas injection design. *Acta Geotech.* **2014**, *9*, 135–144. [[CrossRef](#)]
71. Sidenko, E.; Tertyshnikov, K.; Bona, A.; Pevzner, R. DAS-VSP interferometric imaging: CO₂CRC Otway Project feasibility study. *Interpret. -A J. Subsurf. Charact.* **2021**, *9*, SJ1–SJ12. [[CrossRef](#)]
72. Vandeweyer, V.; van der Meer, B.; Hofstee, C.; Mulders, F.; D'Hoore, D.; Graven, H. Monitoring the CO₂ injection site: K12-B. In Proceedings of the 10th International Conference on Greenhouse Gas Control Technologies, Amsterdam, The Netherlands, 19–23 September 2010; pp. 5471–5478.
73. Jang, E.; Wiese, B.; Pilz, P.; Fischer, S.; Schmidt-Hattenberger, C. Geochemical modeling of CO₂ injection and gypsum precipitation at the Ketzin CO₂ storage site. *Environ. Earth Sci.* **2022**, *81*, 286. [[CrossRef](#)]
74. Sato, K.; Mito, S.; Horie, T.; Ohkuma, H.; Saito, H.; Watanabe, J.; Yoshimura, T. Monitoring and simulation studies for assessing macro- and meso-scale migration of CO₂ sequestered in an onshore aquifer: Experiences from the Nagaoka pilot site, Japan. *Int. J. Greenh. Gas Control* **2011**, *5*, 125–137.
75. Boreham, C.; Underschultz, J.; Stalker, L.; Kirste, D.; Freifeld, B.; Jenkins, C.; Ennis-King, J. Monitoring of CO₂ storage in a depleted natural gas reservoir: Gas geochemistry from the CO₂CRC Otway Project, Australia. *Int. J. Greenh. Gas Control* **2011**, *5*, 1039–1054. [[CrossRef](#)]
76. Gyore, D.; Stuart, F.M.; Gilfillan, S.M.V.; Waldron, S. Tracing injected CO₂ in the Cranfield enhanced oil recovery field (MS, USA) using He, Ne and Ar isotopes. *Int. J. Greenh. Gas Control* **2015**, *42*, 554–561. [[CrossRef](#)]
77. Utley, R.E.; Martin-Roberts, E.; Utting, N.; Johnson, G.; Györe, D.; Zurakowska, M.; Stuart, F.M.; Boyce, A.J.; Darrah, T.H.; Gulliver, P.; et al. Multi-isotope geochemical baseline study of the Carbon Management Canada Research Institutes CCS Field Research Station (Alberta, Canada), prior to CO₂ Injection. *Earth Sci. Syst. Soc.* **2023**, *3*, 10069. [[CrossRef](#)]
78. Lescanne, M.; Hy-Billiot, J.; Aimard, N.; Prinet, C. The site monitoring of the Lacq industrial CCS reference project. *Energy Procedia* **2011**, *4*, 3518–3525.
79. Gilfillan, S.M.V.; Sherk, G.W.; Poreda, R.J.; Haszeldine, R.S. Using noble gas fingerprints at the Kerr Farm to assess CO₂ leakage allegations linked to the Weyburn-Midale CO₂ monitoring and storage project. *Int. J. Greenh. Gas Control* **2017**, *63*, 215–225. [[CrossRef](#)]
80. Morris, J.P.; Hao, Y.; Foxall, W.; McNab, W. In Salah CO₂ Storage JIP: Hydromechanical Simulations of Surface Uplift due to CO₂ Injection at In Salah. *Energy Procedia* **2011**, *4*, 3269–3275.
81. Sun, X.H.; Wang, Z.Y.; Li, H.Y.; He, H.K.; Sun, B.J. A simple model for the prediction of mutual solubility in CO₂-brine system at geological conditions. *Desalination* **2021**, *504*, 114972.
82. Oldenburg, C.M. Joule-Thomson cooling due to CO₂ injection into natural gas reservoirs. *Energy Convers. Manag.* **2007**, *48*, 1808–1815. [[CrossRef](#)]
83. Mathias, S.A.; Gluyas, J.G.; Oldenburg, C.M.; Tsang, C.-F. Analytical solution for Joule-Thomson cooling during CO₂ geo-sequestration in depleted oil and gas reservoirs. *Int. J. Greenh. Gas Control* **2010**, *4*, 806–810. [[CrossRef](#)]
84. Jiang, L.L.; Wang, Y.; Lu, G.H.; Yang, J.G.; Song, Y.C. Experimental Study on the density-driven convective mixing of CO₂ and brine at reservoir temperature and pressure conditions. *Energy Fuels* **2022**, *36*, 10261–10268. [[CrossRef](#)]
85. Taheri, A.; Torsæter, O.; Lindeberg, E.; Hadia, N.; Wessel-Berg, D. Effect of convective mixing process on storage of CO₂ in saline aquifers with layered permeability. *Adv. Chem. Res.* **2021**, *3*, 12. [[CrossRef](#)]
86. Akai, T.; Saito, N.; Hiyama, M.; Okabe, H. Numerical modelling on CO₂ storage capacity in depleted gas reservoirs. *Energies* **2021**, *14*, 3978. [[CrossRef](#)]
87. Hoteit, H.; Fahs, M.; Soltanian, M.R. Assessment of CO₂ injectivity during sequestration in depleted gas reservoirs. *Geosciences* **2019**, *9*, 199. [[CrossRef](#)]
88. Cao, C.; Liao, J.X.; Hou, Z.M.; Xu, H.C.; Mehmood, F.; Wu, X.N. Utilization of CO₂ as cushion gas for depleted gas reservoir transformed gas storage reservoir. *Energies* **2020**, *13*, 576. [[CrossRef](#)]

89. Worden, R.H.; Griffiths, J.; Wooldridge, L.J.; Utley, J.E.P.; Lawan, A.Y.; Muhammed, D.D.; Simon, N.; Armitage, P.J. Chlorite in sandstones. *Earth Sci. -Rev.* **2020**, *204*, 103105. [[CrossRef](#)]
90. McBride-Wright, M.; Maitland, G.C.; Trusler, J.P.M. Viscosity and density of aqueous solutions of carbon dioxide at temperatures from (274 to 449) K and at pressures up to 100 MPa. *J. Chem. Eng. Data* **2015**, *60*, 171–180. [[CrossRef](#)]
91. Seyyedi, M.; Rostami, B.; Pasdar, M.; Pazhoohan, J. Experimental and numerical study of the effects of formation brine salinity and reservoir temperature on convection mechanism during CO₂ storage in saline aquifers. *J. Nat. Gas Sci. Eng.* **2016**, *36*, 950–962. [[CrossRef](#)]
92. Snippe, J.; Tucker, O. CO₂ fate comparison for depleted gas field and dipping saline aquifer. *Energy Procedia* **2014**, *63*, 5586–5601. [[CrossRef](#)]
93. Worden, R.H.; Morrall, G.; Kelly, S.; Mc Ardle, P.; Barshep, D.V. A renewed look at calcite cement in marine-deltaic sandstones: The Brent Reservoir, Heather Field, Northern North Sea, UK. In *Application of Analytical Techniques to Petroleum Systems. Special Publication*; Dowey, P.J., Osborne, M.J., Volk, H., Eds.; Geological Society: London, UK, 2019; Volume 484, pp. 305–335.
94. Kelly, S.; Worden, R.H.; Mc Ardle, P. The Value of core in mature field development—Examples from the UK North Sea. In *The Role of Core in 21st Century Reservoir Characterisation*; Neal, A., Ashton, M., Williams, L., Dee, S., Dodd, T., Marshall, J., Eds.; The Geological Society: London, UK, 2023; Volume 527, pp. 261–278.
95. Hamza, A.; Hussein, I.A.; Al-Marri, M.J.; Mahmoud, M.; Shawabkeh, R.; Aparicio, S. CO₂ enhanced gas recovery and sequestration in depleted gas reservoirs: A review. *J. Pet. Sci. Eng.* **2021**, *196*, 107685. [[CrossRef](#)]
96. Mahabadi, N.; van Paassen, L.; Battiato, I.; Yun, T.S.; Choo, H.; Jang, J. Impact of pore-scale characteristics on immiscible fluid displacement. *Geofluids* **2020**, *2020*, 5759023. [[CrossRef](#)]
97. Sidiq, H.; Amin, R.; Van der Steen, E.; Kennaird, T. Super critical CO₂-methane relative permeability investigation. *J. Pet. Sci. Eng.* **2011**, *78*, 654–663. [[CrossRef](#)]
98. Hellevang, H. Carbon capture and storage (CCS). Chapter 24. In *Petroleum Geoscience: From Sedimentary Environments to Rock Physics*; Bjorlykke, K., Ed.; Springer: Berlin, German, 2015; pp. 591–602.
99. Spycher, N.; Pruess, K.; Ennis-King, J. CO₂-H₂O mixtures in the geological sequestration of CO₂: I.: Assessment and calculation of mutual solubilities from 12 to 100 °C and up to 600 bar. *Geochim. Cosmochim. Acta* **2003**, *67*, 3015–3031. [[CrossRef](#)]
100. Mito, S.; Xue, Z.Q. Post-Injection monitoring of stored CO₂ at the Nagaoka Pilot Site: 5 years time-lapse well logging results. *Energy Procedia* **2011**, *4*, 3284–3289. [[CrossRef](#)]
101. Okwen, R.T.; Stewart, M.T.; Cunningham, J.A. Analytical solution for estimating storage efficiency of geologic sequestration of CO₂. *Int. J. Greenh. Gas Control* **2010**, *4*, 102–107. [[CrossRef](#)]
102. Nordbotten, J.M.; Celia, M.A. Similarity solutions for fluid injection into confined aquifers. *J. Fluid Mech.* **2006**, *561*, 307–327. [[CrossRef](#)]
103. Sidiq, H.; Amin, R. The impact of pore pressure on CO₂-methane displacement. *Pet. Sci. Technol.* **2012**, *30*, 2531–2542. [[CrossRef](#)]
104. Burnside, N.M.; Naylor, M. Review and implications of relative permeability of CO₂/brine systems and residual trapping of CO₂. *Int. J. Greenh. Gas Control* **2014**, *23*, 1–11. [[CrossRef](#)]
105. Kazemifar, F.; Kyritsis, D.C. Experimental investigation of near-critical CO₂ tube-flow and Joule-Thompson throttling for carbon capture and sequestration. *Exp. Therm. Fluid Sci.* **2014**, *53*, 161–170. [[CrossRef](#)]
106. Miri, R.; Hellevang, H. Salt precipitation during CO₂ storage—A review. *Int. J. Greenh. Gas Control* **2016**, *51*, 136–147. [[CrossRef](#)]
107. Tan, X.H.; Shi, J.J.; Hui, D.; Li, Q.; Wu, T.T. Material balance method and dynamic pressure monitoring for water-bearing gas reservoirs with CO₂ injection. *Energies* **2023**, *16*, 4592. [[CrossRef](#)]
108. James, A.; Baines, S.; McCollough, S. *Progressing Development of the UK's Strategic Carbon Dioxide Storage Resource: A Summary of Results from the Strategic UK CO₂ Storage Appraisal Project*; The Energy Technologies Institute: Loughborough, UK, 2016.
109. Doughty, C.; Freifeld, B.M.; Trautz, R.C. Site characterization for CO₂ geologic storage and vice versa: The Frio brine pilot, Texas, USA as a case study. *Environ. Geol.* **2008**, *54*, 1635–1656. [[CrossRef](#)]
110. Ide, S.T.; Jessen, K.; Orr, F.M. Storage of CO₂ in saline aquifers: Effects of gravity, viscous, and capillary forces on amount and timing of trapping. *Int. J. Greenh. Gas Control* **2007**, *1*, 481–491.
111. Zhou, Q.L.; Birkholzer, J.T.; Tsang, C.F.; Rutqvist, J. A method for quick assessment of CO₂ storage capacity in closed and semi-closed saline formations. *Int. J. Greenh. Gas Control* **2008**, *2*, 626–639. [[CrossRef](#)]
112. Bachu, S.; Bonijoly, D.; Bradshaw, J.; Burruss, R.; Holloway, S.; Christensen, N.P.; Mathiassen, O.M. CO₂ storage capacity estimation: Methodology and gaps. *Int. J. Greenh. Gas Control* **2007**, *1*, 430–443. [[CrossRef](#)]
113. IEAGHG. *CO₂ Storage in Depleted Gas Fields*; IEAGHG: Cheltenham, UK, 2009.
114. James, A.; Baines, S.; McCollough, S. *Strategic UK CCS Storage Appraisal—WP5E—Viking Storage Development Plan*; Energy Technologies Institute: Loughborough, UK, 2016.
115. AlNajdi, N.; Worden, R.H. Porosity in mudstones and its effectiveness for sealing carbon capture and storage sites. In *Enabling Secure Subsurface Storage in Future Energy Systems, Special Publication*; Alcalde, J., Miocic, J., Heinemann, N., Edlmann, K., Sundal, A., Schultz, R., Eds.; Geological Society: London, UK, 2022; Volume 528.
116. Bump, A.P.; Bakhshian, S.; Ni, H.L.; Hovorka, S.D.; Olariu, M.I.; Dunlap, D.; Hosseini, S.A.; Meckel, T.A. Composite confining systems: Rethinking geologic seals for permanent CO₂ sequestration. *Int. J. Greenh. Gas Control* **2023**, *126*, 103908. [[CrossRef](#)]
117. Espinoza, D.N.; Santamarina, J.C. CO₂ breakthrough-caprock sealing efficiency and integrity for carbon geological storage. *Int. J. Greenh. Gas Control* **2017**, *66*, 218–229. [[CrossRef](#)]

118. Kaldi, J.G.; Daniel, R.F.; Tenthorey, E.; Michael, K.; Schacht, U.; Nicol, A.; Underschultz, J.R.; Backe, G. *Caprock Systems for Geological Storage of CO₂*; Cooperative Research Centre for Greenhouse Gas Technologies: Canberra Australia, 2011; pp. 1–133.
119. Allen, M.J.; Faulkner, D.R.; Worden, R.H.; Rice-Birchall, E.; Katirtsidis, N.; Utley, J.E.P. Geomechanical and petrographic assessment of a CO₂ storage site: Application to the Acorn CO₂ Storage Site, offshore United Kingdom. *Int. J. Greenh. Gas Control* **2020**, *94*, 102923. [[CrossRef](#)]
120. Rider, M.; Kennedy, M.J. *The Geological Interpretation of Well Logs*; Rider-French Consulting: Cambridge, UK, 2011.
121. Yalız, A.; Taylor, P. The Hamilton and Hamilton North Gas Fields, Block 110/13a, East Irish Sea. In *United Kingdom Oil and Gas Fields, Commemorative Millennium Volume*; Gluyas, J.G., Hitchens, H.M., Eds.; Geological Society: London, UK, 2003; Volume 20, pp. 77–86.
122. Santarelli, F.J.; Tronvoll, J.T.; Svennekjaer, M.; Skeie, H.; Henriksen, R.; Bratli, R.K. Reservoir stress path: The depletion and the rebound. In Proceedings of the SPE/ISRM Rock Mechanics in Petroleum Engineering Conference, Trondheim, Norway, 8–10 July 1998; pp. 203–209.
123. Engelder, T.; Fischer, M.P. Influence of poroelastic behavior on the magnitude of minimum horizontal stress, S_h , in overpressured parts of sedimentary basins. *Geology* **1994**, *22*, 949–952. [[CrossRef](#)]
124. White, J.A.; Foxall, W. Assessing induced seismicity risk at CO₂ storage projects: Recent progress and remaining challenges. *Int. J. Greenh. Gas Control* **2016**, *49*, 413–424. [[CrossRef](#)]
125. Paap, B.; Verdel, A.; Meekes, S.; Steeghs, P.; Vandeweyer, V.; Neele, F. Four years of experience with a permanent seismic monitoring array at the Ketzin CO₂ storage pilot site. In Proceedings of the 12th International Conference on Greenhouse Gas Control Technologies (GHGT), Austin, TX, USA, 5–9 October 2014; pp. 4043–4050.
126. Grude, S.; Landro, M.; Dvorkin, J. Pressure effects caused by CO₂ injection in the Tubæen Fm. the Snohvit field. *Int. J. Greenh. Gas Control* **2014**, *27*, 178–187. [[CrossRef](#)]
127. Smith, N.; Boone, P.; Oguntimhin, A.; van Essen, G.; Guo, R.; Reynolds, M.A.; Friesen, L.; Cano, M.-C.; O’Brien, S. Quest CCS facility: Halite injectivity damage remediation in CO₂ injection wells. In Proceedings of the 15th International Conference on Greenhouse Gas Control Technologies GHGT-15, Abu Dhabi, United Arab Emirates, 15–18 March 2021.
128. Vialle, S.; Vanorio, T. Laboratory measurements of elastic properties of carbonate rocks during injection of reactive CO₂-saturated water. *Geophys. Res. Lett.* **2011**, *38*, L01302. [[CrossRef](#)]
129. Bacci, G.; Korre, A.; Durucan, S. Experimental investigation into salt precipitation during CO₂ injection in saline aquifers. *Energy Procedia* **2011**, *4*, 4450–4456. [[CrossRef](#)]
130. Pruess, K.; Garcia, J. Multiphase flow dynamics during CO₂ disposal into saline aquifers. *Environ. Geol.* **2002**, *42*, 282–295. [[CrossRef](#)]
131. Worden, R.H. Halogen elements in sedimentary systems and their evolution during diagenesis. In *Role of Halogens in Terrestrial and Extraterrestrial Processes: Surface Crust and Mantle*; Harlov, D.E., Aranovich, L., Eds.; Springer: Berlin, German, 2018; pp. 185–260.
132. Worden, R.H. Controls on halogen concentrations in sedimentary formation waters. *Mineral. Mag.* **1996**, *60*, 259–274. [[CrossRef](#)]
133. Worden, R.H.; French, M.W.; Mariani, E. Amorphous silica nanofilms result in growth of misoriented microcrystalline quartz cement maintaining porosity in deeply buried sandstones. *Geology* **2012**, *40*, 179–182. [[CrossRef](#)]
134. Giorgis, T.; Carpita, M.; Battistelli, A. 2D modeling of salt precipitation during the injection of dry CO₂ in a depleted gas reservoir. *Energy Convers. Manag.* **2007**, *48*, 1816–1826. [[CrossRef](#)]
135. Pearce, J.; Czernichowski-Lauriol, I.; Lombardi, S.; Brune, S.; Nador, A.; Baker, J.; Pauwels, H.; Hatziyannis, G.; Beaubien, S.; Faber, E. A review of natural CO₂ accumulations in Europe as analogues for geological sequestration. In *Geological Storage of Carbon Dioxide. Special Publication*; Baines, S.J., Worden, R.H., Eds.; Geological Society: London, UK, 2004; Volume 233, pp. 29–41.
136. Baines, S.J.; Worden, R.H. The long term fate of CO₂ in the subsurface: Natural analogues for CO₂ storage. In *Geological Storage of Carbon Dioxide. Special Publication*; Baines, S.J., Worden, R.H., Eds.; Geological Society: London, UK, 2004; Volume 233, pp. 59–85.
137. Baines, S.J.; Worden, R.H. Geological CO₂ disposal: Understanding the long term fate of CO₂ in naturally occurring accumulations. In *Greenhouse Gas Control Technologies*; Williams, D.J., Durie, B., McMullan, P., Paulson, C., Smith, A., Eds.; CSIRO: Clayton, Australia, 2001; pp. 311–316.
138. Vilarrasa, V.; Makhnenko, R.Y.; Rutqvist, J. Field and laboratory studies of geomechanical response to the injection of CO₂. In *Science of Carbon Storage in Deep Saline Aquifers*; Newell, P., Ilgen, G.A., Eds.; Elsevier: Amsterdam, The Netherlands, 2019; pp. 209–236.
139. Cardoso, S.S.S.; Andres, J.T.H. Geochemistry of silicate-rich rocks can curtail spreading of carbon dioxide in subsurface aquifers. *Nat. Commun.* **2014**, *5*, 5743. [[CrossRef](#)]
140. Kaszuba, J.; Yardley, B.; Andreani, M. Experimental perspectives of mineral dissolution and precipitation due to carbon dioxide-water-rock interactions. *Geochem. Geol. CO₂ Sequestration* **2013**, *77*, 153–188.
141. Griffiths, J.; Worden, R.H.; Wooldridge, L.J.; Utley, J.E.P.; Duller, R.A. Compositional variation in modern estuarine sands: Predicting major controls on sandstone reservoir quality. *Am. Assoc. Pet. Geol. Bull.* **2019**, *103*, 797–833. [[CrossRef](#)]
142. Worden, R.H.; Morad, S. Clay minerals in sandstones: Controls on formation, distribution and evolution. In *Clay Mineral Cements in Sandstones. Special Publication of the International Association of Sedimentologists*; Worden, R.H., Morad, S., Eds.; Blackwells: Oxford, UK, 2003; Volume 34, pp. 3–41.

143. McKinley, J.M.; Worden, R.H.; Ruffell, A.H. Smectite in sandstones: A review of the controls on occurrence and behaviour during diagenesis. In *Clay Mineral Cements in Sandstones, Special Publication of the International Association of Sedimentologists*; Worden, R.H., Morad, S., Eds.; Blackwells: Oxford, UK, 2003; Volume 34, pp. 109–128.
144. Nover, G.; Von Der Gonna, J.; Heikamp, S.; Koster, J. Changes of petrophysical properties of sandstones due to interaction with supercritical carbon dioxide—A laboratory study. *Eur. J. Mineral.* **2013**, *25*, 317–329. [[CrossRef](#)]
145. Singh, K.; Anabaraonye, B.U.; Blunt, M.J.; Crawshaw, J. Partial dissolution of carbonate rock grains during reactive CO₂-saturated brine injection under reservoir conditions. *Adv. Water Resour.* **2018**, *122*, 27–36. [[CrossRef](#)]
146. Shevalier, M.; Dalkhaa, C.; Humez, P.; Mayer, B.; Becker, V.; Nightingale, M.; Rock, L.; Zhang, G.X. Coupling of TOUGHREACT-Geochemist Workbench (GWB) for modeling changes in the isotopic composition of CO₂ leaking from a CCS storage reservoir. *Energy Procedia* **2014**, *63*, 3751–3760. [[CrossRef](#)]
147. Shevalier, M.; Nightingale, M.; Mayer, B.; Hutcheon, I.; Durocher, K.; Perkins, E. Brine geochemistry changes induced by CO₂ injection observed over a 10 year period in the Weyburn oil field. *Int. J. Greenh. Gas Control* **2013**, *16*, S160–S176. [[CrossRef](#)]
148. Alam, M.M.; Hjuler, M.L.; Christensen, H.F.; Fabricius, I.L. Petrophysical and rock-mechanics effects of CO₂ injection for enhanced oil recovery: Experimental study on chalk from South Arne field, North Sea. *J. Pet. Sci. Eng.* **2014**, *122*, 468–487. [[CrossRef](#)]
149. Pham, V.T.H.; Lu, P.; Aagaard, P.; Zhu, C.; Hellevang, H. On the potential of CO₂-water-rock interactions for CO₂ storage using a modified kinetic model. *Int. J. Greenh. Gas Control* **2011**, *5*, 1002–1015. [[CrossRef](#)]
150. Xu, T.F.; Apps, J.A.; Pruess, K. Mineral sequestration of carbon dioxide in a sandstone-shale system. *Chem. Geol.* **2005**, *217*, 295–318. [[CrossRef](#)]
151. Hellevang, H.; Declercq, J.; Aagaard, P. Why is dawsonite absent in CO₂ charged reservoirs? *Oil Gas Sci. Technol. -Rev. D IFP Energ. Nouv.* **2011**, *66*, 119–135. [[CrossRef](#)]
152. Worden, R.H. Dawsonite cement in the Triassic Lam Formation, Shabwa Basin, Yemen: A natural analogue for a potential mineral product of subsurface CO₂ storage for greenhouse gas reduction. *Mar. Pet. Geol.* **2006**, *23*, 61–77. [[CrossRef](#)]
153. Forster, H.-J.; Wilke, F.D.H.; Block, S.; Eisner, D.; Forster, A.; Norden, B.; Schmidt-Hattenberger, C. Mineralogical responses to 9-years of interaction of a CO₂-charged brine with a sandstone aquifer: Observations and implications from the Ketzin CO₂-storage pilot site (Germany). In Proceedings of the 10th Trondheim Conference on Carbon Capture, Transport and Storage TCCS-10, Trondheim, Norway, 17–19 June 2019.
154. Hermanrud, C.; Eiken, O.; Hansen, O.R.; Bolas, H.M.N.; Simmenes, H.; Teige, G.M.G.; Hansen, H.; Johansen, S. Importance of pressure management in CO₂ storage. In Proceedings of the Offshore Technology Conference, Houston, Texas, USA, 6–9 May 2013; p. OTC-23961-MS.
155. Machado, M.V.B.; Delshad, M.; Sepehrnoori, K. Potential benefits of horizontal wells for CO₂ injection to enhance storage security and reduce leakage risks. *Appl. Sci. -Basel* **2023**, *13*, 12830. [[CrossRef](#)]
156. Harding, F.C.; James, A.T.; Robertson, H.E. The engineering challenges of CO₂ storage. *Proc. Inst. Mech. Eng. Part A-J. Power Energy* **2018**, *232*, 17–26. [[CrossRef](#)]
157. Rutqvist, J. The Geomechanics of CO₂ Storage in Deep Sedimentary Formations. *Geotech. Geol. Eng.* **2012**, *30*, 525–551. [[CrossRef](#)]
158. Rutqvist, J.; Rinaldi, A.P.; Vilarrasa, V.; Cappa, F. *Numerical Geomechanics Studies of Geological Carbon Storage (GCS). Process Coupling across Time and Spatial Scales*; Newell, P., Ilgen, A.G., Eds.; Elsevier: Amsterdam, The Netherlands, 2019; pp. 237–252.
159. Carey, J.W.; Wigand, M.; Chipera, S.J.; WoldeGabriel, G.; Pawar, R.; Lichtner, P.C.; Wehner, S.C.; Raines, M.A.; Guthrie, G.D. Analysis and performance of oil well cement with 30 years of CO₂ exposure from the SACROC Unit, West Texas, USA. *Int. J. Greenh. Gas Control* **2007**, *1*, 75–85. [[CrossRef](#)]
160. Hawkes, C.D.; Bachu, S.; McLellan, P.J. Geomechanical factors affecting geological storage of CO₂ in depleted oil and gas reservoirs. *J. Can. Pet. Technol.* **2005**, *44*, 52–61. [[CrossRef](#)]
161. Dean, M.; Tucker, O.D. A risk-based framework for measurement, monitoring and verification (MMV) of the Goldeneye storage complex for the Peterhead CCS project, UK. *Int. J. Greenh. Gas Control* **2017**, *61*, 1–15. [[CrossRef](#)]
162. IEAGHG. *Monitoring and Modelling of CO₂ Storage: The Potential for Improving the Cost-Benefit Ratio of Reducing Risk*; IEAGHG: Cheltenham, Switzerland, 2020; pp. 1–109.
163. Bourne, S.; Crouch, S.; Smith, M. A risk-based framework for measurement, monitoring and verification of the Quest CCS Project, Alberta, Canada. *Int. J. Greenh. Gas Control* **2014**, *26*, 109–126. [[CrossRef](#)]
164. Gaurina-Medimurec, N.; Mavar, K.N. Depleted hydrocarbon reservoirs and CO₂ injection wells—CO₂ leakage assessment. *Rud. -Geol. -Naft. Zb.* **2017**, *32*, 15–27. [[CrossRef](#)]
165. Rutqvist, J.; Vasco, D.W.; Myer, L. Coupled reservoir-geomechanical analysis of CO₂ injection and ground deformations at In Salah, Algeria. *Int. J. Greenh. Gas Control* **2010**, *4*, 225–230. [[CrossRef](#)]
166. Rutqvist, J.; Pio-Rinaldi, A.; Vilarrasa, V.; Cappa, F. Numerical geomechanics studies of geological carbon storage (GCS). In *Science of Carbon Storage in Deep Saline Formations*; Newell, P., Ilgen, A.G., Eds.; Elsevier: Chennai, India, 2019; pp. 179–190.
167. Williams, G.A.; Chadwick, R.A. Influence of reservoir-scale heterogeneities on the growth, evolution and migration of a CO₂ plume at the Sleipner Field, Norwegian North Sea. *Int. J. Greenh. Gas Control* **2021**, *106*, 103260. [[CrossRef](#)]
168. Correa, J.; Pevzner, R.; Bona, A.; Tertyshnikov, K.; Freifeld, B.; Robertson, M.; Daley, T. 3D vertical seismic profile acquired with distributed acoustic sensing on tubing installation: A case study from the CO₂CRC Otway Project. *Interpret. -A J. Subsurf. Charact.* **2019**, *7*, SA11–SA19. [[CrossRef](#)]

169. Freifeld, B.M.; Trautz, R.C.; Kharaka, Y.K.; Phelps, T.J.; Myer, L.R.; Hovorka, S.D.; Collins, D.J. The U-tube: A novel system for acquiring borehole fluid samples from a deep geologic CO₂ sequestration experiment. *J. Geophys. Res. -Solid Earth* **2005**, *110*, B10203. [[CrossRef](#)]
170. Murugan, A.; Brown, R.J.C.; Wilmot, R.; Hussain, D.; Bartlett, S.; Brewer, P.J.; Worton, D.R.; Bacquart, T.; Gardiner, T.; Robinson, R.A.; et al. Performing quality assurance of carbon dioxide for carbon capture and storage. *J. Carbon Res.* **2020**, *6*, 6040076. [[CrossRef](#)]
171. Sidenko, E.; Tertyshnikov, K.; Gurevich, B.; Pevzner, R. DAS signature of reservoir pressure changes caused by a CO₂ injection: Experience from the CO₂CRC Otway Project. *Int. J. Greenh. Gas Control* **2022**, *119*, 103735. [[CrossRef](#)]
172. Martens, S.; Kempka, T.; Liebscher, A.; Luth, S.; Moller, F.; Myrtilinen, A.; Norden, B.; Schmidt-Hattenberger, C.; Zimmer, M.; Kuhn, M.; et al. Europe's longest-operating on-shore CO₂ storage site at Ketzin, Germany: A progress report after three years of injection. *Environ. Earth Sci.* **2012**, *67*, 323–334. [[CrossRef](#)]
173. Xue, Z.Q.; Mito, S.; Kitamura, K.; Matsuoka, T. Case study: Trapping mechanisms at the pilot-scale CO₂ injection site, Nagaoka, Japan. In Proceedings of the 9th International Conference on Greenhouse Gas Control Technologies, Washington, DC, USA, 16–20 November 2008; pp. 2057–2062.
174. Hovorka, S.D. Three-million-metric-ton-monitored injection at the SECARB Cranfield project-project update. In Proceedings of the International Conference on Greenhouse Gas Technologies (GHGT), Kyoto, Japan, 18–22 November 2012; pp. 6412–6423.
175. Roberts, J.J.; Gilfillan, S.M.V.; Stalker, L.; Naylor, M. Geochemical tracers for monitoring offshore CO₂ stores. *Int. J. Greenh. Gas Control* **2017**, *65*, 218–234. [[CrossRef](#)]
176. Wallmann, K.; Reitz, A. *ECO2—Sub-Seabed CO₂ Storage: Impact on Marine Ecosystems*; GEOMAR: Kiel, Germany, 2014.
177. Mathieson, A.; Midgely, J.; Wright, I.; Saoula, N.; Ringrose, P. In Salah CO₂ Storage JIP: CO₂ sequestration monitoring and verification technologies applied at Krechba, Algeria. *Energy Procedia* **2011**, *4*, 3596–3603. [[CrossRef](#)]

Disclaimer/Publisher's Note: The statements, opinions and data contained in all publications are solely those of the individual author(s) and contributor(s) and not of MDPI and/or the editor(s). MDPI and/or the editor(s) disclaim responsibility for any injury to people or property resulting from any ideas, methods, instructions or products referred to in the content.